



AD-A283 530



Miscellaneous Paper CERC-94-14  
July 1994

①

US Army Corps  
of Engineers  
Waterways Experiment  
Station

## Upgrade of Tropical Cyclone Surface Wind Field Model

by Vincent J. Cardone, Andrew T. Cox, J. Arthur Greenwood, Oceanweather, Inc.  
Edward F. Thompson, WES



WZES

Approved For Public Release; Distribution Is Unlimited

DTIC QUALITY INSPECTED 5

94-26566



94 8 19 078

Prepared for Headquarters, U.S. Army Corps of Engineers

# Upgrade of Tropical Cyclone Surface Wind Field Model

by Vincent J. Cardone, Andrew T. Cox, J. Arthur Greenwood

Oceanweather, Inc.  
5 River Road, Suite 1  
Cos Cob, CT 06807

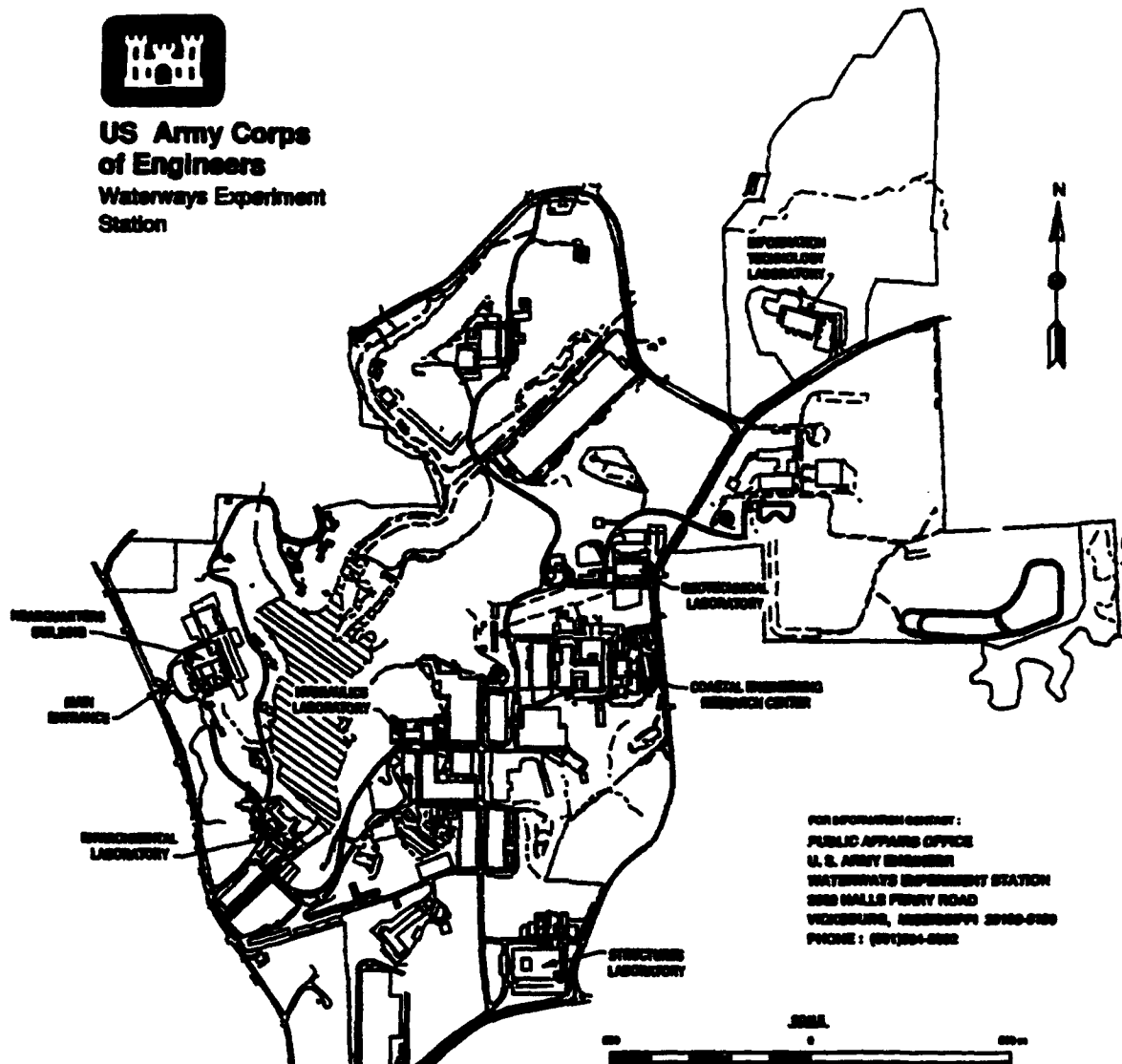
Edward F. Thompson  
U.S. Army Corps of Engineers  
Waterways Experiment Station  
3909 Halls Ferry Road  
Vicksburg, MS 39180-6199

Final report

Approved for public release; distribution is unlimited



**US Army Corps  
of Engineers**  
**Waterways Experiment  
Station**



#### **Waterways Experiment Station Cataloging-in-Publication Data**

**Upgrade of tropical cyclone surface wind field model / by Vincent J. Cardone ... [et al] ; prepared for U.S. Army Corps of Engineers.**

**101 p. : ill. ; 28 cm. -- (Miscellaneous paper ; CERC-94-14)**

**Includes bibliographic references.**

**1. Storm winds -- Mathematical models. 2. Hurricanes -- Mathematical models -- Data processing. 3. Windstorms -- Mathematical models -- Computer programs. 4. Cyclones -- Mathematical models. I. Cardone, Vince J. II. United States. Army. Corps of Engineers. III. U.S. Army Engineer Waterways Experiment Station. IV. Coastal Engineering Research Center (U.S.) V. Series: Miscellaneous paper (U.S. Army Engineer Waterways Experiment Station) ; CERC-94-14.**

**TA7 W34m no.CERC-94-14**

# Contents

---

Preface .....	v
Conversion Factors, Non-SI to SI Units of Measurements .....	vi
1—Introduction .....	1
Background .....	1
Previous Studies .....	2
Scope .....	3
2—Existing Model Limitations .....	4
Physics .....	4
Initialization .....	5
Numerics .....	7
Summary of Limitations .....	9
3—Upgraded Model .....	10
Increased Resolution .....	10
Generalized Pressure Specification .....	12
Pressure profile form .....	12
Modified outflow .....	13
Specification of pressure parameters .....	15
Sample Runs .....	20
4—Summary .....	25
References .....	26
Appendix A: Comparison of Five-Nest and Seven-Nest Models for Hurricane Camille .....	A1
Appendix B: Documentation of CE Model Upgrades .....	B1
Appendix C: Sample Application of Upgraded CE Model to Simulation of 12 Snapshots of Hurricane Gilbert .....	C1
Appendix D: Sample Application of Upgraded CE Model to Simulation of 36-Hr Period of Hurricane Gilbert in the Gulf of Mexico .....	D1
SF 298	

## List of Figures

---

Figure 1.	Temporal changes in the azimuthally averaged wind for NOAA reconnaissance flights into Hurricane Gilbert; changes are normalized to a 6-hr time interval (from Black and Willoughby (1992)) . . . . .	8
Figure 2.	Distribution of maximum wind speed differences between 5-nest and 7-nest model runs for Hurricane Camille . . . . .	12
Figure 3.	Example of Oceanweather tropical storm analysis . . . . .	17
Figure 4.	Some parameters in double exponential profile . . . . .	21
Figure 5.	Comparison of azimuthally averaged reconnaissance winds and fitted gradient winds in 12 cases of Hurricane Gilbert defined by Black and Willoughby (1992) . . . . .	24

## List of Tables

---

Table 1.	Effect of Nest Activation Parameter, INSIDE . . . . .	11
Table 2.	Maximum Inflow Observed in Frictionless Stationary Vortex Solution . . . . .	14
Table 3.	Empirical Correction of Inflow Angle . . . . .	15
Table 4.	Parameter Definitions for Fitting Single Exponential Profile . . . . .	18
Table 5.	Generalized Single Exponential Profile Fits to Selected Hurricane Gilbert Cases . . . . .	18
Table 6.	Parameter Definitions for Fitting Double Exponential Profile . . . . .	20
Table 7.	Observed Pressure and Azimuthally Averaged Pseudo-Gradient Wind Maxima in Hurricane Gilbert and Estimated Generalized Profile Parameters . . . . .	22
Table 8.	Comparison of Measured Flight-Level Wind Maxima and Fitted Gradient Wind Maxima for Double Exponential Pressure Profile . . . . .	23

# Preface

---

This report describes improvements developed for the planetary boundary layer surface wind field model traditionally used by the U.S. Army Corps of Engineers for hurricane modeling. Limitations of the model are also described. The upgraded model has increased flexibility for spatial resolution and pressure profile specification. The wind fields can be used in ocean response modeling, including wave and surge modeling activities.

This study was authorized by Headquarters, U.S. Army Corps of Engineers, under the Coastal Flooding and Storm Protection Area of the Coastal Research Program, Work Unit 32683, "Wind Estimation for Coastal Modeling." Technical Monitors were Messrs. John H. Lockhart, Jr.; John G. Housley; Barry W. Holliday; and John Saucier. Ms. Carolyn M. Holmes of the U.S. Army Engineer Waterways Experiment Station (WES), Coastal Engineering Research Center (CERC), was the Program Manager.

The study was conducted under Contract No. DACW39-93-C-0022 by Oceanweather, Inc. (OWI), Cos Cob, Connecticut. The report was prepared by Dr. Vincent J. Cardone and Messrs. Andrew T. Cox and J. Arthur Greenwood, all of OWI, and Dr. Edward F. Thompson of the Coastal Oceanography Branch (COB), Research Division (RD), CERC. Dr. Thompson was Principal Investigator of the research work unit funding this study. The work unit was under the direct supervision of Dr. Martin C. Miller, Chief, COB, and Mr. H. Lee Butler, Chief, RD, and under the general supervision of Mr. Charles C. Calhoun, Jr., Assistant Director, CERC, and Dr. James R. Houston, Director, CERC.

At the time of publication of this report, Director of WES was Dr. Robert W. Whalin. Commander was COL Bruce K. Howard, EN.

Accession For	
NTIS GRA&I	<input checked="" type="checkbox"/>
DTIC TAB	<input type="checkbox"/>
Unannounced	<input type="checkbox"/>
Justification	
By _____	
Distribution/ _____	
Availability Codes	
Distr	Avail and/or Special
A-1	

*The contents of this report are not to be used for advertising, publication, or promotional purposes. Citation of trade names does not constitute an official endorsement or approval of the use of such commercial products.*

# **Conversion Factors, Non-SI to SI Units of Measurement**

---

Non-SI units of measurement used in this report can be converted to SI units as follows:

Multiply	By	To Obtain
degrees (angle)	0.01745329	radians
knots (international)	0.5144444	meters per second
miles (U.S. nautical)	1.852	kilometers

# 1 Introduction

---

## Background

The unprecedented destruction of parts of the United States caused by hurricanes Andrew and Iniki last summer has aroused increased interest in the wind structure of tropical cyclones among the scientific and engineering communities. Unlike most past destructive storms, much of the loss in these recent storms was associated with direct wind damage. While simple parametric tropical cyclone wind models remain in use to model surface winds and to provide forcing for ocean response models, a few numerical vortex boundary layer models based upon solution of the primitive equations of motion have emerged, including most prominently the so-called U.S. Army Corps of Engineers (CE) wind model (Cardone et al. 1992). The model was developed originally at New York University in the early 1970's and later further developed at Oceanweather Inc. (OWI) under CE support in 1979. Recently the format of the CE model was modified to conform with the requirements of the CE Coastal Modeling System (Thompson 1993).

The CE numerical model was reviewed as part of a Workshop on Tropical Wind Modeling convened at the U.S. Army Engineer Waterways Experiment Station on 24-25 March, 1992. Invited participants in the review were:

- Dr. Wilson A. Schaffer, Techniques Development Laboratory, National Weather Service (NWS), National Oceanic and Atmospheric Administration (NOAA)
- Dr. Mark D. Powell, Hurricane Research Division (HRD), Atlantic Oceanographic and Meteorological Laboratory, Environmental Research Laboratories, NOAA
- Dr. Mukut B. Mathur, National Meteorological Center, NWS, NOAA
- Dr. Vincent J. Cardone, OWI

The workshop stressed the relationship between surface wind modeling and more general questions of the dynamical and thermodynamic nature of tropical cyclones. It also emphasized the need to carefully evaluate the reliability and representativeness of the scant surface marine wind data available in intense cyclones, before such data are used to further develop and validate numerical models.

The workshop addressed the potential for further development of existing numerical models, particularly the CE model. A number of specific research needs for improving wind models were identified and prioritized in terms of both importance to ocean response modeling and feasibility of success. These needs are summarized more fully in a "white paper" (Cardone and Thompson 1992).

Subsequent to the workshop, a study was initiated to address high priority upgrades to the CE model which could be accomplished with the limited funds available. The following tasks were chosen: (1) increase resolution and domain of the nested grid system; (2) generalize the surface pressure specification. The enhancements developed for the CE wind model are the subject of this report. The enhancements will be incorporated into the Coastal Modeling System in the near future.

## Previous Studies

The CE wind model has been used mainly to provide wind fields in historical tropical cyclones to drive ocean response models operated in a hindcast mode (surface waves, mixed layer currents, storm surge). Those wind fields generally provide unbiased ocean predictions when used to drive CE and OWI ocean response models (e.g. Reece and Cardone 1982). They have also been used to drive ocean response models developed by other scientists independently, wherein CE model winds have also repeatedly been shown to provide unbiased hindcasts (e.g. Forristall 1980, WAMDI Group 1988, Cooper and Thompson 1989, Ly and O'Connor 1991, Grosskopf et al. 1991, Mairs et al. 1992). At OWI the model has been used in over three dozen studies to drive ocean response models to establish offshore design criteria in many parts of the world affected by tropical cyclones.

The CE model has been extensively used for both ocean wave and storm surge modeling for CE applications. Abel et al. (1989) applied the model to estimate wave statistics due to hurricanes in the Atlantic Ocean and Gulf of Mexico during 1956-75. Tracy and Hubertz (1990) estimated waves produced by 10 hurricanes impacting southern California during 1956-89. Mark and Scheffner (1993) describe a hurricane surge study for the coast of Delaware. A similar approach is presently being applied to the entire U.S. Atlantic Coast.

The generality of the CE model was also demonstrated when it was used to provide winds to test the third generation wave model (3GWAM) (WAMDI Group 1988). Winds supplied to the WAM model were exactly the same as winds for the subject storms (three intense Gulf of Mexico hurricanes) which had been used in previous studies to drive first and second generation models, and which had been used by other investigators. The WAM model was found to provide unbiased and skillful wave hindcasts in these storms, with WAM using its own calibration of source terms developed completely independently of CE winds. The same tuning on WAM has also been shown to provide

nearly perfect hindcasts in severe extratropical storms as well when driven by extremely accurate wind fields derived by direct kinematic analysis of wind measurements (Cardone et al. 1994).

## Scope

In many of the studies cited above, ocean response models were used to evaluate the most extreme response (storm peak winds, waves, surge and currents) in a storm at a fixed site. In general, in storms in which the assumed storm pressure profile fits the actual radial distribution well, modeled storm peaks are unbiased in the mean and exhibit scatter index of 15 percent or less. The method is less successful in modeling the entire spatial and temporal distribution of the wind field in such storms. There are some storms in which even the storm peaks are difficult to simulate, where the storm structure departs from the simple structure implied by the presumed pressure distribution. This and other limitations of the CE model are described in more detail in Chapter 2.

In this study, two limitations of the CE tropical storm wind model are addressed and remedied. The first change is simply the addition of two additional nests to the grid system used to implement the numerical vortex model. This change provides lower truncation errors near the center of small intense storms, greater resolution near the vortex center, and an expanded solution domain. The second change is generalization of the radial surface pressure profile upon which the surface pressure initialization of the vortex model is based. The form adopted also allows the specification of profiles with two maxima in the radial pressure gradient. These changes are described in Chapter 3. A summary is given in Chapter 4.

## 2 Existing Model Limitations

---

The CE wind model developed by Cardone et al. (1992) has proved to be a powerful tool in ocean response modeling. However, the model, developed in 1979, includes a number of limitations. In light of enhanced computing power now available and the increasing field measurements and understanding of tropical storm behavior, it is timely to review the model limitations. Limitations of the CE model may be described in three basic categories: physics, initialization, and numerics.

### Physics

The CE model evolved from the model of Chow (1971) who solved the momentum equations of an integrated boundary layer flow for a boundary layer of constant depth. The vertical friction force was taken parallel to the wind relative to the earth. Horizontal friction was also considered. The equations, however, were solved numerically on a nested cartesian grid system centered on the vortex and translating at constant velocity with the vortex. The steady solution in the moving coordinate system referred back to the earth yielded qualitatively realistic boundary layer wind patterns. The solution included supergradient flows inside the radius of maximum gradient wind and a decrease in the radius of maximum wind. It also included an asymmetric wind distribution with maxima in the right front quadrant for a typical superposition of a symmetric vortex and ambient gradient, and a boundary layer convergence pattern consistent with observed patterns of convection in typical storms.

Shapiro (1983) solved the same slab momentum equation as Chow (1971) but used a truncated spectral analysis in cylindrical coordinates, in order to allow a more convenient separation of the role of linear and non-linear asymmetric effects in the boundary layer flow. Chow's model and solution method provide the same patterns as that of Shapiro's model except that inside the radius of maximum wind truncation errors are larger than for the spectral solution. As a consequence, Chow's model may slightly overestimate the degree of supergradient flow inside the eye. These studies show that the essential physics governing the boundary layer flow are included in Chow's and Shapiro's models. The main physical processes missing are the feedback of

the convection (induced in part by the modelled convergence field) on the wind field, and strong non-steady effects (for example rapid deepening of the vortex in the moving frame) which may cause even the overlying vortex to be unbalanced.

The CE model is derived directly from Chow's formulation and uses Chow's numerical solution. Several improvements to Chow's solution were made to insure that it not only gives qualitatively realistic wind fields, but also provides a quantitatively correct surface stress vector distribution, from which the model diagnoses winds within the surface boundary layer as well. The main enhancements to Chow's model are in the inclusion of a similarity boundary layer formulation relating vertically integrated flow to the surface drag (magnitude and direction), adoption of more realistic boundary layer depths than considered by Chow or Shapiro, consideration of the effects of boundary layer stratification and variable surface roughness (expressed in terms of wind alone with no sea state effects considered), and incorporation of greater flexibility in the specification of the imposed pressure distribution of the vortex over the possibilities considered by Chow.

The CE model was developed with a secondary objective to provide winds over inland lake surfaces and land surfaces of arbitrary roughness. The theoretical development of this part of the model met with less success than the over-water treatment. A simplified equilibrium boundary layer approach was adopted which ignores the adjustment of the planetary boundary layer (PBL) wind field across discontinuities of roughness. Thus, while the model validation against winds measured over land indicated good agreement when the wind fetch was over a homogeneous roughness, little is known about the effect on ocean response modeling associated with failure in the CE model (probably) to resolve small scale PBL wind changes downwind of abrupt changes in roughness (e.g. the coast).

## Initialization

The model is generally applied with boundary layer height in the range of 500 m - 650 m, slightly unstable stratification, a Charnock type surface roughness formulation (Charnock constant 0.035 with Karman constant 0.35), and a value of unity for the Ekman scale height parameter. This combination produces unbiased surface winds over the open sea when the model is applied to real storms and validated against measured surface wind time histories obtained by calibrated instruments (e.g. NOAA buoys, offshore rigs).

The pressure field is generally described as the superposition of the pressure gradient computed from the exponential pressure profile form for the symmetric part of the vortex:

$$p(r) = p_o + (p_\infty - p_o) e^{-\frac{r}{R_p}} \quad (1)$$

where

$p(r)$  = pressure

$p_o$  = central pressure (at the eye)

$p_\infty$  = axisymmetric ambient pressure (far field pressure)

$R_p$  = scaling radius

$r$  = radius

and an uniform ambient gradient given by

$$f \bar{k} \times \nabla_s = - \frac{1}{\rho} \nabla p_\infty \quad (2)$$

where

$f$  = Coriolis parameter

$\bar{k}$  = unit vector in the vertical direction

$\nabla_s$  = ambient uniform geostrophic flow

$\rho$  = mean air density

$\nabla p_\infty$  = uniform ambient pressure gradient

This pressure initialization scheme (it is also a boundary condition since the model is solved to a steady state solution) often provides a very realistic simulation of the actual pressure field about a tropical cyclone. However, in some storms the actual pressure field departs from this simple picture in several possible ways. Often, particularly as a tropical cyclone enters the mid-latitudes, the ambient pressure field is inhomogeneous. The effect is especially evident if the tropical cyclone begins to interact with a frontal system or an extratropical cyclone or both. Within the tropics, some storms have been shown (Holland 1980) to follow the more general form:

$$p(r) = p_0 + (p_\infty - p_0) e^{-\left(\frac{r}{r_c}\right)^B} \quad (3)$$

where

$B$  = constant in the general range 0.5-2.5

Finally, in some storms the radial pressure profile in the inner core is more irregular than either of the above forms, with a shape which implies two maxima in the radial pressure gradient, accompanied by two distinct maxima in the wind speed. Willoughby (1990) and Black and Willoughby (1992) have described the tendency for "concentric rings" in the radial wind distribution to be a fairly typical characteristic of intense tropical cyclones. The rings appear to be related intimately to storm intensity evolution. For example, Figure 1 shows the evolution of concentric rings in Hurricane Gilbert (1988) over a six-day period. In this storm, the CE model might be expected to provide reasonably accurate wind fields in the initial stage of vortex development and intensification between September 11-13, but it would fail to model the complicated double maxima structures later. The impact on ocean response modeling of this failure to model concentric rings is unknown.

## Numerics

The CE model is computationally demanding. For example, computational considerations drove the decision to presolve the boundary layer model for spatially homogeneous (constant) boundary layer height and stability and to use a table look-up procedure for the drag coefficient during the marching of the solution toward steady state. To relax the constraint of constant boundary layer height and stability would greatly increase computer time, unless a more efficient integration scheme could be found. The minimum grid spacing on the inner nest of the solution grid (as opposed to the target grid) is 5 km, which is a bit too large to resolve details of the wind field near the center in very tight storms. (For example, as Hurricane Andrew approached the south Florida coast, the radius of maximum wind was only about 11 km.) The grid spacing is also not sufficient to resolve boundary layer adjustments near roughness discontinuities, though that physical process is not presently incorporated in the numerical model. Further, the grid spacing is too coarse to resolve detailed gradients of wind over inland bays and estuaries. Limitations in temporal resolution are less serious, within the constraint of the steady-state model, since the "time step" of the windfields is simply the temporal resolution of the storm track. That temporal resolution can be refined within reason (say to intervals of 15 minutes or so) without significant computational cost.

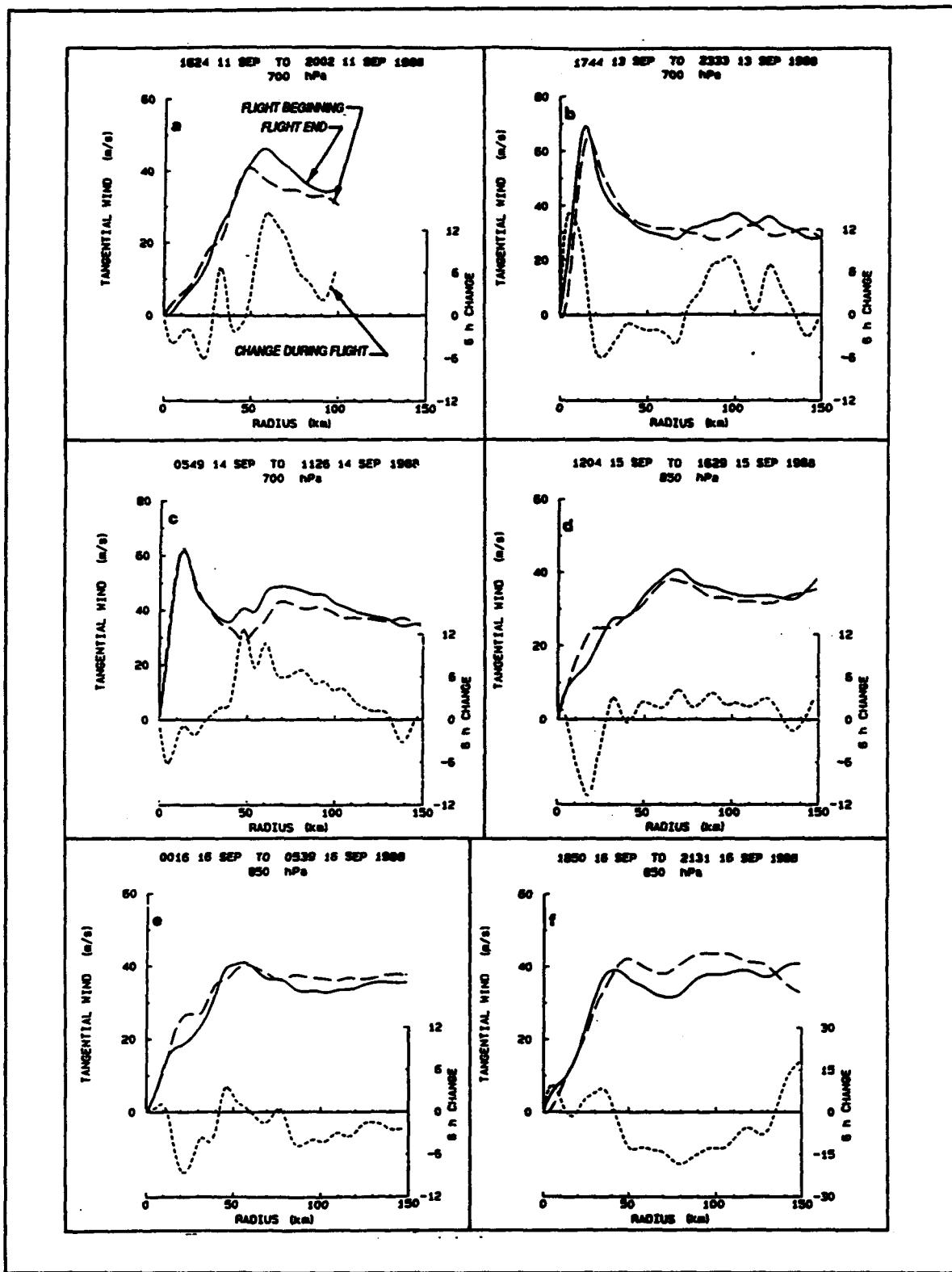


Figure 1. Temporal changes in the azimuthally averaged wind for NOAA reconnaissance flights into Hurricane Gilbert; changes are normalized to a 6-hr time interval (from Black and Willoughby (1992))

## **Summary of Limitations**

The main model limitations described in each category above may be listed as follows:

*a. Physics.*

- (1) Decoupling of boundary layer from full vortex dynamics, precluding mutual adjustment of pressure and wind fields; and feedback of convective scale effects on wind field.
- (2) Simplified PBL theory (e.g. constant Ekman scale height).
- (3) Extrapolation of Charnock roughness to extreme wind speeds, with no sea state dependence.
- (4) No boundary layer adjustment across roughness discontinuity.

*b. Initialization.*

- (1) Constant and homogeneous boundary layer height.
- (2) Constant and homogeneous stratification.
- (3) Relatively simple pressure specification:
  - (a) Exponential pressure profile provides only one radius of maximum wind (no concentric rings).
  - (b) Pressure profile may be inadequate even for unimodal maximum gradient pressure distributions.
  - (c) Homogeneous ambient linear pressure gradient.

*c. Numerics.*

- (1) Practical limit of spatial resolution to 5 km may be inadequate for very tight storms.
- (2) Large number of iterations (800) required for each steady state configuration, or snapshot (using the terminology of Cardone et al. 1992).

In this study, two of the above limitations are addressed and remedied, as described in the next section.

# 3 Upgraded Model

---

## Increased Resolution

The CE program consists basically of two main programs (Cardone et al. 1992). The first, SNAP, solves the numerical vortex model on a nested grid a number of times to represent the storm wind field at discrete times within an event, thereby producing a number of *snapshot* wind fields on a nested grid. SNAP also writes the snapshots to a file for use by the second main program HIST, which among other functions, interpolates the nested grid solutions to hourly intervals and then interpolates the winds to an output or *target* grid (typically that of an ocean response model).

The nested grid consists of five square 21 by 21 grid point arrays. The grid spacing increases by a factor of two from nest to nest. In the program input, the user specifies a desired spacing of the inner nest (the variable DX in name-list NAME3 of SNAP). For the default value of 5 km, the grid spacing in the coarsest nest becomes 80 km and the entire grid covers an area of (1,600 km<sup>2</sup>). While the existing CE program allows users to set DX smaller than 5 km, this is not recommended since the grid coverage shrinks commensurately. The simplified boundary condition applied on the outer boundary of the outermost nest becomes increasingly tenuous as the gridded domain shrinks.

The upgraded program allows the use of up to seven nests. However, the user may specify the number of nests (from three to seven) in a given run. The new parameter INSIDE is used to specify the number of active nests. It designates which is the finest active nest, where nests are numbered from 1 to 7 going from finest to coarsest. For example, INSIDE = 1 activates all seven nests, and INSIDE = 2 activates only nests 2 through 7. The grid spacing of nest 1, the innermost nest, is specified as before with variable DX, regardless of whether or not the nest is active. The relationships between INSIDE, active nests, and spacing of the finest active nest are summarized in Table 1. The default value of DX is 2 km. If all seven nests are exercised, the execution time per snapshot is roughly four times as long as the existing CE model. For this case the number of iterations on the inner nest is set to the default value of 3200.

**Table 1**  
**Effect of Nest Activation Parameter, INSIDE**

INSIDE	Active Nests	Spacing of Finest Active Nest
1	1 - 7	DX
2	2 - 7	2 DX
3	3 - 7	4 DX
4	4 - 7	8 DX
5	5 - 7	16 DX

The program with the new nesting was tested in two ways using the Hurricane Camille snapshots as test cases. First, vortex model winds were produced by the CE model (and its OWI equivalent) for the case of  $DX = 8 \text{ km}$ . Then, the same SNAP inputs were used to generate winds with the new code for the case  $DX = 2 \text{ km}$ ,  $\text{INSIDE} = 3$ , which provides the equivalent number of nests and inner nest grid spacing as the CE model run. Winds produced by the two alternative programs were interpolated to a target grid covering the Gulf of Mexico (nominal spacing of  $0.2 \text{ deg}^1$ ), compared and found to agree to within roundoff error of the VAX computer used for these tests.

The second test compared winds for Camille produced by the new code for the case  $DX = 2 \text{ km}$  and  $\text{INSIDE} = 1$ ; that is, all seven nests are live with inner nest grid spacing of  $2 \text{ km}$ , with winds produced by the CE program with  $DX = 5 \text{ km}$ . These results are shown in Appendix A which gives, at 30-minute intervals, the maximum scalar wind speed, the location and the corresponding wind speeds and directions, and the same data for the maximum vector wind difference magnitude. The results (see also Figure 2) indicate that the largest differences (scalar differences of up to about  $7 \text{ m/s}$ ), occur inside the eyewall, where truncation errors on the 5-km solution are expected to be large for an intense tight vortex such as Camille. Maximum scalar wind speed differences in the area of the eyewall are generally less than  $1 \text{ m/sec}$ . However, maximum vector difference magnitudes of up to  $9 \text{ m/sec}$  were observed occasionally in the vicinity of the eyewall reflecting a tendency for the wind direction on the 2-km solution to be turned systematically in the direction of less inflow, by up to  $10 \text{ deg}$  from the 5-km solution. The 2-km solutions are no doubt the more accurate solutions.

---

<sup>1</sup> A table of factors for converting non-SI units of measurement to SI units is presented on page vi.

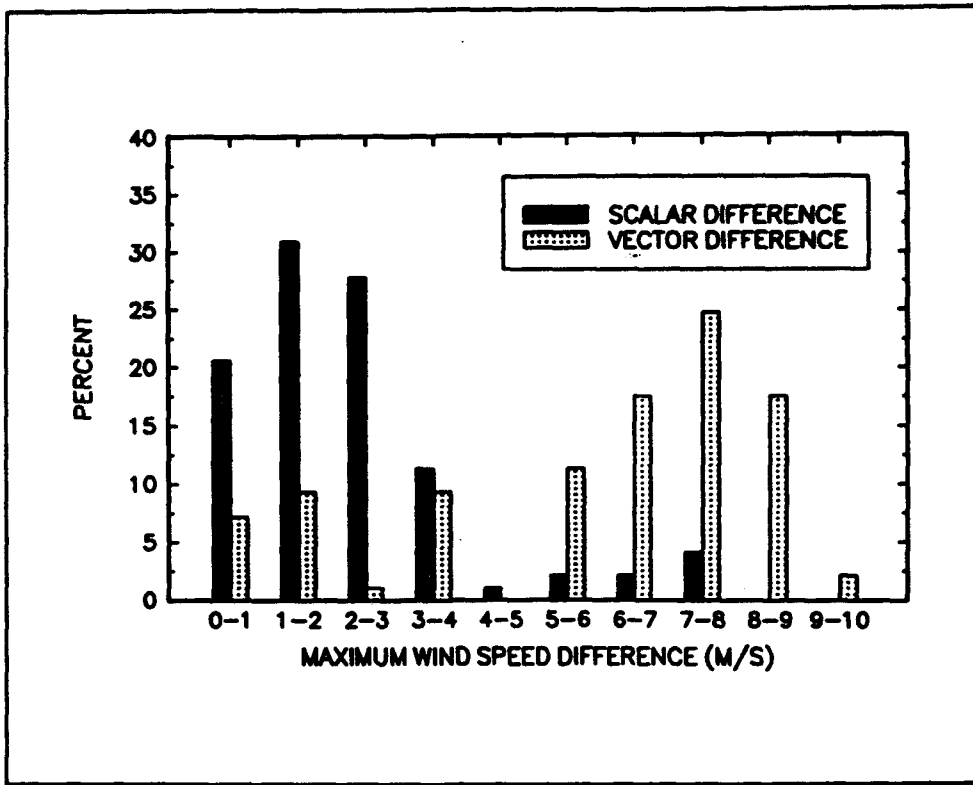


Figure 2. Distribution of maximum wind speed differences between 5-nest and 7-nest model runs for Hurricane Camille

## Generalized Pressure Specification

### Pressure profile form

The upgrade to the pressure specification uses a generalized form of Holland's (1980) exponential pressure profile

$$p(r) = p_o + \sum_{i=1}^n dp_i e^{\left(\frac{R_o}{r}\right)^{p_i}} \quad (4)$$

where

$n$  = number of components

$dp_i$  = pressure anomaly for the  $i$ 'th component ( $dp_1+dp_2+\dots+dp_n=p_o-p_e$ )

$R_{pi}$  = scaling radius for the  $i$ 'th component

$B_i$  = Holland's  $B$  coefficient for the  $i$ 'th component

The corresponding tangential and radial pressure gradients are:

$$\frac{\partial p}{\partial \theta} = 0 \quad (\text{tangential}) \quad (5)$$

$$\frac{\partial p}{\partial r} = \sum_{i=1}^n B_i \frac{dp_i}{dr} \left( \frac{R_{pi}}{r} \right)^n \left( \frac{1}{r} \right) e^{-\left(\frac{R_{pi}}{r}\right)^n} \quad (\text{radial})$$

The CE model was modified to provide options for a single or double exponential component ( $n = 1$  or  $n = 2$ ). This form allows the specification of pressure profiles with two separate maxima in the radial pressure gradient, though the mere form does not guarantee two maxima. For example, the sum of two exponentials also allows the modeling of pressure profiles which have only one maximum but with shapes very different from those predicted by the single exponential even with the variable  $B$  included.

Incorporation of this model into the seven-nest version of the program led to extensive changes to program SNAP, in particular to Subroutines GRAD and PXYM and further changes to namelist NAME3, as documented in Appendix B. One immediate consequence of this model is that the quadrantal specification of profile parameters allowed in the single exponential form with  $B = 1$  is lost. To retain this option in the CE model portfolio, two versions of the upgraded program were developed as follows:

**SNAP\_ADC.7NE and HIST\_ADC.7NE** - This version only upgrades the current CE program (which includes quadrantal variation of parameters for a single exponential with  $B = 1$ ) to incorporate the additional nests.

**SNAP\_HOL.7NE** - This version upgrades the current CE model to allow both 7 nests and the generalized pressure specification scheme, but without quadrantal variation. Note, however, that asymmetry in the pressure field is still modeled through superposition of the vortex pressure field and the background steering gradient. The background pressure gradient is required to be homogeneous (that is, the parameter ST12 is eliminated).

### Modified outflow

In early tests of the upgraded CE program with hypothetical snapshot inputs estimated roughly to apply to several stages of Hurricane Gilbert (inputs for

Gilbert snapshots were derived more rigorously as described below), it was demonstrated that the program could produce the pattern of annular concentric wind maxima. However, it was noticed that the inflow characteristics of the model appeared to have changed somewhat from the unimodal mode!. In the standard CE model, Subroutine OUTFLOW serves to remove 8 degrees of inflow from the snapshot solution throughout the domain to compensate approximately for inflow believed to be spuriously introduced through the numerical solution. This spurious inflow is revealed by solving the model for a motionless vortex with all friction terms deactivated and comparing the modeled wind direction to the purely circular flow expected of a vortex in gradient balance.

The frictionless, motionless vortex test was repeated with the upgraded model for the series of nine snapshots indicated in Table 2. For the unimodal case (Case 1) and the bimodal cases with  $B = 1$  for both exponentials (cases 2 and 6), the maximum inflow (which tends to occur just outside the wind maxima) averages 7.5 deg. As the value of  $B$  increases, however, there is a proportional increase in the inflow. In the bimodal profile with  $B$  varying between the two exponentials, the inflow varies with radius. Subroutine OUTFLOW was modified to compensate for dependence of spurious inflow on  $B$  (Table 3).

**Table 2**  
**Maximum Inflow Observed in Frictionless Stationary Vortex Solution<sup>1</sup>**

Case	$p_0$ , mb	$R_{in}$ , mm	$R_{ex}$ , mm	$\Delta p_0$ , mb	$\Delta p_0$ , mb	$B_1$	$B_2$	(Max inflow) <sub>1</sub> , deg	(Max inflow) <sub>2</sub> , deg
1	970	27	0	40	0	1.00	0.00	7.2	—
2	915	8	58	68	27	1.00	1.00	7.3	7.3
3	915	8	58	68	27	1.00	2.00	6.6	13.1
4	915	8	58	68	27	2.52	1.00	18.7	6.6
5	915	8	58	68	27	2.52	2.00	28.8	16.5
6	890	6	42	53	67	1.00	1.00	8.0	7.7
7	890	6	42	53	67	1.00	1.26	8.1	9.1
8	890	6	42	53	67	2.52	1.00	12.7	7.5
9	890	6	42	53	67	2.52	1.26	15.1	9.0

<sup>1</sup> All runs were done with the upgraded CE model with 7 nests and generalized pressure specification;  $p_0 = 1010$  mb for all runs

**Table 3**  
**Empirical Correction of Inflow Angle**

Exponential	Reduction Applied To Inflow Angle deg
Unimodal $B = 1$	8
Unimodal $B \neq 1$	8.8
Bimodal	$8 \left( \frac{B_1 + B_2}{2} \right)$

### Specification of pressure parameters

**Single Exponential Profile:**  $B = 1$ . In the standard CE model, the pressure profile may be specified in basically two ways. The most fundamental way is to fit the profile to sea level pressure measurements available at different radii at a given time, or transformed from time to space using single station data acquired at a station in the path of the storm. There are several examples of this approach as applied to historical U.S. Gulf of Mexico and East Coast hurricanes in Graham and Hudson (1960). The eye pressure may be prescribed, if it is known, for a more accurate fit, or the eye pressure may be extrapolated from a fit determined exclusively from data outside the center. A simplification to this procedure is often followed for oceanic storms, for which eye pressure may be known from aircraft dropsonde data, far field pressure is estimated from weather maps, and a few estimates of pressure at various radii about the storm are known from ship or island station synoptic reports. Then, the unknown parameter scale radius may be estimated from Equation 1 as follows for each such report and an average or weighted average of the estimates taken to represent the storm profile at map time:

$$R_p = -r \ln \left( \frac{p(r) - p_o}{p_m - p_o} \right) \quad (6)$$

If there are insufficient pressure data but eye pressure is known and an estimate of the radius of maximum wind,  $R_m$ , is known (e.g. from aircraft vortex message reports filed upon penetration of the eye and assuming that  $R_m$  at flight level is the same as  $R_m$  at the surface, or more crudely from radar or satellite eye diameter estimates),  $R_p$  may be estimated directly from  $R_m$  using the average relationship found between these two variables by the vortex model.

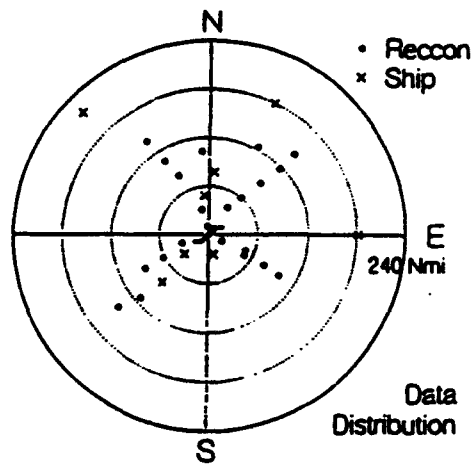
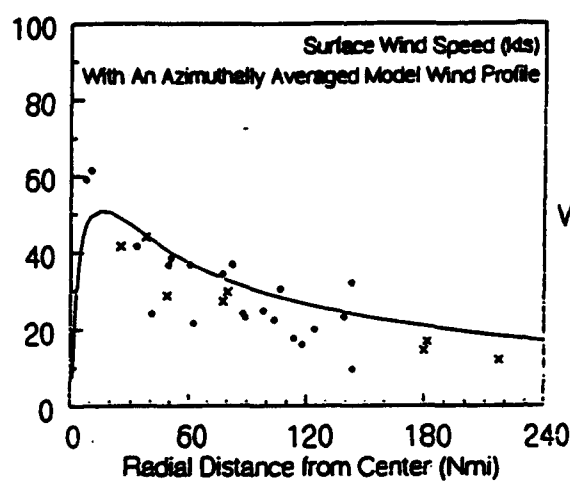
**Single Exponential Profile: Variable  $B$ .** Variants of these same two approaches may be followed to estimate the parameters of the generalized unimodal model, for which the additional parameter  $B$  must also be specified. Again, if there are sufficient pressure data, the profile may be fitted directly. For example, Figure 3 shows the screen display of a PC-based interactive system developed at OWI using a commercially available plotting/statistical analysis software package. The pressure data are composited (see window in upper right hand corner of screen) as a function of radius in a South China Sea typhoon from reduced (from flight level) aircraft pressures and pressures reported by ships within a 3-hr time window of analysis time. The aircraft also provided estimates of eye pressure (note the two conflicting estimates at the origin in the lower window of Figure 3). Far field pressure was estimated from weather maps. The best fit shown is for  $p_e = 968$  mb,  $B = 0.8$ , and  $R_s = (14 \text{ nm})^{0.8}$ . The window at the upper left of the screen compares the azimuthally averaged solution for the model surface wind (downloaded from a run made on a VAX) and reduced aircraft and ship reports of wind.

The second approach is more indirect and emphasizes the use of aircraft wind data. In recent years such data have become quite accurate after the introduction of inertial navigation systems, onboard processing and the availability of coded messages (so-called supplementary or peripheral flight level winds) containing measured winds at flight level outside the eye. Figure 1 shows the complete analysis carried out by Black and Willoughby (1992) of flight data acquired over the main lifetime of Hurricane Gilbert in the Caribbean Sea and Gulf of Mexico. These curves show 12 separate radial profiles of the azimuthally averaged flight level (700 mb or 850 mb) tangential wind speed composited from flight legs near the indicated times. Most of the wind profiles exhibit two distinct wind maxima. On the assumption that the azimuthally averaged flow is approximately in gradient balance with the axisymmetric pressure field, the pressure profile associated with double concentric wind maxima should also exhibit two local maxima in the pressure gradient. Therefore they might be fitted by a double exponential profile. Even those profiles which do not exhibit two distinct peaks, such as those in panels *b*, *d*, and *e*, exhibit atypical shapes for tropical cyclones, with a single maximum and broad regions with little or no change of wind speed with radius. Nevertheless, we have selected five of these cases to illustrate the fitting of the single exponential profile using aircraft wind data and eye pressure. Parameters are defined in Table 4 and results from the fitting process are given in Table 5.

The fitting method is basically a systematic search of many possible solutions of the single exponential for that solution whose radial distribution of implied gradient wind provides a close match to the location and magnitude of the azimuthal average flight level wind. This searching program (implemented in a preprocessing program called 1EYEWALL.nJL) requires the input information listed in Table 5. Additional documentation is given in Appendix B. The searching program fixes the profile anomaly parameter ( $p_e - p_o$ ), loops through possible values of the scale radius  $R_s$  (from  $R_m$  to  $2R_m$ ) and  $B$  (from 0.5 to 2.52) and finds the pressure profile whose gradient wind simultaneously

**Oceanweather Tropical System Analysis**  
 Surface Winds and Pressures Estimated from  
 Recon, Vortex and Periperal Data Messages

**Typhoon WAYNE86**  
 86090212 +/- 3hrs



Created on Aug 16, 1993 3:52:20 pm

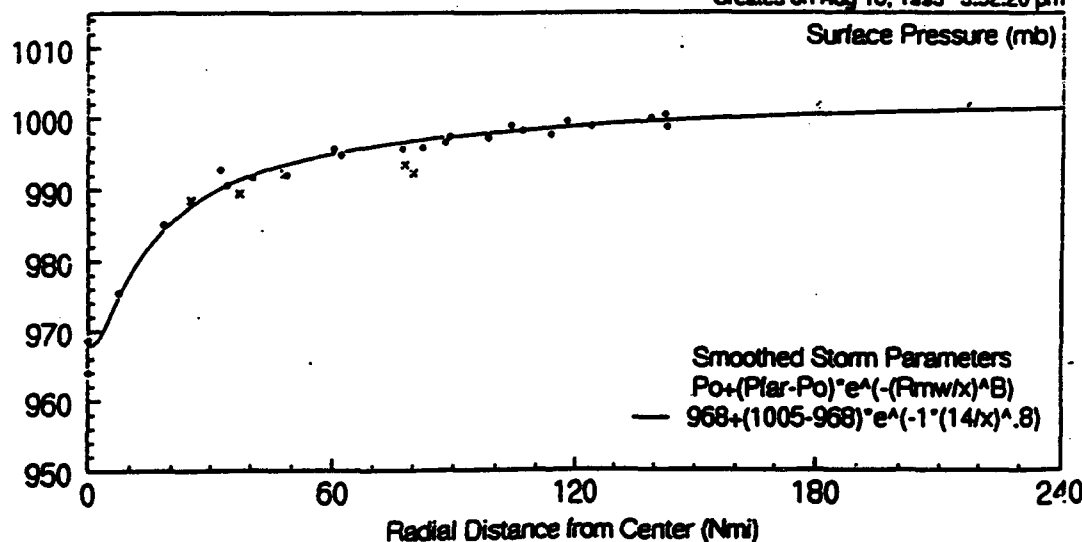


**Figure 3.** Example of Oceanweather tropical storm analysis

**Table 4**  
**Parameter Definitions for Fitting Single Exponential Profile**

Parameter	Definition
$R_m$	Observed radius of maximum wind
$V_m$	Azimuthally averaged tangential flight level wind at $R_m$
$V_{m150}$	Azimuthally averaged tangential flight level wind at 150 km from center
$r_p$	Scale radius of single exponential profile
$dp$	Storm pressure anomaly parameter of single exponential profile
$B$	Holland's $B$
$R_{pm}$	Radius of maximum gradient of fitted pressure profile
$V_{pm}$	Maximum gradient wind of fitted pressure profile
$V_{p150}$	Gradient wind of fitted profile 150 km from center

**Table 5**  
**Generalized Single Exponential Profile Fits to Selected Hurricane Gilbert Cases**

Case	Input						Output					
	$P_o$ mb	$P_{\infty}$ mb	$R_m$ km	$V_m$ m/s	$V_{m150}$ m/s	$r_p$ km	$dp$ mb	$B$	$V_{pm}$ m/s	$R_{pm}$ km	$V_{p150}$ m/s	
3	905	1012	16	65	30	20	107	1.50	67.2	20	21	
4	888	1012	13	69	30	16	124	1.41	70.3	16	20	
7	951	1012	65	38	36	97	61	1.00	39.3	87	36	
8	950	1012	69	41	38	92	62	1.12	42.2	85	38	
9	949	1010	57	40	37	85	61	1.12	41.9	79	37	

best matches the observed wind speeds at  $R_m$  and at 150 km in terms of absolute difference. For example, in Case 3 of Table 5 the selected profile gradient wind (not shown) is within 1 m/s of the  $V_m$  of 65 m/s at  $R_m$ . However the searching program places the absolute profile maximum of 67.2 m/s at a radius of 20 km, and fails to maintain the observed broad region of little change in wind speed between 50 and 150 km, resulting in a profile wind speed of only 21 m/s at 150 km, about 10 m/s lower than measured. Cases 7, 8 and 9 are somewhat more successful. The parameter  $B$  varies between 1.0 and 1.5 for these fits, or in the same general range reported by Holland for a single exponential.

**Double Exponential Profile.** While it is conceivable that there may be sufficiently voluminous and accurate pressure data in some tropical cyclones to

attempt to directly fit a double exponential profile to measurements of surface pressure as a function of radius, we have not attempted to construct such a data set and perform such a fit. We did try, without success, to develop useful fits to the profile from just the total storm anomaly, estimates of the two radii of maximum wind and a single pressure along the profile in the region between the two maxima. However, a generalization of the searching algorithm described above for a single exponential has met with some success.

The searching algorithm (called 2EYEWALL.HOL) as applied to a double exponential is documented in Appendix B. Parameters involved are defined in Table 6 and Figure 4. The searching program fixes the total storm anomaly, assumes the scale radius for the inner exponential is equal to the observed radius of maximum wind of the inner maximum, or ring, and loops through ranges of the outer scale radius,  $R_{p2}$  (from  $R_{m2}$  to  $2R_{m2}$ ), inner and outer  $B$  (from 0.5 to 2.52) and the ratio of  $dp_1/dp_2$  (from 1/8 to 8). The algorithm seeks the combination whose pressure profile provides a gradient wind profile that has maxima at  $R_{m1}$  and  $R_{m2}$  within  $\pm 1$  m/s of observed and which maximizes the following:

$$V_{g1} + V_{g2} - 2 V_{gm} \quad (7)$$

where

$$V_{gm} = \text{gradient wind at } (R_{m1} + R_{m2})/2$$

If it succeeds in finding such a profile it checks that the wind at 150 km is lower than the outer maximum,  $V_{m2}$ , and if it is, prints the solution. If these conditions are not met, another cycle is attempted. The matching criterion is relaxed to  $\pm 2$  m/s, this time requiring that the wind at  $(R_{m1} + R_{m2})/2$  is less than the winds prescribed at  $R_{m1}$  and  $R_{m2}$ , and minimizing the wind at 150 km. The program also prints the profile parameters for the selected profile. If, after the second cycle the program still does not find a successful fit, it prints the closest fit found in each cycle.

Table 7 shows the results of the application of this searching algorithm to all 12 of the azimuthal average tangential flight level wind profiles in Hurricane Gilbert derived by Black and Willoughby (1992). The double exponential appears to require large values of  $B$  to resolve two distinct peaks in the radial profile of gradient wind, at least for most of these cases. Table 8 compares the location and magnitude of the double wind maxima derived from the fitted profile to those observed. Figure 5 compares the fitted and observed radial profiles of pseudo-gradient wind. The inner ring is usually fitted very closely. In 11 out of 12 of the cases a distinct outer wind maximum is resolved, and it is usually placed within  $\pm 20$  km of the observed maximum. In 9 out of those 11 cases, the maximum is within about  $\pm 2$  m/s of that observed. Case 8 is the poorest fit, but in practice Case 7 and Case 8 are so close in time

**Table 6**  
**Parameter Definitions for Fitting Double Exponential Profile**

Parameter	Definition
$R_{m1}$	Radius of maximum wind, inner ring
$R_{m2}$	Radius of maximum wind, outer ring
$V_{m1}$	Azimuthally averaged tangential flight level wind, inner ring
$V_{m2}$	Azimuthally averaged tangential flight level wind, outer ring
$R_{p1}$	Scale radius, inner exponential
$R_{p2}$	Scale radius, outer exponential
$dp_1$	Pressure anomaly, inner exponential
$dp_2$	Pressure anomaly, outer exponential
$B_1$	Holland's $B$ , inner exponential
$B_2$	Holland's $B$ , outer exponential
$R_g1$	Radius of maximum gradient wind of fitted profile, inner ring
$R_g2$	Radius of maximum gradient wind of fitted profile, outer ring
$V_{g1}$	Maximum gradient wind of fitted profile, inner ring
$V_{g2}$	Maximum gradient wind of fitted profile, outer ring

(in fact they are derived from the same flight) that Case 7 may be used to represent this phase of the storm history.

## Sample Runs

The upgraded program, including seven nests and the generalized pressure specification, has been applied to provide sample wind fields on target grids using as test input the snapshots developed for Hurricane Gilbert. Two runs were made. The first generates a snapshot wind field for each of the 12 Gilbert cases (including realistic forward motion and steering flow parameters) and interpolates each snapshot to a polar grid using a test history table. Interpolations are also made from pairs of adjacent snapshots (equal time weight). Winds for the 23 wind fields so produced on the polar grid are then azimuthally averaged. These results are given in Appendix C.

A second test run was made which modeled Gilbert during its passage across the Gulf of Mexico between 1200 UT 15 September through 0000 UT 17 September, 1988. Snapshots for this run consisted of Cases 7, 9, 11, and 12. The target grid for this run was a grid of nominal 12 nm spacing covering the Gulf of Mexico. The wind fields were output at 12-hourly intervals. Additional details and surface wind field plots are given in Appendix D.

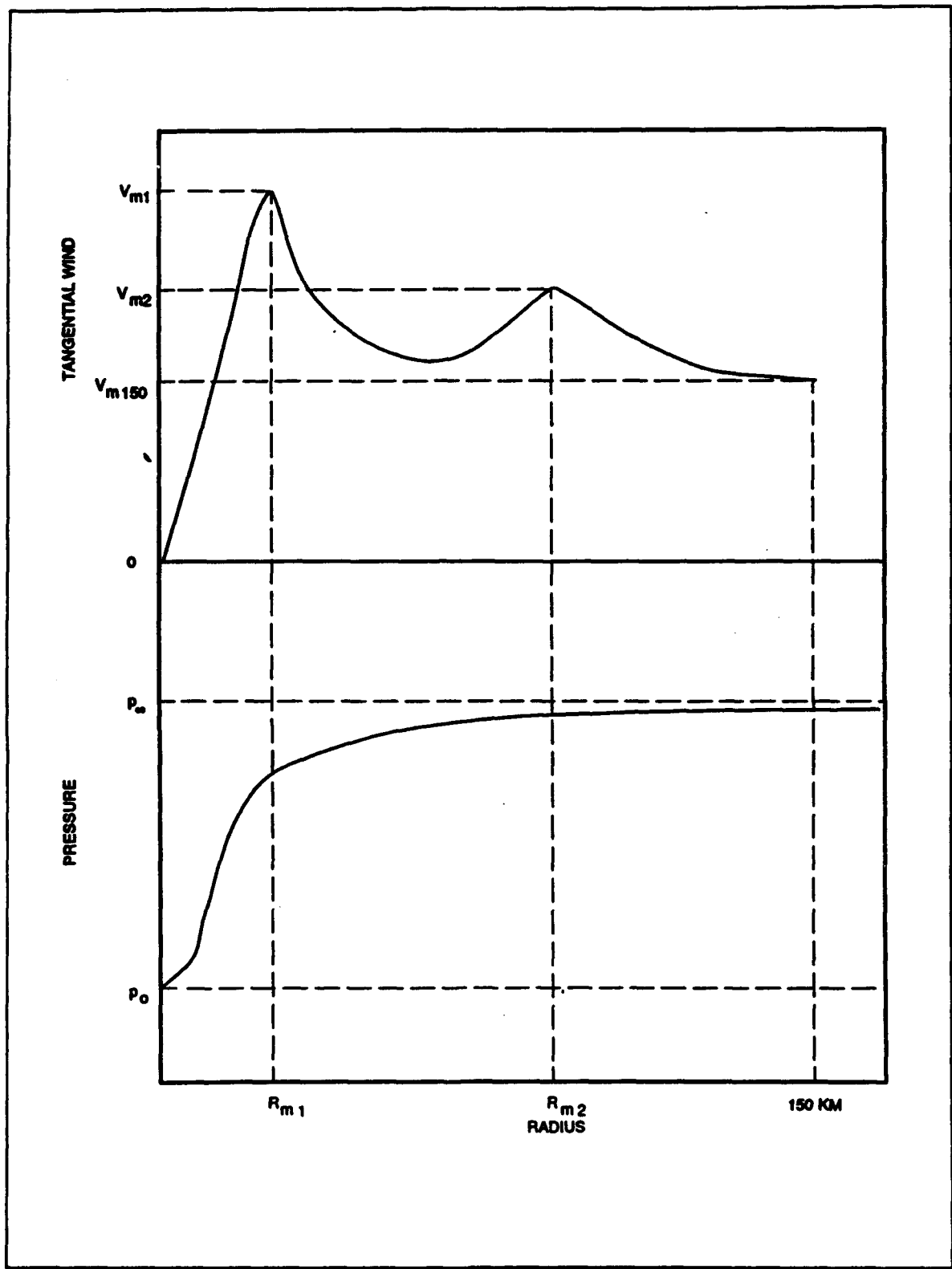


Figure 4. Some parameters in double exponential profile

**Table 7**
**Observed Pressure and Azimuthally Averaged Pseudo-Gradient Wind Maxima  
In Hurricane Gilbert<sup>1</sup> and Estimated Generalized Profile Parameters**

Case	Date/ Time (UTC)	Input							Output					
		$p_o$ mb	$p_e$ mb	$R_{m1}$ km	$R_{m2}$ km	$V_{m1}$ m/s	$V_{m2}$ m/s	$R_{p1}$ km	$R_{pe}$ km	$dp_1$ mb	$dp_2$ mb	$B_1$	$B_2$	
1	11/1624	972	1011	47	90	40	35	47	127	23	16	2.52	2.52	
2	11/2002	968	1011	58	108	47	36	58	162	32	11	2.52	2.52	
3	13/1744	905	1012	16	111	65	32	16	125	94	13	1.68	2.39	
4	13/2333	888	1012	13	100	69	38	13	100	110	14	1.59	2.52	
5	14/0549	893	1012	13	70	62	44	13	70	101	18	1.41	2.52	
6	14/1126	890	1012	13	69	62	48	13	69	102	20	1.41	2.52	
7	15/1204	951	1012	22	65	25	38	22	87	45	16	0.56	2.52	
8	15/1629	950	1012	32	69	28	41	32	103	35	27	0.94	2.51	
9	16/0016	949	1010	22	57	27	40	22	81	41	20	0.75	2.52	
10	16/0539	950	1011	55	120	41	37	55	170	52	9	1.12	2.24	
11	16/1850	953	1010	50	100	42	43	50	119	47	10	1.33	2.52	
12	16/2131	954	1009	40	100	39	40	40	112	45	10	1.19	2.52	

<sup>1</sup> Cases correspond to Black and Willoughby's (1992) analysis of aircraft data in Hurricane Gilbert

**Table 8**  
**Comparison of Measured Flight-Level Wind Maxima and Fitted  
 Gradient Wind Maxima for Double Exponential Pressure Profile<sup>1</sup>**

Case	Inner Ring				Outer Ring				
	Measured		Fitted		Measured		Fitted		
	$R_{m1}$ km	$V_{m1}$ m/s	$R_{g1}$ km	$V_{g1}$ m/s	$R_{m2}$ km	$V_{m2}$ m/s	$R_{g2}$ km	$V_{g2}$ m/s	$V_g$ at $R_{m2}$ m/s
1	47	40	47	39.6	90	35	110	37.1	35.7
2	58	47	58	46.6	108	36	108 <sup>2</sup>	35.7 <sup>2</sup>	—
3	16	65	16	66.7	111	32	105	33.7	33.6
4	13	69	13	70.3	100	38	85	37.2	36.3
5	13	62	13	63.5	70	44	59	46.2	45.4
6	13	62	13	63.7	69	48	59	48.4	47.3
7	22	25	22	26.3	65	38	82	39.2	36.1
8	32	28	30	29.7	69	41	98	48.1	39.2
9	22	27	21	28.9	57	40	78	43.4	38.1
10	55	41	55	39.2	120	37	120	37.1	—
11	50	42	50	40.7	100	43	93	41.5	41.3
12	40	39	40	32.9	100	40	92	38.4	38.2

<sup>1</sup> Cases correspond to Black and Willoughby's (1992) analysis of Hurricane Gilbert

<sup>2</sup> Second ring maximum not resolved, profile gradually decays from inner maximum

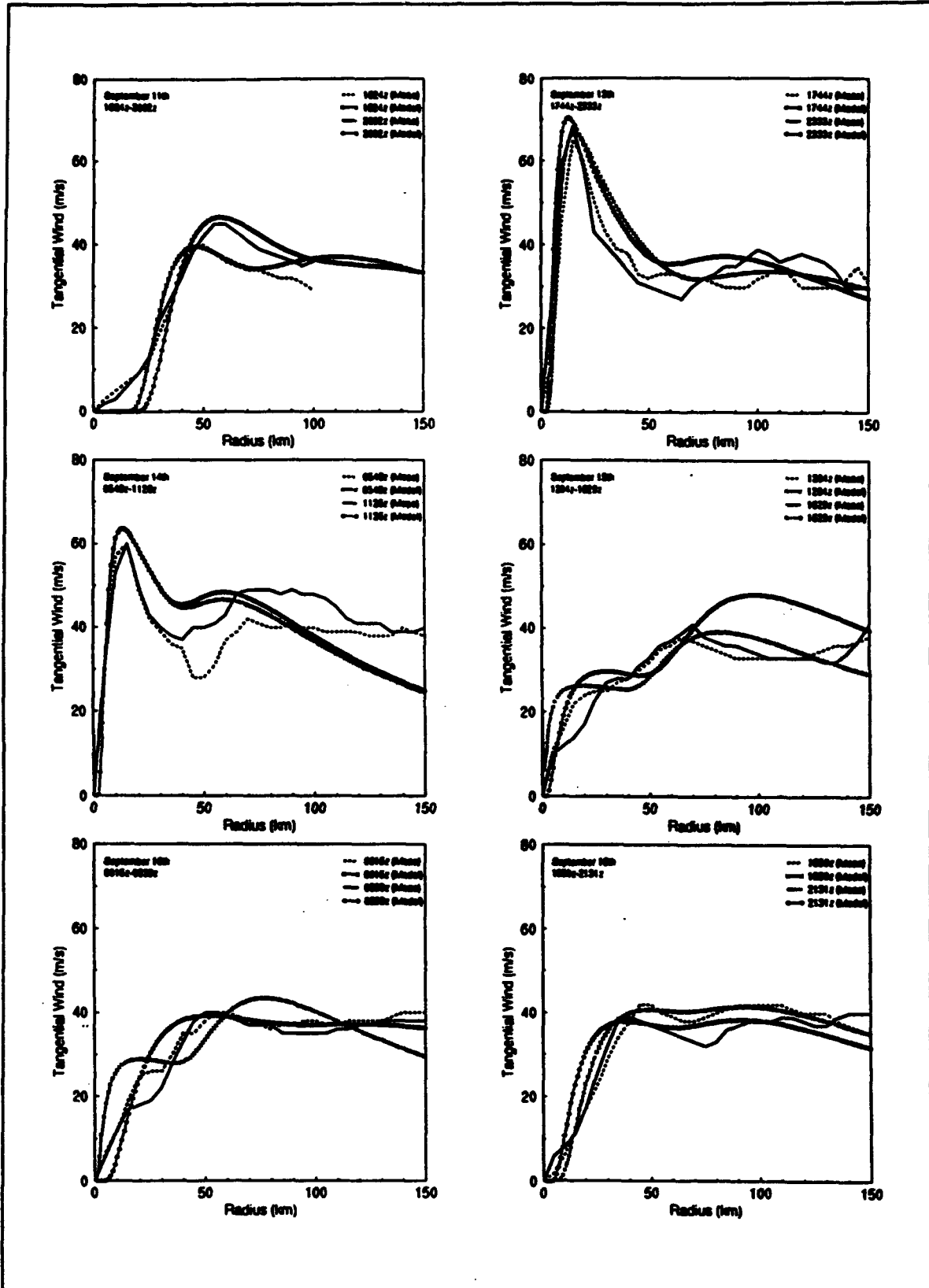


**Figure 5.** Comparison of azimuthally averaged reconnaissance winds and fitted gradient winds in 12 cases of Hurricane Gilbert defined by Black and Willoughby (1992)

## 4 Summary

---

The CE tropical cyclone surface wind field model has been a very useful tool in ocean response modeling for more than a decade. The model continues to be used regularly. The CE recently held a workshop to reassess model assumptions, particularly in light of modern advances in computing technology and field measurement of hurricane structure. Model limitations were identified and evaluated in terms of their perceived importance to ocean response modeling and the level of effort required to develop improved solutions. The limitations are summarized in this report.

Two aspects of the CE model were targeted for improvement. This report describes the improvements developed for the upgraded model. First, the standard CE model represents a compromise between spatial resolution in the central region of very high gradients, coverage of the full ocean area affected by the tropical cyclone, and computer requirements. Computing resources are much more available now than at the time the model was developed in the late 1970's. The model was upgraded to include more computationally intensive options which give improved resolution and areal coverage. Up to seven nested grids are now available, compared to only five nests in the standard model. In a typical application, this upgrade can be used to achieve 2-km resolution around the eye (as compared to 5-km resolution often used in the standard model) and an expanded total coverage area.

The second upgrade to the standard CE model allows a more general specification of the axisymmetric pressure profile. This upgrade can be used to create wind fields with maxima at two different radii or with a broad maximum extending over a range of radii. It also provides more flexibility in fitting the shape of single peaked wind profiles.

The upgraded model is demonstrated with historical hurricanes. The five-nest and seven-nest models are applied to Hurricane Camille. The fully upgraded model, with seven nests and general pressure specification, is applied to Hurricane Gilbert. This hurricane was chosen because it is well-documented by Black and Willoughby (1992) and it evolved into some non-traditional storm structures. The upgraded model was more effective than the standard CE model in simulating the storm.

## References

---

- Abel, C. E., Tracy, B. A., Vincent, C. L., and Jensen, R. E. (1989). "Hurricane hindcast methodology and wave statistics for Atlantic and Gulf hurricanes from 1956-1975," WIS Report 19, U.S. Army Engineer Waterways Experiment Station, Vicksburg, MS.
- Black, M. L., and Willoughby, H. E. (1992). "The concentric eyewall cycle of Hurricane Gilbert," *Mon. Weather Rev.*, American Meteorological Society, 120, 947-957.
- Cardone, V. J., and Thompson, E. F. (1992). "Numerical modeling of tropical cyclone boundary layer winds: status, limitations and priorities," unpublished report prepared for U.S. Army Engineer Waterways Experiment Station, Vicksburg, MS.
- Cardone, V. J., Graber, H. C., Jensen, R. E., Hasselmann, S., and Caruso, M. J. (1994). "In search of the true surface wind field in SWADE IOP-1: ocean wave modelling perspective," to be submitted to *Atmosphere-Ocean System Journal*.
- Cardone, V. J., Greenwood, C. V., and Greenwood, J. A. (1992). "Unified program for the specification of hurricane boundary layer winds over surfaces of specified roughness," Contract Report CERC-92-1, U.S. Army Engineer Waterways Experiment Station, Vicksburg, MS.
- Chow, S. H. (1971). "A study of the wind field in the planetary boundary layer of a moving tropical cyclone," M. S. thesis in Meteorology, School of Engineering and Science, New York University, New York, N.Y.
- Cooper, C., and Thompson, J. D. (1989). "Hurricane-generated currents on the outer continental shelf, 1, model formulation and verification," *J. Geophys. Res.* 94(C9), 12513-12540.
- Forristall, G. Z. (1980). "A two-layer model for hurricane driven currents on an irregular grid," *J. Phys. Oceanogr.* 10(9), 1417-1438.

- Graham, H. E., and Hudson, G. N. (1960). "Surface winds near the center of hurricanes and other cyclones," National Hurricane Research Project Report No. 39, Wash., DC.
- Grosskopf, W. D., Griffon, D. L., Berek, E. P., and Sharma, J. N. (1991). "Gulf of Mexico wind, wave, and current database," *Proc., Offshore Tech. Conf.* OTC 6539, Houston, TX, 1, 357-364.
- Holland, G. J. (1980). "An analytic model of the wind and pressure profiles in hurricanes," *Mon. Weather Rev.* 108, 1212-1218.
- Ly, L. N., and O'Connor, W. P. (1991). "Gulf coast hurricane surge simulations using a numerical ocean circulation model," *Proc., MTS '91 Conf.*, Marine Technology Society, New Orleans, LA.
- Mairs, H. L., Koch, S. P., Gordon, R. B., and Cuellar, R., Jr. (1992). "The storm current response of Gulf of Mexico hurricanes," *Proc., Offshore Tech. Conf.* OTC 6833, Houston, TX, 235-242.
- Mark, D. J., and Scheffner, N. W. (1993). "Validation of a continental-scale storm surge model for the coast of Delaware," *Proc. Estuarine and Coastal Modeling Conference*, ASCE, Chicago, IL, 249-263.
- Reece, A. M., and Cardone, V. J. (1982). "Test of wave hindcast model results against measurements during four different meteorological systems," *Proc., Offshore Tech. Conf.* OTC 4323, Houston, TX, 269-293.
- Shapiro, L. J. (1983). "The asymmetric boundary layer flow under a translating hurricane," *J. Atmospheric Sci.* 39(Feb.).
- Thompson, E. F. (1993). "HURWIN: Tropical Storm Planetary Boundary Layer Wind Model," *Coastal Modeling System (CMS) User's Manual*, Instruction Report CERC-91-1, Supplement 2, M. A. Cialone, ed., U.S. Army Engineer Waterways Experiment Station, Vicksburg, MS.
- Tracy, B. A., and Hubertz, J. M. (1990). "Hindcast hurricane swell for the coast of southern California," WIS Report 21, U.S. Army Engineer Waterways Experiment Station, Vicksburg, MS.
- WAMDI Group. (1988). "The WAM model - a third generation ocean wave prediction model," *J. Phys. Oceanog.* 18, 1275-1810.
- Willoughby, H. E. (1990). "Temporal changes of the primary circulation in tropical cyclones," *J. Atmospheric Sci.* (47), 242-264.

# **Appendix A**

## **Comparison of Five-Nest and Seven-Nest Models for Hurricane Camille**

---

Comparison of modeled winds at 20-m height and at 30-min intervals in alternative hindcasts of Hurricane Camille in the Gulf of Mexico during August 1969. The run labelled "5-Nests" used the standard CE model with 5-km spacing on the inner nest. The run labelled "7-Nests" used the upgraded CE model with seven-nests and grid spacing of 2 km on the inner nest. The first (second) line at each time step gives: maximum scalar (vector magnitude) wind speed difference found on the grid between the two runs, latitude and longitude of the grid point, and wind speed and direction of the alternative solutions at that grid point.

Table A1

Comparison of Wind Estimates from 5-Nest and 7-Nest Models,  
Hurricane Camille

Day/ Hour	Max. Speed Diff. m/s	Grid Point Coord.		5-Nest Model		7-Nest Model	
		Lat. deg	Long. deg	Speed m/s	Dir. deg az	Speed m/s	Dir. deg az
161200	7.1	24.1	-85.7	27.9	151.7	20.8	162.6
	8.4	24.1	-85.7	27.9	151.7	20.8	162.6
161230	3.0	24.1	-86.0	39.7	338.6	36.7	342.5
	6.0	24.1	-85.7	42.0	172.2	43.1	180.1
161300	1.2	24.1	-85.7	41.6	181.0	42.8	183.7
	7.0	24.3	-86.0	52.6	47.1	52.9	54.6
161330	2.2	24.3	-86.0	43.6	78.8	41.4	88.0
	7.2	24.3	-86.0	43.6	78.8	41.4	88.0
161400	1.5	24.3	-86.0	38.1	131.1	36.7	140.6
	6.7	24.3	-86.2	51.0	2.0	50.1	9.5
161430	3.4	24.3	-86.2	40.7	359.4	37.3	5.4
	7.3	24.3	-86.0	43.5	150.1	45.2	159.3
161500	2.1	24.3	-86.2	21.2	312.9	23.2	306.1
	5.3	24.5	-86.2	53.0	52.8	54.0	58.3
161530	2.4	24.3	-86.2	31.2	240.3	33.6	242.5
	8.2	24.5	-86.2	49.6	80.5	49.2	90.0
161600	1.0	24.3	-86.4	46.5	312.6	45.5	316.1
	8.9	24.5	-86.2	47.6	106.6	46.9	117.4
161630	3.8	24.5	-86.4	39.5	16.6	35.7	22.6
	6.2	24.5	-86.2	46.3	138.6	47.9	145.9
161700	1.5	24.5	-86.4	9.8	339.9	8.4	342.7
	3.6	24.8	-86.4	53.0	57.2	54.1	60.8
161730	1.9	24.5	-86.4	23.2	226.5	25.1	232.6
	5.4	24.8	-86.4	52.2	74.4	52.9	80.2
161800	2.0	24.5	-86.4	36.8	209.7	38.8	212.5
	6.9	24.8	-86.4	49.9	103.1	51.0	110.8
161830	3.4	24.8	-86.7	43.7	27.9	40.3	36.3
	7.0	24.8	-86.7	43.7	27.9	40.3	36.3
161900	2.1	24.8	-86.7	14.7	2.9	12.7	359.3
	3.0	25.0	-86.7	53.2	53.0	54.2	55.9
161930	2.8	24.8	-86.7	25.2	226.3	28.0	231.6
	6.0	25.0	-86.7	52.0	76.3	52.6	82.9
162000	1.9	24.8	-86.7	36.1	217.8	38.0	219.8
	7.0	25.0	-86.7	48.9	102.0	49.9	111.1
162030	3.1	25.0	-86.9	44.4	20.2	41.3	28.9
	7.2	25.0	-86.9	44.4	20.2	41.3	28.9

(Sheet 1 of 6)

**Table A1 (Continued)**

Day/ Hour	Max. Speed Diff. m/s	Grid Point Coord.		5-Nest Model		7-Nest Model	
		Lat. deg	Long. deg	Speed m/s	Dir. deg az	Speed m/s	Dir. deg az
162100	1.2 3.2	25.0 25.0	-86.7 -86.7	44.1 44.1	159.6 159.6	45.3 45.3	163.4 163.4
162130	2.4 6.8	25.0 25.3	-86.9 -86.9	24.7 51.9	255.5 68.2	27.0 52.2	257.8 75.7
162200	1.7 9.3	25.2 25.2	-86.9 -86.9	47.8 47.8	95.4 95.4	46.2 46.2	106.5 106.5
162230	2.8 7.6	25.2 25.2	-87.1 -86.9	45.4 46.9	13.3 132.4	42.6 46.9	22.2 141.6
162300	1.6 3.7	25.2 25.2	-86.9 -86.9	43.4 43.4	163.1 163.1	44.9 44.9	167.5 167.5
162330	2.1 7.7	25.2 25.4	-87.1 -87.1	26.5 51.0	267.8 64.2	28.6 51.3	268.0 72.8
170000	1.8 8.2	25.4 25.4	-87.1 -87.1	44.0 44.0	94.1 94.1	42.2 42.2	104.8 104.8
170030	1.2 6.1	25.4 25.4	-87.4 -87.4	48.6 48.6	345.6 345.6	47.3 47.3	352.7 352.7
170100	2.2 7.2	25.4 25.6	-87.4 -87.4	41.8 51.9	313.1 29.6	39.6 51.8	318.0 37.5
170130	2.4 5.0	25.6 25.6	-87.4 -87.1	31.0 45.7	7.0 149.9	28.6 46.8	6.2 155.9
170200	0.9 7.8	22.6 25.8	-88.5 -87.4	8.4 51.4	265.9 54.0	7.4 51.4	271.6 62.7
170230	7.3 9.0	25.8 25.8	-87.4 -87.4	19.8 19.8	104.9 104.9	12.6 12.6	124.3 124.3
170300	3.5 6.7	25.8 26.0	-87.4 -87.4	28.9 51.2	221.5 81.4	32.3 52.0	226.8 88.8
170330	1.0 7.5	26.0 26.0	-87.6 -87.4	51.3 42.1	7.4 121.2	50.4 41.2	14.3 131.4
170400	2.8 5.5	26.0 26.0	-87.6 -87.4	38.2 41.5	333.4 175.3	35.4 42.9	336.4 182.5
170430	2.9 7.6	26.2 26.2	-87.6 -87.6	45.2 45.2	39.4 39.4	42.3 42.3	48.6 48.6
170500	1.3 3.7	26.2 26.4	-87.4 -87.6	44.2 53.4	161.7 53.5	45.5 54.4	164.7 57.3
170530	1.7 8.1	26.2 26.4	-87.6 -87.6	32.2 46.2	250.2 78.9	34.1 45.2	251.5 89.0

(Sheet 2 of 6)

**Table A1 (Continued)**

Day/ Hour	Max. Speed Diff. m/s	Grid Point Coord.		5-Nest Model		7-Nest Model	
		Lat. deg	Long. deg	Speed m/s	Dir. deg az	Speed m/s	Dir. deg az
170600	6.9	26.4	-87.6	22.5	163.9	15.7	177.4
	8.1	26.4	-87.6	22.5	163.9	15.7	177.4
170630	2.5	26.4	-87.6	37.7	192.9	40.2	190.6
	5.2	26.4	-87.6	37.7	192.9	40.2	190.6
170700	4.0	26.6	-87.8	42.8	29.2	38.8	36.7
	6.7	26.6	-87.8	42.8	29.2	38.8	36.7
170730	2.4	26.6	-87.8	6.5	353.2	4.1	20.6
	3.4	26.6	-87.8	6.5	353.2	4.1	20.6
170800	3.2	26.6	-87.8	30.1	229.2	33.2	234.5
	7.9	26.8	-87.8	51.4	81.1	51.1	89.9
170830	1.5	26.8	-88.0	49.3	7.7	47.8	16.1
	7.3	26.8	-87.8	41.8	129.6	40.9	139.7
170900	2.9	26.8	-88.0	35.2	344.8	32.3	345.8
	6.3	26.8	-87.8	43.9	163.9	45.6	171.6
170930	0.9	24.5	-80.1	8.8	290.2	8.0	206.4
	8.6	27.0	-88.0	49.4	53.7	48.5	63.7
171000	5.9	27.0	-88.0	19.5	102.7	13.6	113.0
	6.6	27.0	-88.0	19.5	102.7	13.6	113.0
171030	1.4	27.0	-88.3	45.3	342.6	43.9	349.2
	6.4	27.0	-88.0	32.6	186.0	33.3	187.1
171100	2.0	27.0	-88.3	39.4	312.5	37.3	315.8
	7.1	27.2	-88.3	51.2	31.4	50.1	39.4
171130	2.3	27.2	-88.3	26.3	24.5	24.0	20.5
	5.3	27.2	-88.0	48.7	145.2	49.6	151.4
171200	1.0	27.2	-88.0	45.1	168.0	46.1	170.2
	6.3	27.4	-88.3	52.9	64.7	53.4	70.4
171230	3.7	27.4	-88.3	39.6	96.0	35.9	102.8
	5.8	27.4	-88.3	39.6	96.0	35.9	102.8
171300	1.8	27.4	-88.5	44.1	346.3	42.4	352.7
	7.1	27.4	-88.3	35.3	180.2	33.6	191.7
171330	1.7	27.4	-88.5	40.1	313.1	38.4	316.2
	7.5	27.6	-88.3	50.7	111.3	51.0	119.7
171400	1.4	27.6	-88.5	28.0	12.5	26.6	8.4
	5.9	27.6	-88.3	48.2	149.0	49.5	155.8
171430	2.3	27.6	-88.5	30.2	280.3	32.6	279.7
	8.4	27.8	-88.5	48.7	58.4	47.3	68.2

(Sheet 3 of 6)

**Table A1 (Continued)**

Day/ Hour	Max Speed Diff. m/s	Grid Point Coord.		5-Nest Model		7-Nest Model	
		Lat. deg	Long. deg	Speed m/s	Dir. deg az	Speed m/s	Dir. deg az
171500	6.0 6.8	27.8 27.8	-88.5 -88.5	19.3 19.3	114.2 114.2	13.3 13.3	125.6 125.6
171530	1.7 6.5	27.8 28.0	-88.7 -88.5	45.9 52.5	338.5 81.4	44.2 53.2	342.8 88.4
171600	1.6 7.6	28.0 28.0	-88.5 -88.5	41.8 41.8	126.4 126.4	40.1 40.1	136.8 136.8
171630	1.7 7.5	28.0 28.0	-88.7 -88.5	34.0 45.2	338.7 169.1	32.3 46.3	338.4 178.4
171700	3.1 7.5	28.3 28.3	-88.7 -88.7	44.9 44.9	45.2 45.2	41.8 41.8	54.2 54.2
171730	2.0 3.2	28.3 28.5	-88.7 -88.7	6.9 53.8	324.1 59.8	4.9 53.9	340.6 63.2
171800	2.6 8.5	28.3 28.5	-88.7 -88.7	33.7 47.2	240.9 81.6	36.4 45.0	246.3 91.9
171830	7.8 8.3	28.5 28.5	-88.7 -88.7	24.5 24.5	167.5 167.5	16.7 16.7	175.6 175.6
171900	2.5 8.9	28.5 28.7	-88.7 -88.7	38.2 50.1	214.3 97.5	40.7 49.6	221.1 107.7
171930	2.9 7.7	28.7 28.7	-89.0 -88.7	41.2 41.2	1.6 154.8	38.3 40.8	6.5 165.5
172000	1.8 7.2	28.7 28.9	-88.7 -89.0	43.2 50.0	192.8 38.1	45.0 49.0	197.7 46.4
172030	1.5 7.1	28.9 28.9	-88.7 -88.7	47.9 47.9	150.2 150.2	49.4 49.4	158.3 158.3
172100	2.0 8.2	28.9 29.1	-89.0 -89.0	31.1 47.6	283.6 55.6	33.2 46.1	283.5 65.4
172130	3.1 3.5	29.1 29.1	-89.0 -89.0	15.6 15.6	79.7 79.7	12.5 12.5	86.5 86.5
172200	3.6 8.5	29.1 29.3	-89.0 -89.0	27.7 50.1	250.0 72.7	31.3 49.6	255.4 82.6
172230	7.2 8.2	29.3 29.3	-89.0 -89.0	23.8 23.8	135.6 135.6	16.6 16.6	147.2 147.2
172300	1.6 7.1	29.3 29.5	-89.0 -89.0	37.8 51.5	205.3 93.0	39.4 52.0	214.6 100.9
172330	2.2 6.2	29.5 29.5	-89.2 -89.0	44.9 39.1	7.8 143.3	42.7 37.6	15.1 152.3

(Sheet 4 of 6)

**Table A1 (Continued)**

Day/ Hour	Max. Speed Diff. m/s	Grid Point Coord.		5-Nest Model		7-Nest Model	
		Lat. deg	Long. deg	Speed m/s	Dir. deg az	Speed m/s	Dir. deg az
180000	1.7	29.5	-89.0	43.4	188.7	45.1	195.4
	5.5	29.5	-89.0	43.4	188.7	45.1	195.4
180030	1.8	29.7	-89.2	27.4	30.7	25.6	26.6
	6.0	29.7	-89.0	49.7	142.6	50.7	149.4
180100	3.2	29.7	-89.2	27.0	274.3	30.2	276.4
	8.4	29.9	-89.2	50.6	62.6	49.5	72.1
180130	6.9	29.9	-89.2	20.1	126.8	13.2	141.7
	8.0	29.9	-89.2	20.1	126.8	13.2	141.7
180200	1.4	29.9	-89.2	36.5	197.3	37.9	208.1
	7.1	29.9	-89.2	36.5	197.3	37.9	208.1
180230	2.9	30.1	-89.4	43.9	16.8	41.0	24.2
	9.2	30.1	-89.2	46.9	132.5	45.5	143.9
180300	1.4	30.1	-89.2	45.9	176.3	47.3	181.7
	6.0	30.3	-89.4	52.0	47.1	52.1	53.6
180330	2.5	30.3	-89.4	23.1	71.2	20.6	66.5
	3.3	30.3	-89.2	49.9	139.7	50.5	143.4
180400	1.9	30.3	-89.4	24.1	245.7	26.0	252.7
	3.6	30.3	-89.4	24.1	245.7	26.0	252.7
180430	0.9	28.3	-92.2	8.4	293.9	7.5	299.6
	1.4	30.3	-89.4	38.9	234.0	39.7	235.6
180500	0.9	28.3	-92.2	8.3	291.2	7.5	296.5
	1.4	29.5	-94.0	4.4	353.8	4.3	11.9
180530	0.9	28.5	-92.2	8.8	292.6	7.9	298.1
	1.5	30.3	-89.4	39.5	236.7	38.8	234.8
180600	0.9	28.5	-92.4	7.8	293.4	7.0	299.2
	1.4	29.5	-93.3	6.5	334.2	6.0	345.8
180630	0.9	28.7	-92.4	7.5	293.6	6.6	299.3
	1.3	29.7	-92.9	8.0	328.1	7.2	336.0
180700	0.9	29.5	-92.6	7.6	315.2	6.7	322.1
	1.3	29.5	-92.6	7.6	315.2	6.7	322.1
180730	0.9	29.5	-92.6	6.7	310.7	5.8	317.2
	1.1	29.5	-92.6	6.7	310.7	5.8	317.2
180800	0.9	29.5	-92.4	6.8	301.6	5.9	306.7
	1.1	29.5	-92.4	6.8	301.6	5.9	306.7
180830	0.9	29.7	-92.2	7.2	298.6	6.3	302.9
	1.0	29.7	-92.0	8.2	294.2	7.3	298.0

(Sheet 5 of 6)

**Table A1 (Concluded)**

Day/ Hour	Max. Speed Diff. m/s	Grid Point Coord.		5-Nest Model		7-Nest Model	
		Lat. deg	Long. deg	Speed m/s	Dir. deg az	Speed m/s	Dir. deg az
180900	0.9	29.7	-92.0	7.2	289.3	6.3	292.2
	0.9	29.7	-92.0	7.2	289.3	6.3	292.2
180930	0.9	29.7	-92.0	6.3	282.5	5.5	284.1
	0.9	30.3	-89.4	17.4	218.1	17.3	215.2
181000	0.8	29.7	-92.0	5.5	275.1	4.7	274.8
	0.8	30.3	-89.4	15.8	216.9	15.8	213.8
181030	0.7	29.7	-92.0	4.8	265.3	4.1	262.5
	0.8	30.3	-86.4	11.9	161.5	12.1	165.0
181100	0.5	29.7	-91.7	4.9	253.5	4.3	249.7
	0.8	30.3	-86.4	11.4	162.2	11.5	165.9
181130	0.4	28.3	-83.4	8.2	156.8	8.5	160.7
	0.8	30.1	-85.7	10.0	160.4	10.2	164.6
181200	0.4	29.7	-93.8	3.1	170.9	3.5	170.8
	0.8	30.3	-86.4	10.3	163.0	10.4	167.3

(Sheet 6 of 6)

# **Appendix B**

## **Documentation of CE Model Upgrades**

---

This appendix provides brief documentation of new and modified programs in the upgraded CE tropical cyclone surface wind field model. The material is a supplement to the primary documentation of Cardone et al. (1992). Five FORTRAN programs are discussed. The programs HIST\_ADC.7NE, SNAP\_ADC.7NE, and SNAP\_HOL.7NE are modified versions of the previous HIST and SNAP programs. Programs 1EYEWALL.HOL and 2EYEWALL.HOL are new. They are helpful in implementing the new generalized surface pressure specification.

### **Program HIST\_ADC.7NE**

HIST\_ADC.7NE is a slight modification of HIST\_ADC.F. All input files except LSNAP, and all output files, are unchanged from HIST\_ADC.F to HIST\_ADC.7NE. The changes to file LSNAP are as follows:

- pressure arrays, formerly dimensioned (21,21,5), are now dimensioned (21,21,7);
- wind arrays, formerly dimensioned (21,21,10), are now dimensioned (21,21,14);
- in the variables at the end of records in LSNAP, variable DX is followed by the new variable INSIDE. INSIDE is an integer indexing the innermost live nest of the 7 nests supported, so that the effective grid spacing is  $DX*2^{**}(INSIDE-1)$ .

### **Program SNAP\_ADC.7NE**

SNAP\_ADC.7NE is derived from SNAP\_ADC.F. The modifications allow the user to run up to 7 grid nests rather than the previous mandatory 5 nests.

Arrays of pressure, pressure gradient, wind, formerly dimensioned (21,21,5), are now dimensioned (21,21,7). Two changes are made to namelist /NAME3/ as follows:

- a variable name NOMEN (CHARACTER\*4) for storm identification has been included;
- integer variable INSIDE has been added. INSIDE indexes the finest live nest of the 7 nests provided. Thus the number of live nests is (8-INSIDE), and the grid spacing of the finest live nest is  $DX*2^{**}(INSIDE-1)$ . Default values are DX = 2, and INSIDE = 1, yielding a 2 km grid spacing and an execution time roughly 4 times as long as the existing 5-nest model. The combination DX = 6.25, INSIDE = 3, (lines 304, 305) reproduces the 25 km spacing often used by the CE for global studies. In the great majority of applications, the useful values of INSIDE are 1, 2, and 3. INSIDE = 4 may be tried for running a quick preliminary study on a coarse grid.

## **Program SNAP\_HOL.7NE**

SNAP\_HOL.7NE is an extensive modification of SNAP\_ADC.7NE to include the generalized pressure profile as well as the capability for modeling up to 7 nests. The variable ST12 and the quadrantal variation of PFAR and RADIUS have been excised. In OWI's experience with the hurricane model, they have been used only once: for hurricane Eloise, September 13, 1975. Variable ITRACK has been excised: its use pertained to a 1969 study in which direction was specified in points. Namelist /NAME3/ is changed materially. Each variable and array in /NAME3/ is documented below. The method of computation of pressure and pressure gradient is discussed in a later part on Mathematical Method.

### **Revisions at beginning of program**

```
REAL RADIUS(2),DPRESS(2),HOLL(2)
CHARACTER*4 NOMEN
EQUIVALENCE (RAD1,RADIUS), (RAD2,RADIUS(2)), (B1,HOLL),
$ (B2,HOLL(2)), (DP1,DPRESS), (DP2,DPRESS(2))
NAMELIST /NAME3/ SGW, AN1, NOMEN,
$ EYELAT, EYLONG, DIREC, SPEED, EYPRES, RADIUS, RAD1,
$ RAD2, PFAR, NM, DX, INSIDE, HOLL, B1, B2, DPRESS, DP1,
$ DP2
```

### Definition of variables in namelist NAME3

SGW	Magnitude of surface geostrophic wind, m/sec
AN1	Angle between SGW and east, counterclockwise from east
NOMEN	Designator for tropical storm, e.g. two digits and one letter
EYELAT	Latitude of eye of storm at snap time, north positive
EYLONG	Longitude of eye of storm at snap time, east positive (EYLONG is included for archival purposes but not presently used in computation)
DIREC	Direction of forward motion of storm, clockwise from north
SPEED	Speed of forward motion, in kt (but redefinable according to the switch variable UNITS)
EYPRES	Pressure at eye of storm, in mb
RADIUS	Scale radius of the two components of exponential pressure profile
RAD1,RAD2	Alternate names for specifying RADIUS; convenient when only one exponential is modeled
PFAR	Ambient pressure exterior to storm, in mb
NM	Number of computational cycles in nest 1; NM should be a multiple of 64 (default: NM = 3200)
DX	Grid spacing in nest 1, in km (default: DX = 2.)
INSIDE	Index of finest nest actually used for computations; the finest active grid spacing is DX*2** (INSIDE-1) (default: INSIDE = 1)
HOLL	Power to which radius is raised in the modified Holland's (1980) pressure profile model. When HOLL(2) = 0., only one exponential is used; RADIUS(2) and DPRESS(2) are then ignored.
B1,B2	Alternate names for specifying HOLL; convenient when only one exponential is modeled. Default values are B1 = 1., B2 = 0. These defaults are reinstated for every snapshot. Use of the defaults reverts to a standard exponential pressure profile, as used in SNAP_ADC.7NE.
DPRESS	DPRESS(I) is the pressure difference associated with RADIUS(I) and HOLL(I) in OWI's double-eyewall extension of Holland's (1980) modified exponential profile.
DP1,DP2	Alternate names for specifying DPRESS. As explained in the part on Mathematical Method, it is never advantageous to include DP2 in an input list; it is in the NAMELIST in order to force its appearance in the output file.

**SPECIAL WARNING:** Do not input both members of an equivalence. Input either RADIUS or RAD and RAD2; either HOLL or B1 and B2; either DPRESS or DP1 and DP2. The program imposes consistency checks on RADIUS, HOLL, and DPRESS; it does not check EYPRES and PFAR, so that it remains the user's duty to verify that PFAR > EYPRES.

## **Mathematical method**

The program performs the following consistency checks:

1. If  $B1 < 0$  or  $B2 < 0$ , stop.
2. If  $B2 = 0$ , run Holland's modified exponential model (ignore RAD2 and DP2).
  - 2.1 If  $RAD1 \leq 0$ , stop.
  - 2.2 If DP1 not specified, compute it as PFAR-EYPRES.
  - 2.3 If DP1 specified, but inconsistent with PFAR-EYPRES, stop.
  - 2.4 Set N = 1.
3. If  $B2 > 0$ , run OWI's extension of Holland's pressure profile.
  - 3.1 If  $RAD1 \leq 0$  or  $RAD2 \leq 0$ , stop.
  - 3.2 If DP2 not specified, compute it as PFAR-EYPRES-DP1.
  - 3.3 If DP2 specified, but inconsistent with PFAR-EYPRES-DP1, stop.
  - 3.4 Set N = 2.

## **Program 1EYEWALL.HOL**

Program 1EYEWALL.HOL attempts to fit snapshot parameters to a guessed wind profile. It considers only the case of one exponential ( $B2 = 0.0$ ). 1EYEWALL.HOL requires the following input arguments (in namelist /INN/):

BLAT	Absolute value of latitude of eye, degrees & decimals; used in computation of the Coriolis parameter. Also, the value BLAT=99 is used as a flag to stop computation.
EYPRES	Pressure at eye, in mb
PFAR	Pressure at large (theoretically infinite) distance from eye, in mb
RW1	Radius at which a wind speed is guessed, in km
SP1	Wind speed corresponding to RW1, in m/sec
V150	Wind speed at radius of 150 km, in m/sec

The following outputs are printed:

1. In namelist /INN/:

SP11, SP12 = SP1 minus & plus 1 m/sec  
SP31, SP32 = V150 minus & plus 1 m/sec  
DP2 = pressure difference (far field minus eye), in pascal

2. In namelist /VORTEX/:

COR = Coriolis parameter,  $2*\omega*\sin(\text{BLAT})$

**FR22** = the quantity  $0.5 * \text{COR} * \text{RW1}$  (used in the computation of gradient wind)

**FR23** =  $0.5 * \text{COR} * r$ , where  $r$  is 150000 m or 150 km

**PEYE** = pressure at eye, in pascal

3. Below namelist /VORTEX/, six parameters are printed, defined from left to right as:

3.1 DP2 (see above)

3.2 Fitted value of scale radius, in m

3.3 Fitted value of Holland's exponent

3.4 Fitted value of gradient wind at radius RW1, in m/sec  
(in a good fit, this will be nearly equal to SP1)

3.5 Fitted value of gradient wind at radius 150 km, in m/sec  
(in a good fit, this will be nearly equal to V150)

3.6 Goodness of fit measure: absolute value of gradient wind minus in put wind at radius RW1, plus the same at radius 150 km. A value less than 3.0 implies a tolerably well-fitting solution.

4. Table with 6 columns and 150 lines:

4.1 Radius, in km

4.2 Pressure, in mb

4.3 First component of pressure gradient, in pascal/m

4.4 Second component (this is zero, since only one exponential was fitted)

4.5 Pressure gradient (here equal to output #4.3)

4.6 Gradient wind, m/sec

5. Below the table are numbers that, if the fit is satisfactory, the user can insert into namelist /NAME3/ of SNAP\_HOL.7NE:

**EYELAT** = echo of the input BLAT

**EYPRES** = echo of input

**PFAR** = echo of input

**RAD1** = scale radius, in nm

**HOLL** = two values of Holland's exponent; the second value is zero, because only one exponential was fitted

## Program 2EYEWALL.HOL

Program 2EYEWALL.HOL attempts to fit snapshot parameters to a guessed wind profile. It considers the case of two exponentials ( $B2 > 0.0$ ).  
2EYEWALL.HOL requires the following inputs in namelist /INN/:

**BLAT**      Same usage as in 1EYEWALL.HOL

**EYPRES**    Same usage as in 1EYEWALL.HOL

**PFAR**      Same usage as in 1EYEWALL.HOL

RS1	Scale radius of inner ring, in km (numerical experiments with this scheme have shown that the inner scale radius can safely be taken equal to the inner radius to local maximum wind)
RW2	Radius to maximum wind of outer ring, in km
DRING	An integer switch variable indexing the shape of the wind profile

DRING = 1: the maximum wind is greater in the inner ring  
 DRING = 2: the maximum wind is greater in the outer ring

SP1	Desired wind speed at radius RS1, in m/sec
SP2	Desired wind speed at radius RW2, in m/sec

The following outputs are printed:

1. In namelist /INN/:

SP11, SP12 = SP1 minus and plus 1 m/sec  
 SP21, SP22 = SP2 minus and plus 1 m/sec

2. In namelist /VORTEX/:

BLAT = echo of input  
 COR = same usage as in 1EYEWALL.HOL  
 RAD1 = RS1, in m  
 RAD2 = RW2, in m  
 RAD3 =  $0.5 * (RAD1 + RAD2)$ ; a local minimum of wind speed, if found, will be near RAD3  
 RAD4 = 150000 m (= 150 km)  
 FR21 = the quantity  $0.5 * COR * RAD1$ ; used in the computation of gradient wind  
 FR22 = the quantity  $0.5 * COR * RAD2$   
 FR23 = the quantity  $0.5 * COR * RAD3$   
 PEYE = same usage as in 1EYEWALL.HOL  
 DP = pressure difference (far field minus eye), in pascal

3. Below namelist /VORTEX/, nine parameters are printed, defined from left to right as:

- 3.1 Fitted value of DP1 (partial pressure difference for first exponential), in pascal
- 3.2 Fitted value of DP2 (partial pressure difference for second exponential), in pascal
- 3.3 Scale radius of second exponential, in m (the scale radius of first exponential has been fixed at RAD1)
- 3.4 Exponent for first exponential (Holland 1980)
- 3.5 Exponent for second exponential (OWI extension of Holland (1980))
- 3.6 Fitted wind speed at radius RAD1, m/sec
- 3.7 Fitted wind speed at radius RAD2, m/sec

3.8 Fitted wind speed at radius RAD3, m/sec  
3.9 (printed below 3.1): fitted wind speed at radius 150 km

4. Second printing of namelist /INN/, if given:

The fit in the above two-line summary was unsatisfactory in that the wind at 150 km was greater than the wind at RAD2; a second fit will be attempted, this time minimizing the wind speed at 150 km.

SP11, SP12 = SP1 minus and plus 2 m/sec  
SP21, SP22 = SP2 minus and plus 2 m/sec

5. Below second printing of /INN/: the same nine parameters as in #3 above, for the second attempted fit.

6. Table with 6 columns and 150 lines:

6.1 Radius, in km  
6.2 Pressure, in mb  
6.3 First component of pressure gradient, in pascal/m  
6.4 Second component of pressure gradient, in pascal/m  
6.5 Pressure gradient (sum of the two components), in pascal/m  
6.6 Gradient wind, in m/sec

7. Below the table are numbers that, if the fit is satisfactory, the user can insert into namelist /NAME3/ of SNAP\_HOL.7NE:

EYELAT = echo of the input BLAT  
EYPRES = echo of input  
PFAR = echo of input  
RADIUS = two values of scale radius, in nm  
HOLL = two values of Holland's exponent  
DP1 = pressure difference for first component, in mb  
(program SNAP\_HOL.7NE computes DP2 by subtraction)

# **Appendix C**

## **Sample Application of Upgraded CE Model to Simu- lation of 12 Snapshots of Hurricane Gilbert**

---

This appendix provides input file information used by OWI in test runs with the upgraded CE model, including seven nests and the generalized pressure specification. Snapshots were generated at 6-hr intervals for Hurricane Gilbert, which occurred during September 1988. The first snapshot represents 1200 UTC (Universal Time Coordinate, formerly known as Greenwich Mean Time) 15 September 1988. In all, 12 snapshots were generated. Inputs for the programs SNAP\_HOL.7NE and HIST\_ADC.7NE are included as implemented on the OWI VAX computer. The listed values of parameter AN1 follow a meteorological convention (deg azimuth coming from ) rather than the convention used by the Cardone et al. (1992).

Listings of the full field of surface (19-m elevation) wind speed and direction were generated on a polar output grid. They are included here at 6-hr intervals (snapshot times). Wind speed is in m/sec. Wind direction is in deg azimuth coming from. Printed output of the azimuthally averaged, surface wind speed and inflow angle is also given in this appendix. In addition to the 12 snapshot wind fields, this output includes a wind field interpolated halfway between each pair of snapshots.

```

S ASSIGN GRID.312    FDR012
S ASSIGN 05GILBERT21 FDR005
S ASSIGN GILB.WIN021 FDR052
S RUN MOLL3
SNAME1
KZM      =      8309,
KDM      =     151200,
KMIN     =      180,
DX       =   2.000030      ,
KSTRES   =          0,
NSTRES   =     17227,
KWIND    =      19,
NWIND    =     312,
MM       =  500.0030      ,
INSIDE   =          1,
KTIME    =          1
SEND
SNAME2
EYELAT  =  16.00030      ,
DIREC   =  290.0030      ,
SPEED   =  11.03030      ,
EYPRES   =  972.0030      ,
PFAR    =  1011.030      ,
RAD1    =  25.38030      ,
RAD2    =  68.73030      ,
RADIUS   =  25.38030      ,  68.73000      ,
DP1     =  22.85030      ,
DP2     =  16.15030      ,
DPRES   =  22.85030      ,  16.15000      ,
B1      =  2.520030      ,
B2      =  2.520030      ,
HOLL    =  2*2.520030
SGW     =  7.000030      ,
AN1     =  110.0030      ,
ST12    =  0.0000030E+00
SEND
SNAME2
EYELAT  =  16.00030      ,
DIREC   =  290.0030      ,
SPEED   =  11.00030      ,
EYPRES   =  968.0030      ,
PFAR    =  1011.030      ,
RAD1    =  31.32030      ,
RAD2    =  87.37030      ,
RADIUS   =  31.32030      ,  87.37000      ,
DP1     =  31.77030      ,
DP2     =  11.23030      ,
DPRES   =  31.77030      ,  11.23000      ,
B1      =  2.520030      ,
B2      =  2.520030      ,
HOLL    =  2*2.520030
SGW     =  7.000030      ,
AN1     =  110.0030      ,
ST12    =  0.0000030E+00
SEND

```

Snapshot 1

Snapshot 2

Figure C1. Program inputs, Hurricane Gilbert (Sheet 1 of 6)

SNAME2			
EYELAT	=	19.00000	,
DIREC	=	290.00000	,
SPEED	=	11.00000	,
EYPRES	=	905.00000	,
PFAR	=	1012.000	,
RAD1	=	8.640000	,
RAD2	=	67.28000	,
RADIUS	=	8.640000	,
DP1	=	93.83000	,
DP2	=	13.17000	,
DPRES	=	93.83000	,
B1	=	1.680000	,
B2	=	2.380000	,
HOLL	=	1.680000	,
SGW	=	7.000000	,
AN1	=	110.0000	,
ST12	=	0.000000E+00	
SEND			
SNAME2			
EYELAT	=	20.00000	,
DIREC	=	290.00000	,
SPEED	=	11.00000	,
EYPRES	=	888.00000	,
PFAR	=	1012.000	,
RAD1	=	7.020000	,
RAD2	=	54.00000	,
RADIUS	=	7.020000	,
DP1	=	110.2200	,
DP2	=	13.78000	,
DPRES	=	110.2200	,
B1	=	1.590000	,
B2	=	2.520000	,
HOLL	=	1.590000	,
SGW	=	7.000000	,
AN1	=	110.0000	,
ST12	=	0.000000E+00	
SEND			
SNAME2			
EYELAT	=	20.00000	,
DIREC	=	290.00000	,
SPEED	=	11.00000	,
EYPRES	=	893.00000	,
PFAR	=	1012.000	,
RAD1	=	7.020000	,
RAD2	=	37.80000	,
RADIUS	=	7.020000	,
DP1	=	101.1200	,
DP2	=	17.88000	,
DPRES	=	101.1200	,
B1	=	1.410000	,
B2	=	2.520000	,
HOLL	=	1.410000	,
SGW	=	7.000000	,
AN1	=	110.0000	,
ST12	=	0.000000E+00	
SEND			

Snapshot 3

Snapshot 4

Snapshot 5

Figure C1. (Sheet 2 of 6)

SNAME2				
EYELAT	=	21.00000	,	
DIREC	=	290.00000	,	
SPEED	=	11.00000	,	
EYPRES	=	890.00000	,	
PFAR	=	1012.000	,	
RAD1	=	7.020000	,	
RAD2	=	37.26000	,	
RADIUS	=	7.020000	,	37.26000
DP1	=	101.80000	,	
DP2	=	20.20000	,	
DPRES	=	101.80000	,	20.20000
B1	=	1.410000	,	
B2	=	2.520000	,	
HOLL	=	1.410000	,	2.520000
SGW	=	7.000000	,	
AN1	=	110.0000	,	
ST12	=	0.000000E+00		
SEND				
SNAME2				
EYELAT	=	22.00000	,	
DIREC	=	290.00000	,	
SPEED	=	11.00000	,	
EYPRES	=	951.00000	,	
PFAR	=	1012.000	,	
RAD1	=	11.88000	,	
RAD2	=	46.85000	,	
RADIUS	=	11.88000	,	46.85000
DP1	=	45.07000	,	
DP2	=	15.93000	,	
DPRES	=	45.07000	,	15.93000
B1	=	0.5600000	,	
B2	=	2.5200000	,	
HOLL	=	0.5600000	,	2.5200000
SGW	=	7.000000	,	
AN1	=	110.0000	,	
ST12	=	0.0000000E+00		
SEND				
SNAME2				
EYELAT	=	22.00000	,	
DIREC	=	290.00000	,	
SPEED	=	11.00000	,	
EYPRES	=	950.00000	,	
PFAR	=	1012.000	,	
RAD1	=	17.28000	,	
RAD2	=	55.82000	,	
RADIUS	=	17.28000	,	55.82000
DP1	=	34.57000	,	
DP2	=	27.43000	,	
DPRES	=	34.57000	,	27.43000
B1	=	0.9400000	,	
B2	=	2.5200000	,	
HOLL	=	0.9400000	,	2.5200000
SGW	=	7.000000	,	
AN1	=	110.0000	,	
ST12	=	0.0000000E+00		
SEND				

Snapshot 6

Snapshot 7

Snapshot 8

Figure C1. (Sheet 3 of 6)

```

SNAME2
EYELAT = 23.00000 , Snapshot 9
DIREC = 290.00000 ,
SPEED = 11.00000 ,
EYPRES = 949.00000 ,
PFAR = 1010.000 ,
RAD1 = 11.89000 ,
RAD2 = 43.53000 ,
RADIUS = 11.88000 , 43.53000 ,
DP1 = 40.67000 ,
DP2 = 20.33000 ,
DPRES = 40.67000 , 20.33000 ,
B1 = 0.7500000 ,
B2 = 2.5200000 ,
HDLL = 0.7500000 , 2.5200000 ,
SGW = 7.0000000 ,
AN1 = 110.00000 ,
ST12 = 0.0000000E+00
SEND

SNAME2
EYELAT = 23.00000 , Snapshot 10
DIREC = 290.00000 ,
SPEED = 11.00000 ,
EYPRES = 950.00000 ,
PFAR = 1011.000 ,
RAD1 = 29.70000 ,
RAD2 = 91.63000 ,
RADIUS = 29.70000 , 91.63000 ,
DP1 = 51.84000 ,
DP2 = 9.1600000 ,
DPRES = 51.84000 , 9.1600000 ,
B1 = 1.1200000 ,
B2 = 2.2400000 ,
HDLL = 1.1200000 , 2.2400000 ,
SGW = 7.0000000 ,
AN1 = 110.00000 ,
ST12 = 0.0000000E+00
SEND

SNAME2
EYELAT = 24.00000 , Snapshot 11
DIREC = 290.00000 ,
SPEED = 11.00000 ,
EYPRES = 953.00000 ,
PFAR = 1010.000 ,
RAD1 = 27.00000 ,
RAD2 = 64.21000 ,
RADIUS = 27.00000 , 64.21000 ,
DP1 = 46.62000 ,
DP2 = 10.38000 ,
DPRES = 46.62000 , 10.38000 ,
B1 = 1.3300000 ,
B2 = 2.5200000 ,
HDLL = 1.3300000 , 2.5200000 ,
SGW = 7.0000000 ,
AN1 = 110.00000 ,
ST12 = 0.0000000E+00
SEND

```

Figure C1. (Sheet 4 of 6)

Snapshot 12

```

SNAME2
EYELAT = 24.00000      ,
DIREC = 290.00000      ,
SPEED = 11.00000      ,
EYPRES = 954.0000      ,
PFAIR = 1009.000      ,
RAD1 = 21.60000      ,
RAD2 = 60.61000      ,
RADIUS = 21.60000      , 60.61000      ,
DP1 = 44.98000      ,
DP2 = 10.02000      ,
DPRES = 44.98000      , 10.02000      ,
B1 = 1.190000      ,
B2 = 2.520000      ,
HOLL = 1.190000      , 2.520000      ,
SGW = 7.000000      ,
AN1 = 110.0000      ,
ST12 = 0.000000E+00
SEND
SNAME2
EYELAT = 999.0000      ,
DIREC = 290.0000      ,
SPEED = 11.00000      ,
EYPRES = 954.0000      ,
PFAIR = 1009.000      ,
RAD1 = 0.000000E+00,
RAD2 = 0.000000E+00,
RADIUS = 2#0.000000E+00,
DP1 = 0.000000E+00,
DP2 = 0.000000E+00,
DPRES = 2#0.000000E+00,
B1 = 1.000000      ,
B2 = 0.000000E+00,
HOLL = 1.000000      , 0.0000000E+00,
SGW = 7.000000      ,
AN1 = 110.0000      ,
ST12 = 0.000000E+00
SEND

```

	0	20	0	0	0	1	0
0	20	0	0	0	0	0	0
2	20	0	0	0	2	0	0
4	20	0	0	0	3	0	0
6	20	0	0	0	4	0	0
8	20	0	0	0	5	0	0
10	20	0	0	0	6	0	0
12	20	0	0	0	7	0	0
14	20	0	0	0	8	0	0
16	20	0	0	0	9	0	0
18	20	0	0	0	10	0	0
20	20	0	0	0	11	0	0
22	20	0	0	0	12	0	0
999	0	0	0	0	0	0	0

Figure C1. (Sheet 5 of 6)

HOUR	LAT	LONG	STORM HISTORY SNAPS	ZERO HOUR IS INTERP ROT	8809 151200
0	20	0	0 0 1 0	0.0000	0
1	20	0	0 0 1 2	0.5000	0
2	20	0	0 0 2 0	0.0000	0
3	20	0	0 0 2 3	0.5000	0
4	20	0	0 0 3 0	0.0000	0
5	20	0	0 0 3 4	0.5000	0
6	20	0	0 0 4 0	0.0000	0
7	20	0	0 0 4 5	0.5000	0
8	20	0	0 0 5 0	0.0000	0
9	20	0	0 0 5 6	0.5000	0
10	20	0	0 0 6 0	0.0000	0
11	20	0	0 0 6 7	0.5000	0
12	20	0	0 0 7 0	0.0000	0
13	20	0	0 0 7 8	0.5000	0
14	20	0	0 0 8 0	0.0000	0
15	20	0	0 0 8 9	0.5000	0
16	20	0	0 0 9 0	0.0000	0
17	20	0	0 0 9 10	0.5000	0
18	20	0	0 0 10 0	0.0000	0
19	20	0	0 0 10 11	0.5000	0
20	20	0	0 0 11 0	0.0000	0
21	20	0	0 0 11 12	0.5000	0
22	20	0	0 0 12 0	0.0000	0

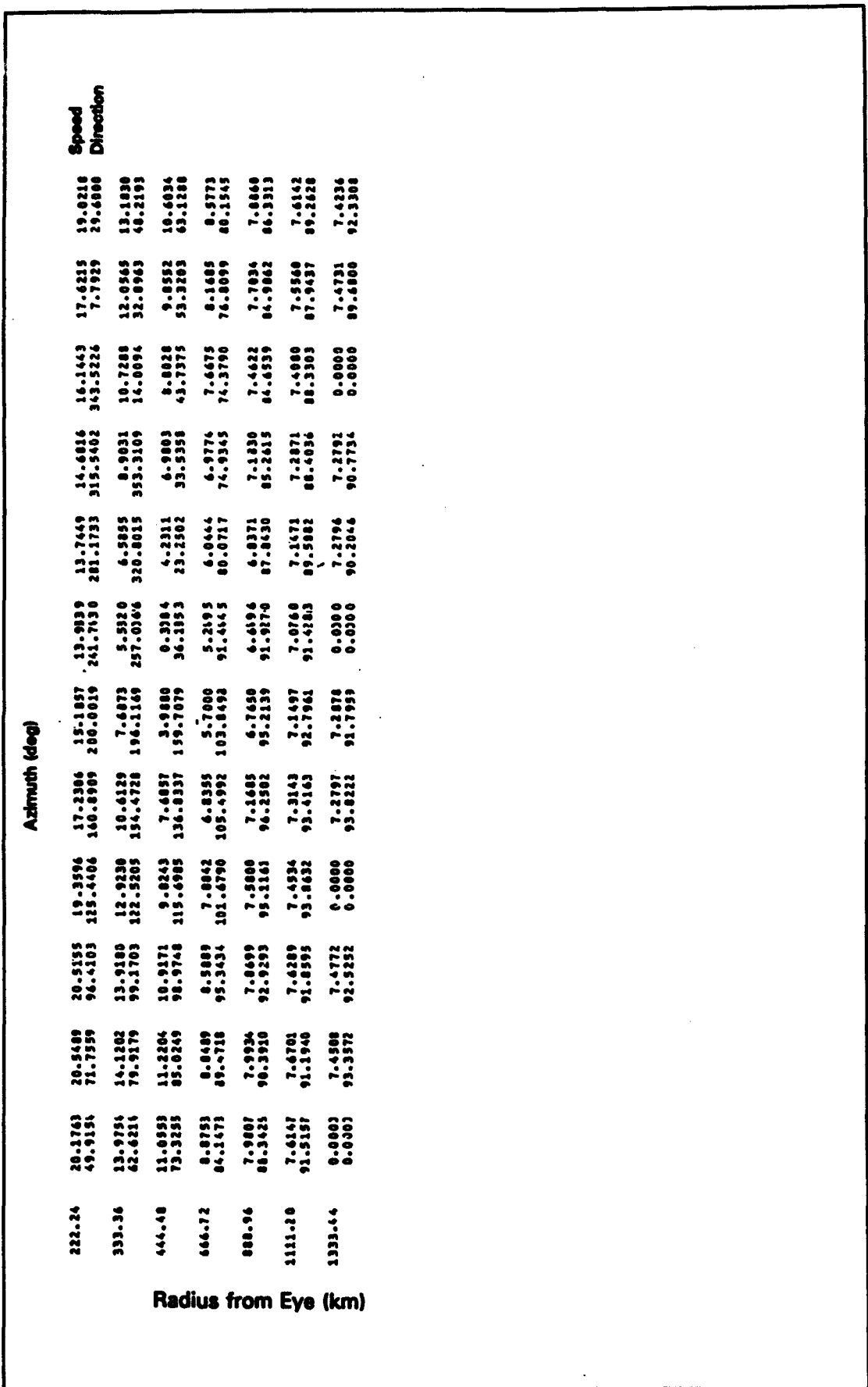
\$WHAT  
 KSTEP2 = 22  
 \$END  
 WORKK: 0 8809 151200  
 WORKK: 1 8809 151500  
 WORKK: 2 8809 151800  
 WORKK: 3 8809 152100  
 WORKK: 4 8809 160000  
 WORKK: 5 8809 160300  
 WORKK: 6 8809 160600  
 WORKK: 7 8809 160900  
 WORKK: 8 8809 161200  
 WORKK: 9 8809 161500  
 WORKK: 10 8809 161800  
 WORKK: 11 8809 162100  
 WORKK: 12 8809 170000  
 WORKK: 13 8809 170300  
 WORKK: 14 8809 170600  
 WORKK: 15 8809 170900  
 WORKK: 16 8809 171200  
 WORKK: 17 8809 171500  
 WORKK: 18 8809 171800  
 WORKK: 19 8809 172100  
 WORKK: 20 8809 180000  
 WORKK: 21 8809 180300  
 WORKK: 22 8809 180600  
 END OF STRESS RUN

Figure C1. (Sheet 6 of 6)

Hour	Radius from Eye (km)	Azimuth (deg)												Speed Direction
		0.	30.	60.	90.	120.	150.	180.	210.	240.	270.	300.	330.	
1.85	5.2191	5.2045	5.0998	5.0868	5.0242	5.0450	5.0535	5.0752	5.0781	5.0587	5.0396	5.0228	5.0474	98.6693
3.70	5.0953	5.0707	5.0574	5.0731	5.0165	5.0367	5.0306	5.0111	6.0155	6.0031	5.9781	5.9342	5.9342	98.5902
5.56	5.0887	5.0381	5.0130	5.0349	5.0075	5.0668	6.0199	6.0671	6.0521	6.0429	6.0169	5.9667	5.9667	99.4205
7.43	5.0663	5.0081	5.0649	5.0764	5.0964	5.0836	5.0507	6.0029	6.0006	6.0066	6.0031	6.0009	6.0009	100.3353
9.26	5.0783	5.7813	5.7133	5.7486	5.8676	5.9662	6.0311	6.1189	6.1304	6.1428	6.1333	6.0610	6.0610	102.4407
11.11	5.2002	5.7649	5.6561	5.6882	5.6429	6.0117	6.1163	6.1807	6.2273	6.2359	6.1741	6.1741	6.1741	101.3340
12.96	6.1181	5.7660	5.5923	5.6034	5.8023	6.0255	6.1500	6.1925	6.2732	6.4122	6.3545	6.4462	6.4462	102.4407
14.82	6.5915	5.4091	5.5224	5.4666	5.7212	6.0349	6.1339	6.2316	6.4952	6.9506	7.1461	7.1547	7.1547	103.7215
16.67	7.5062	5.9973	5.4917	5.2330	5.5279	5.9943	6.1598	6.2660	6.3522	6.4947	6.5797	6.7210	6.8364	105.0828
18.52	9.6965	6.0193	5.8063	5.2179	5.0923	5.6764	6.2315	6.4014	6.2251	6.5958	7.0201	7.0500	7.0500	102.8374
27.78	32.0373	24.3052	21.3874	18.7590	15.5180	11.9773	11.5172	21.4211	36.7541	41.4234	44.2547	42.3971	42.3971	102.0379
37.04	46.2677	46.0264	33.2342	29.2763	27.3211	26.8793	32.0644	40.2791	43.2172	44.8667	46.8933	47.3146	47.3146	102.8326
46.30	45.5667	43.5132	37.4322	35.4423	32.9499	34.1627	37.0834	39.7371	41.2559	42.8003	44.4086	45.2970	45.2970	101.8326
55.56	43.2333	43.2629	39.0072	35.5084	36.4821	35.3937	36.7984	37.8656	38.9099	40.4397	41.9891	42.8609	42.8609	101.8326
74.08	46.2472	46.5314	39.2017	36.5206	35.2295	33.9128	33.0255	34.7682	35.2842	36.6579	38.1599	39.2419	39.2419	101.8326
92.40	37.4363	37.9756	37.6074	35.7166	33.8160	32.3110	31.7723	31.9663	32.5325	33.9074	35.2797	36.5343	36.5343	101.8326
130.90	30.2692	30.7611	30.7445	29.4682	27.5210	25.7919	24.7662	24.9025	26.9451	26.2332	27.6136	29.0277	29.0277	101.8326
166.68	26.2361	26.4758	26.7038	25.5612	23.4929	21.1182	20.3507	20.1863	20.7486	22.1619	23.5127	24.9486	24.9486	101.8326
174.00	43.2022	67.7149	96.7039	125.9559	162.2886	198.2862	236.4804	270.1249	301.8995	319.9995	356.8800	26.5199	26.5199	101.8326

Figure C2. Wind speed and direction fields, Snapshot 1, Hurricane Gilbert (Continued)

**Figure C2. (Concluded)**



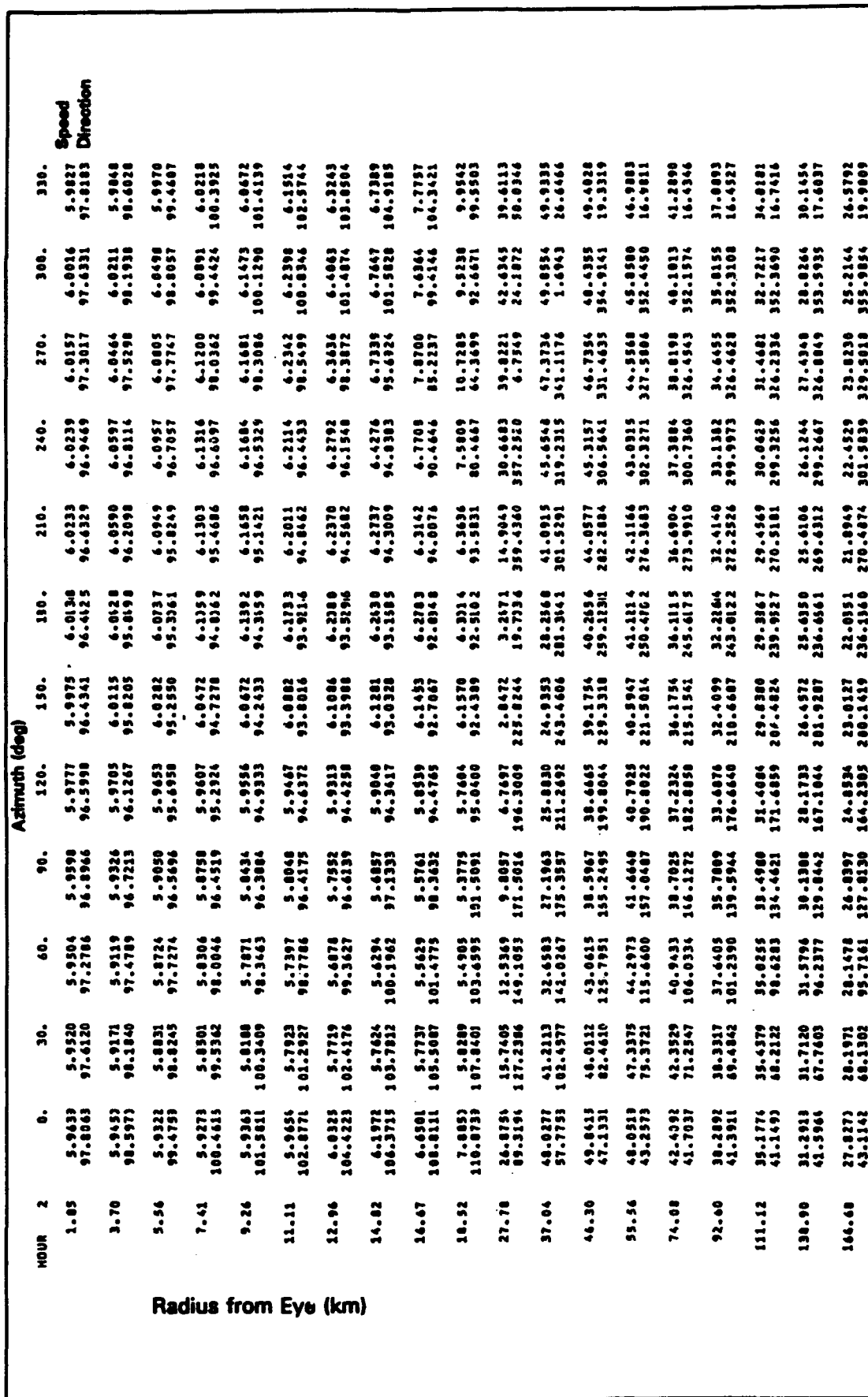


**Figure C3. Wind speed and direction fields, Snapshot 2, Hurricane Gilbert (Continued)**

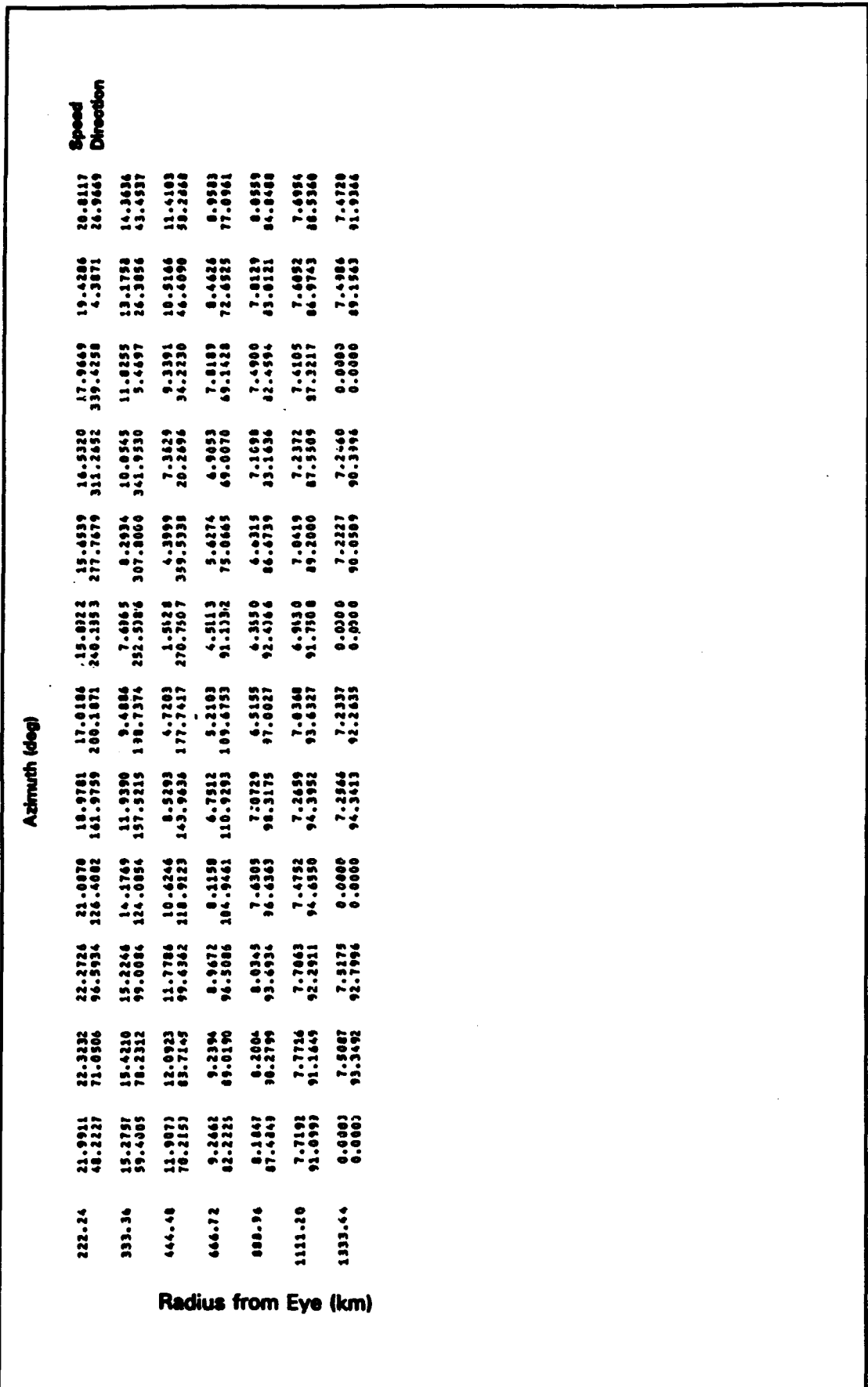


Figure C3. (Concluded)

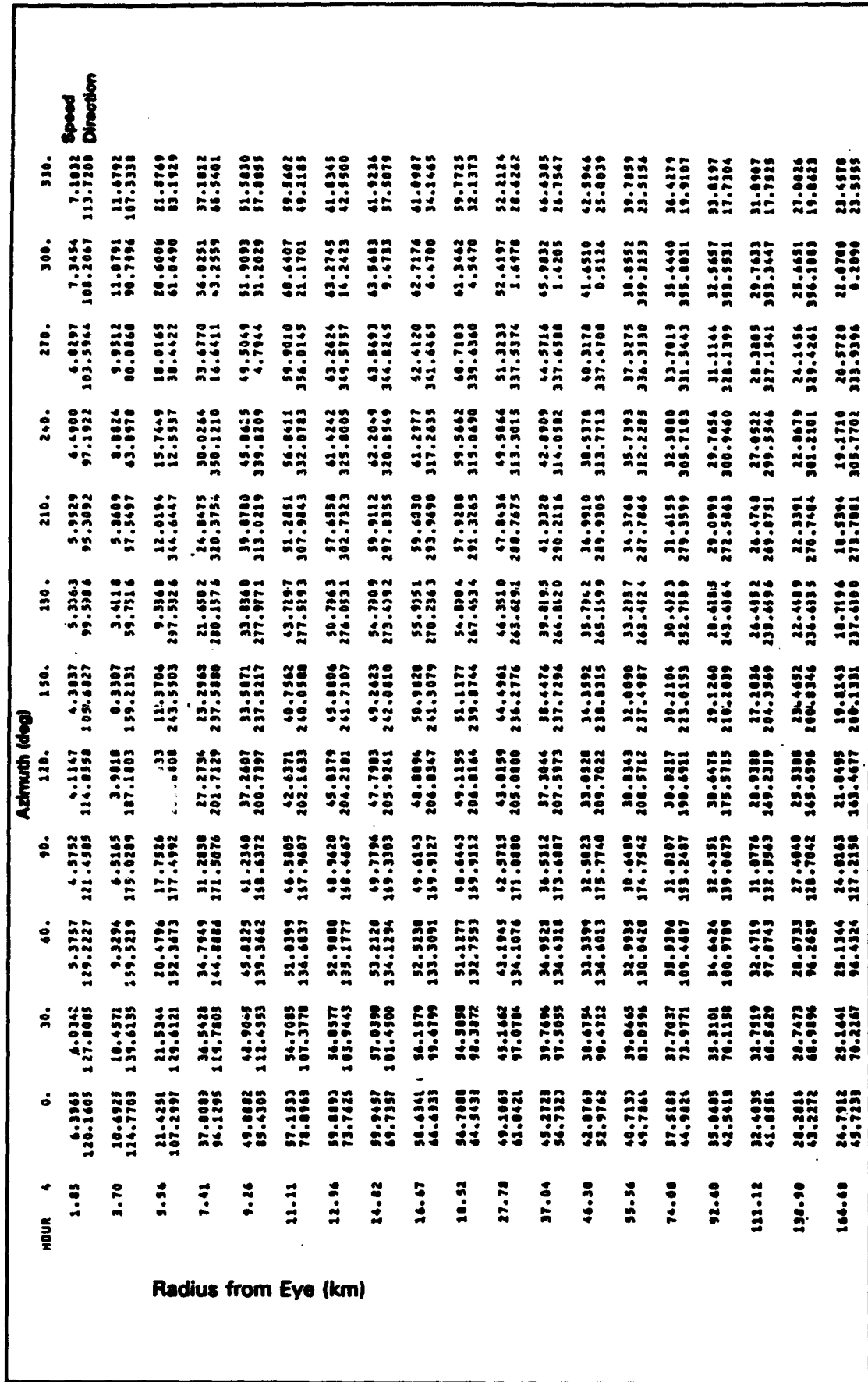
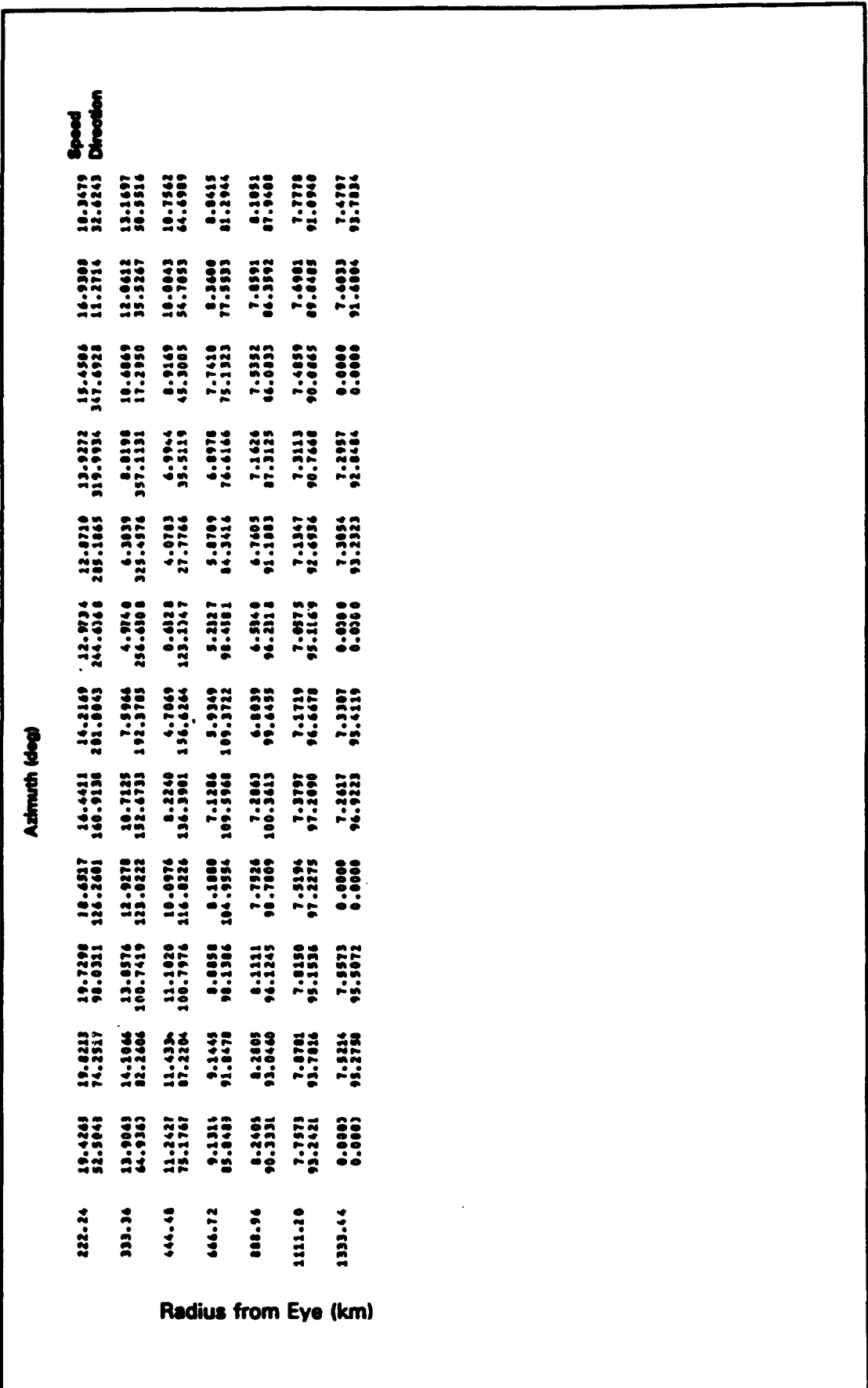


Figure C4. Wind speed and direction fields, Snapshot 3, Hurricane Gilbert (Continued)



**Figure C4. (Concluded)**

Hour	6.	Azimuth (deg)										Speed Direction
		30.	60.	90.	120.	150.	180.	210.	240.	270.	300.	
1.45	8.7587	8.8469	7.3751	6.2912	2.9668	2.7953	6.3706	6.2876	6.6405	6.6346	9.4994	9.8593
136.1323	144.1176	153.1153	155.2415	156.7932	158.7933	92.6150	75.2947	81.8592	95.7165	103.4593	114.1064	
3.70	18.8375	19.1938	18.1798	16.5379	12.9362	8.7114	6.3546	9.5660	13.7629	15.3382	17.4939	19.7043
116.3443	130.2980	150.3503	156.0237	209.0165	215.5932	321.2597	319.1177	26.7669	52.7107	70.0027	92.7229	
5.16	27.5673	36.8985	35.8393	31.5210	26.9226	23.0200	21.5235	24.4005	26.9389	32.3592	35.3477	37.1543
95.0591	119.5443	144.4468	171.3501	202.3593	218.3506	200.2772	321.0060	351.1961	18.9060	44.2365	69.2312	
7.41	52.3123	51.7840	48.8768	63.8776	39.4607	35.9773	36.1742	41.3764	46.8507	50.9407	54.2249	
83.7693	110.5392	137.4012	156.9833	199.4220	236.5291	276.5392	311.6202	339.1288	5.1511	31.0071	56.8460	
9.26	69.2722	58.3196	54.4180	49.4179	45.6254	43.7122	46.7360	50.4535	56.4512	61.0504	63.1035	62.2220
74.3502	104.9284	136.3890	166.1550	200.7326	239.1822	276.5372	307.2585	312.3792	356.6454	21.5529	48.5523	
11.11	61.7753	59.2260	55.3876	51.2279	48.1242	48.5398	53.3904	60.4504	65.7414	65.5473	65.2947	63.7561
72.4413	102.2594	133.6112	157.2567	203.7365	261.7451	276.0103	303.1263	326.7779	310.5916	15.0671	42.6163	
12.96	61.2395	58.3482	54.4777	51.2481	51.7784	57.3164	61.9924	64.4035	64.4035	65.6483	65.3220	63.4411
69.4763	100.8050	133.7936	169.1574	204.5296	243.0662	274.3847	299.2185	322.2239	346.0483	10.7110	38.2669	
14.82	59.8243	56.6520	53.1556	50.5644	50.0220	53.9123	58.3169	61.5660	63.3714	64.5352	64.3750	62.3946
67.5272	99.9166	134.2455	171.3573	208.4510	243.2396	271.3716	295.6800	318.7166	342.8263	7.7321	35.6183	
16.67	57.4673	54.6111	51.3413	49.4066	50.9395	52.7386	57.5953	60.2171	61.6226	62.7707	63.8473	63.4411
66.6825	99.6391	130.4933	172.7232	209.8978	242.6661	269.3732	293.6667	316.7347	340.5663	5.6443	33.5158	
18.52	55.4693	52.3469	49.3679	47.8010	49.4753	52.1007	55.4111	58.9281	60.4404	60.8260	61.3003	59.7045
64.5177	99.5459	135.2461	173.6429	210.2333	241.4376	247.4376	271.4279	291.1797	314.7226	330.9867	3.9918	31.9120
27.79	58.1195	45.7728	41.1246	43.2747	42.7690	44.4606	46.3540	47.9773	49.4243	51.3451	52.4901	51.1543
60.0335	100.9063	140.0168	177.4193	210.2338	239.2319	264.8191	288.0164	312.7312	336.5460	6.2422	26.8616	
37.84	47.3952	42.0494	37.3719	36.9136	38.1612	39.5896	40.8154	42.1046	43.4624	45.0299	46.5221	47.3943
52.1713	93.4259	140.2711	178.4746	210.9635	237.0774	262.9554	287.4566	311.6602	335.6173	356.7277	23.3724	
46.30	44.6671	43.0687	37.9987	35.4313	35.5413	36.4519	37.5746	39.3551	41.5723	42.5760	43.5639	42.9014
47.7362	81.1588	126.2334	170.9221	204.7558	232.5748	258.3649	283.3655	307.9482	332.8180	356.6253	26.9060	
55.56	42.3251	42.2377	39.3022	36.2876	35.1939	34.9469	35.0557	36.1846	37.9296	38.4960	40.0002	41.0002
44.5223	74.1461	110.6455	157.2176	182.7632	223.4742	251.9712	278.0220	304.2259	329.9261	356.4931	38.3977	
74.88	38.4597	29.0401	38.2046	36.3213	34.8021	33.8439	32.3117	32.3117	32.3117	32.3117	36.0990	37.3913
41.4574	68.7123	160.5228	137.4882	174.4264	207.9711	248.3510	269.4181	298.0038	325.1404	351.1395	15.8077	
92.44	34.7072	35.1943	35.9497	33.5277	31.5231	29.8140	28.9198	28.9198	29.8140	29.8140	31.9501	33.3974
130.98	24.9083	26.3179	26.3597	25.4229	23.2679	21.2990	20.3232	19.3232	21.2990	21.2990	23.2420	24.4864
144.68	22.7019	22.7141	22.7297	21.7449	19.4088	17.2160	16.0168	16.0168	16.0168	16.0168	19.5601	21.0074
48.7092	72.2471	97.3235	126.3743	137.4489	158.0082	219.1773	277.9183	310.9147	339.0565	359.8434	22.2374	

Radius from Eye (km)

Figure C5. Wind speed and direction fields, Snapshot 4, Hurricane Gilbert (Continued)

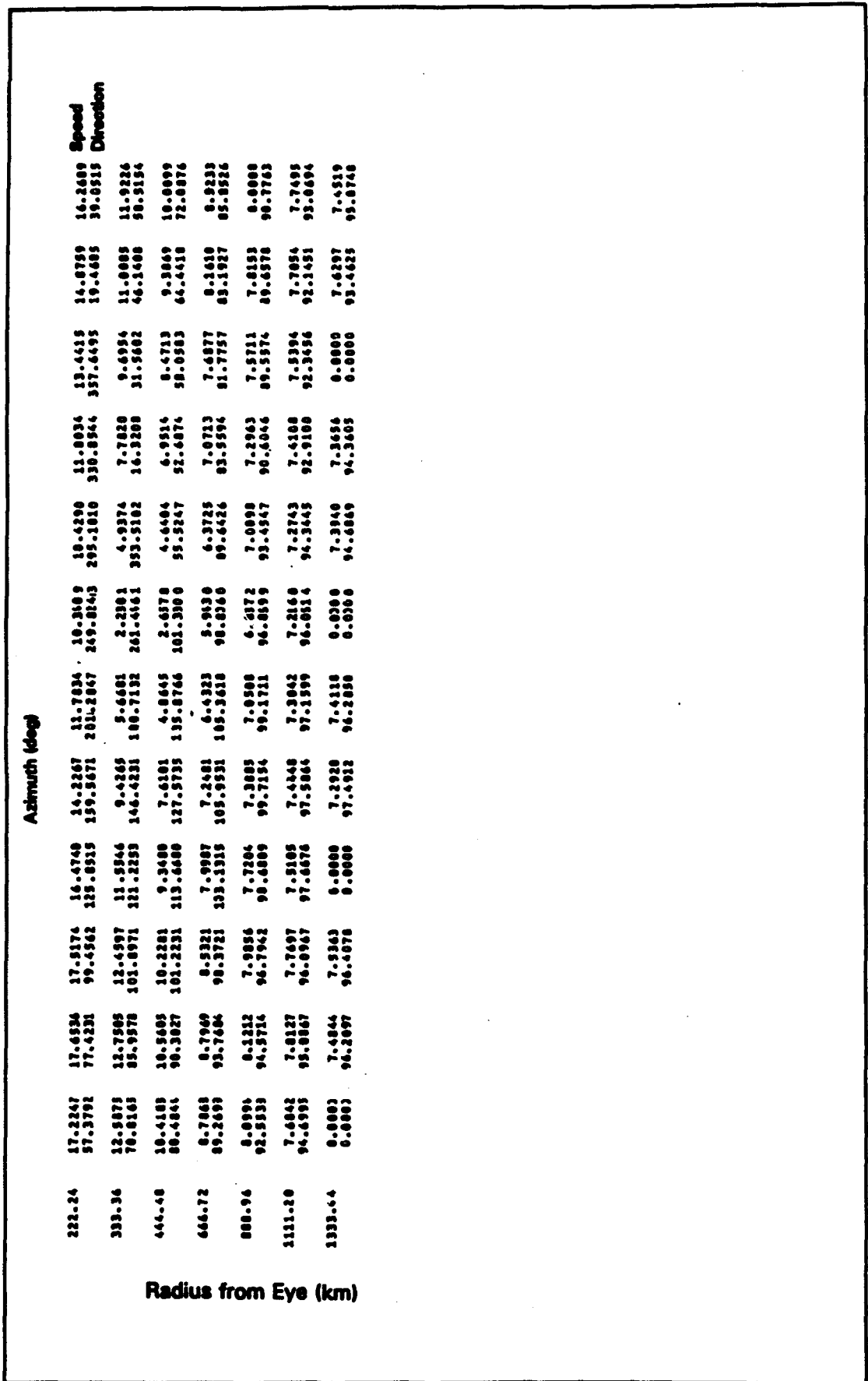


Figure C5. (Concluded)

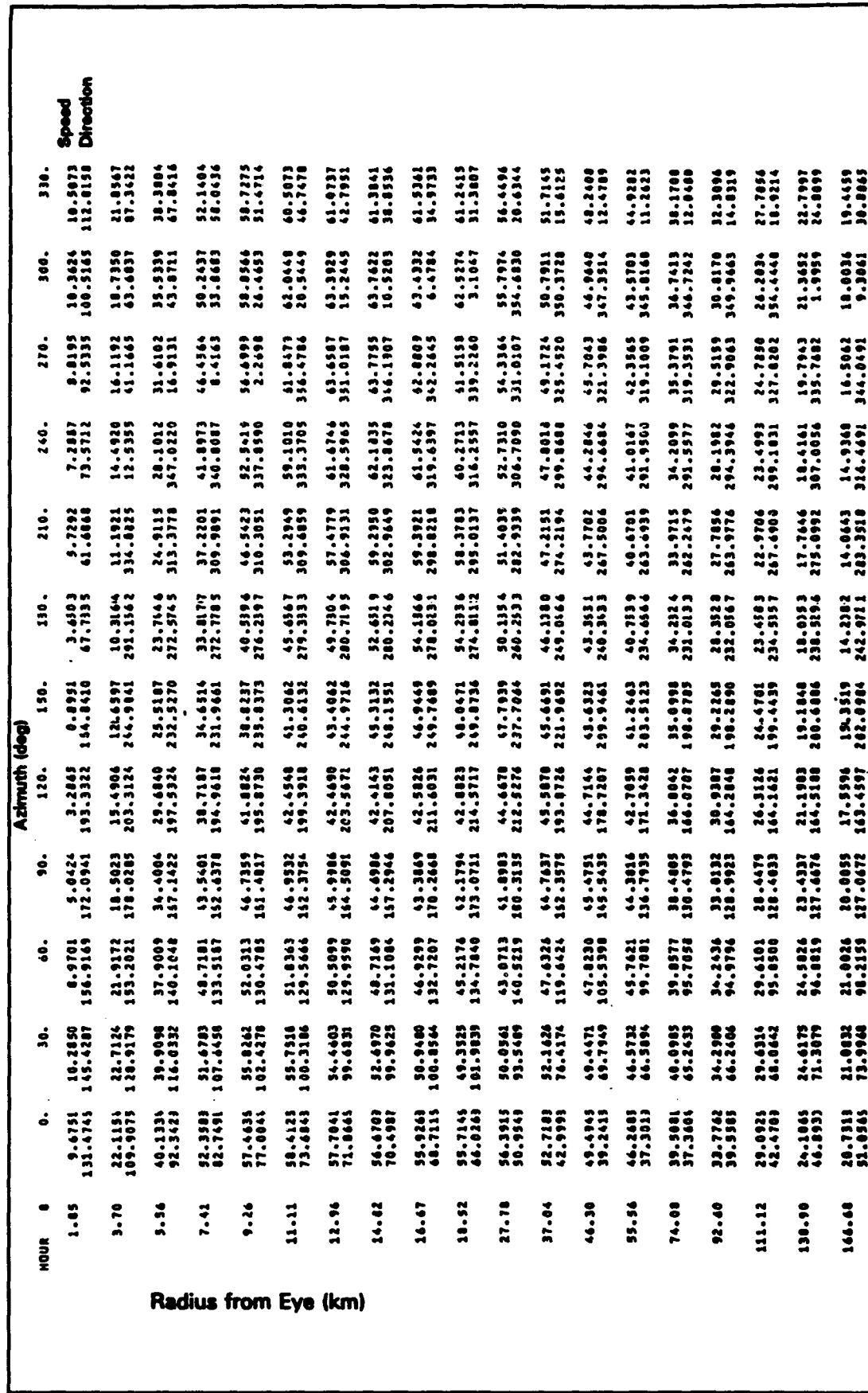


Figure C6. Wind speed and direction fields, Snapshot 5, Hurricane Gilbert (Continued)

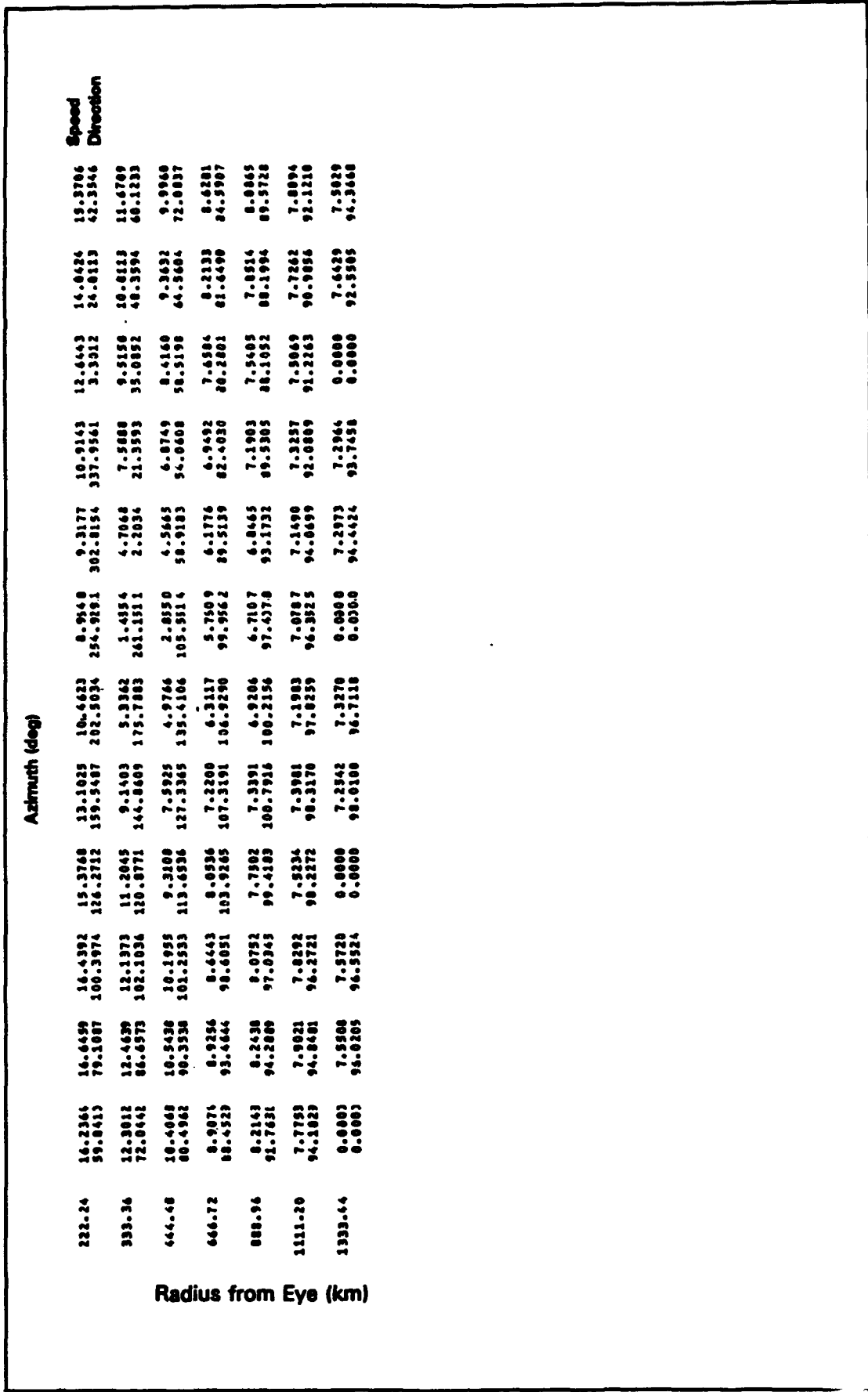
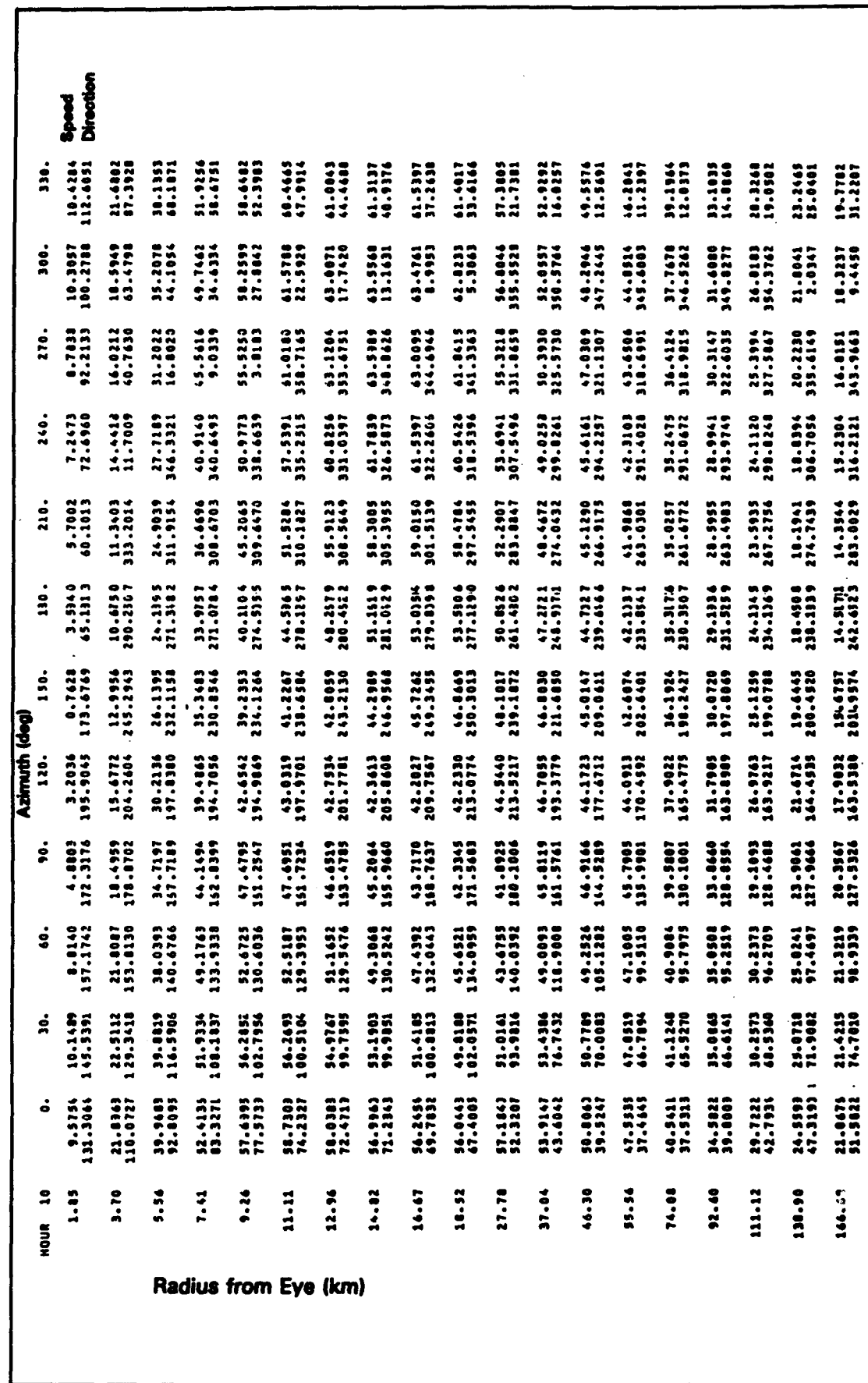


Figure C6. (Concluded)



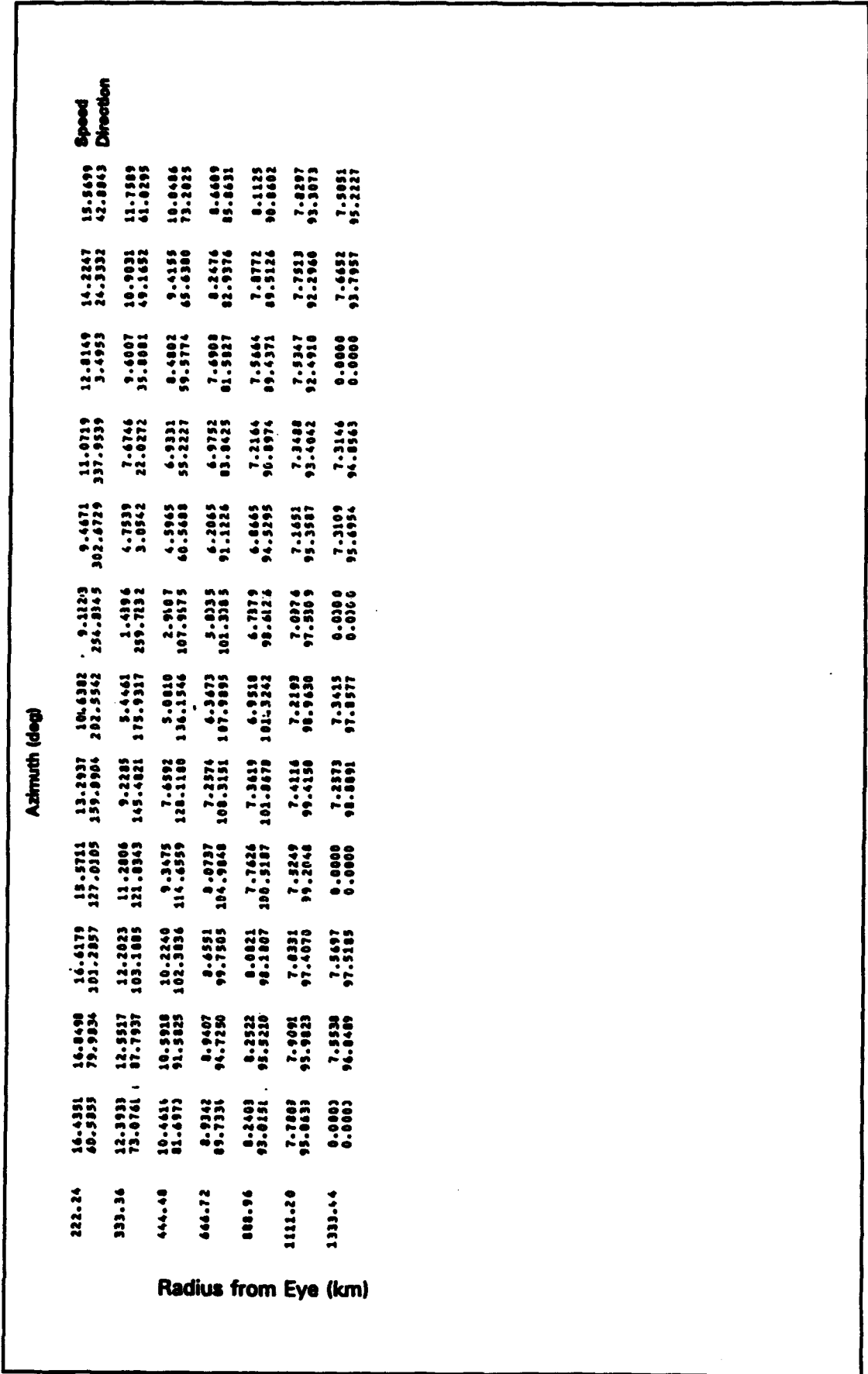


Figure C7. (Concluded)

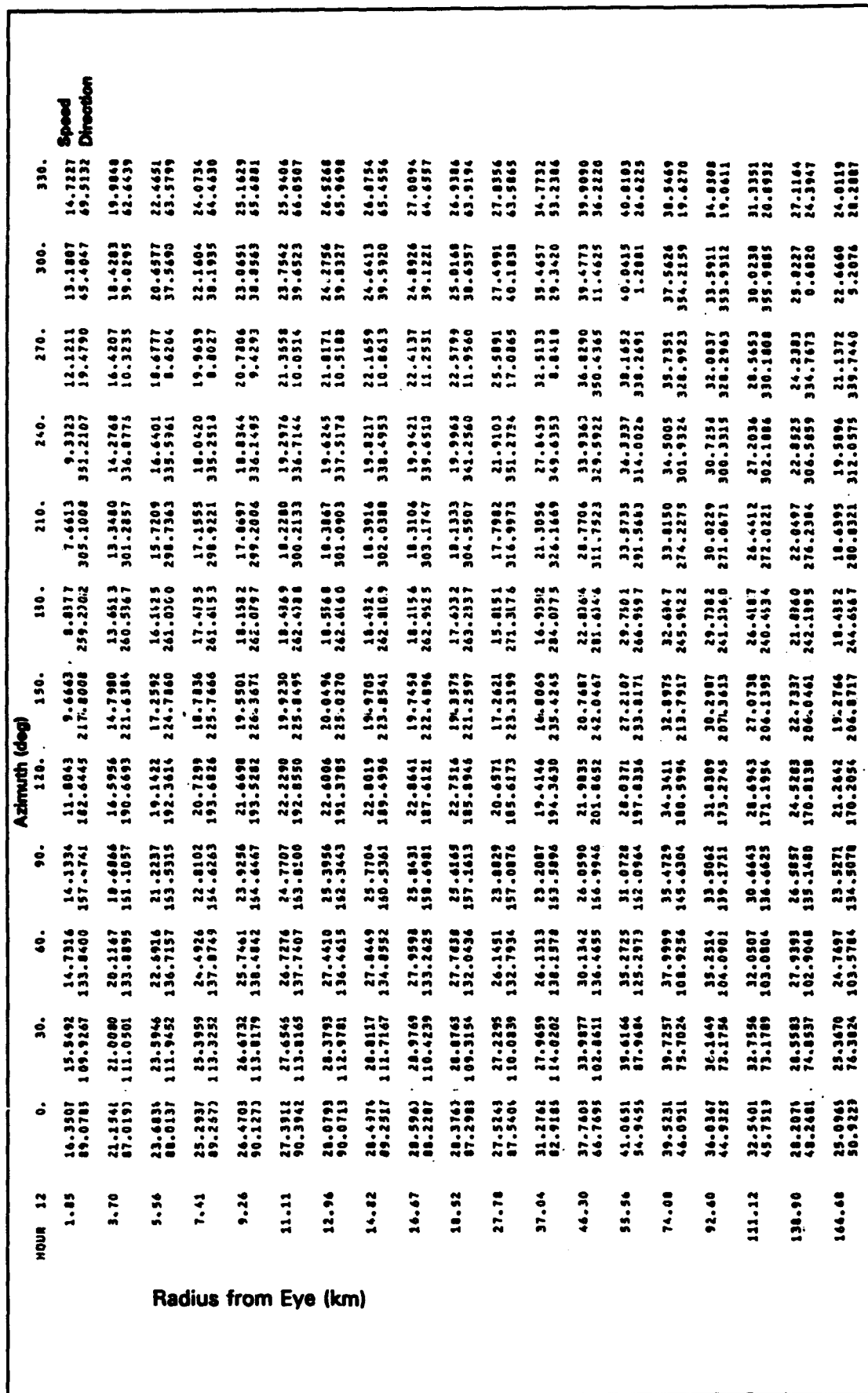


Figure C8. Wind speed and direction fields, Snapshot 7, Hurricane Gilbert (Continued)

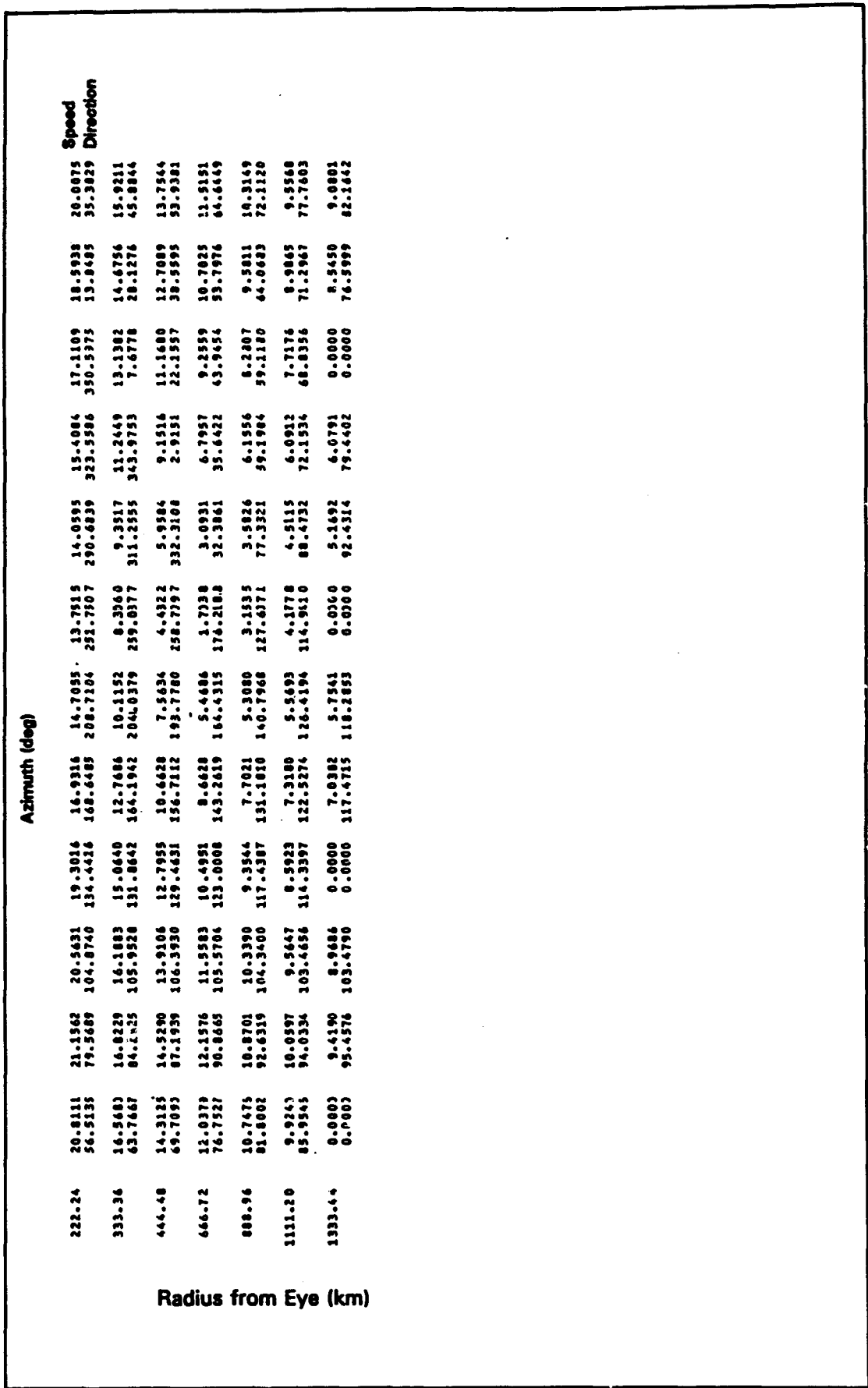


Figure C8. (Concluded)

HOUR	Radius from Eye (km)	Azimuth (deg)									Speed	Direction	
		0.	30.	60.	90.	120.	150.	180.	210.	240.			
1.85	6.3167	6.2123	5.7882	5.1633	4.7461	4.7461	5.1345	5.4502	5.8912	6.4114	6.8043	6.7548	
3.70	9.3112	9.0862	8.2132	6.4910	4.1880	2.4063	2.4063	3.6093	5.8876	7.4573	8.6332	107.4558	
5.56	13.2142	13.0437	12.2754	10.6279	8.2434	5.1929	3.9355	5.1488	7.9992	10.1942	12.7349	12.7349	
7.41	16.8883	17.0289	16.2297	14.5931	12.3905	10.0180	8.8706	9.8225	11.5762	13.3150	15.0222	16.1679	
9.26	9.79123	11.93265	14.16770	16.53396	19.3507	230.2839	277.5774	322.8787	337.6623	26.3510	31.7243	75.3035	
11.11	23.10222	23.7701	23.0668	21.1463	18.5180	16.0879	14.9322	15.4324	16.6294	18.3807	20.1093	21.8452	
12.96	25.6683	26.3959	25.6746	23.6869	20.7933	18.6016	16.7268	17.0477	18.0475	19.5045	22.0999	24.0113	
14.82	27.6935	27.64618	27.64645	25.95662	22.4223	19.3911	17.8150	18.0439	19.4860	21.5614	23.6559	25.7190	
16.67	93.90931	116.54061	139.22286	164.24666	192.3346	227.2160	267.0525	304.0743	341.5164	13.0513	42.1914	69.1750	
18.52	29.14692	30.71179	29.56551	27.7269	24.1947	20.3251	16.3937	19.3817	21.0763	23.7232	26.1338	26.1338	
20.37	80.2622	112.1667	136.6959	159.7269	188.0776	223.4442	265.3289	304.8276	343.5373	13.6230	40.4521	64.4047	
22.22	30.12255	29.9086	28.9396	26.7639	23.5632	20.0442	18.3633	18.7669	20.3842	22.7366	25.075	27.1694	
24.08	35.90441	36.45463	28.3870	25.1491	21.2910	16.0711	19.7367	25.7924	33.8092	39.1071	42.2181	44.1126	
25.94	47.7531	45.9381	39.9193	34.2497	30.9906	31.6531	35.6531	48.2667	43.6494	44.7797	46.7222	47.1961	
26.30	43.7292	38.1410	32.6844	26.4438	22.9905	19.2543	17.7383	20.4126	25.5789	30.1293	32.2792	31.9115	
28.16	43.3261	40.91747	32.7295	37.6473	186.7729	224.4622	273.0611	310.7719	352.2397	16.5688	39.3419	62.5939	
30.02	47.7271	46.7271	46.1813	32.5712	27.3968	23.1957	23.2959	34.3186	40.5223	43.2903	45.9395	46.11238	
31.88	51.4451	85.39882	113.9165	136.9709	154.9358	196.1668	238.3922	286.6393	322.8619	347.6337	5.1933	24.8514	49.1850
33.74	47.3931	47.7292	46.1813	32.5712	27.3968	23.1957	23.2959	34.3186	40.5223	43.2903	45.9395	46.11238	
35.60	43.3261	40.91747	32.7295	37.6473	186.7729	224.4622	273.0611	310.7719	352.2397	16.5688	39.3419	62.5939	
37.46	44.2671	64.4299	64.1783	62.7210	41.4710	39.4451	38.9101	39.0944	39.4565	40.7029	41.9655	43.1862	
39.32	40.1929	39.71190	34.9954	33.9626	32.1515	30.4496	29.3938	29.2223	29.5757	30.7724	32.1345	33.4266	
41.18	36.1693	38.4352	30.3078	29.4091	27.3710	25.3397	24.6243	24.2397	24.7240	26.0802	27.4366	28.7774	
43.04	43.9341	47.51160	57.6649	327.8675	162.9317	197.5139	232.4844	267.1837	298.4638	326.8257	354.3222	19.1913	

Figure C9. Wind speed and direction fields, Snapshot 8, Hurricane Gilbert (Continued)

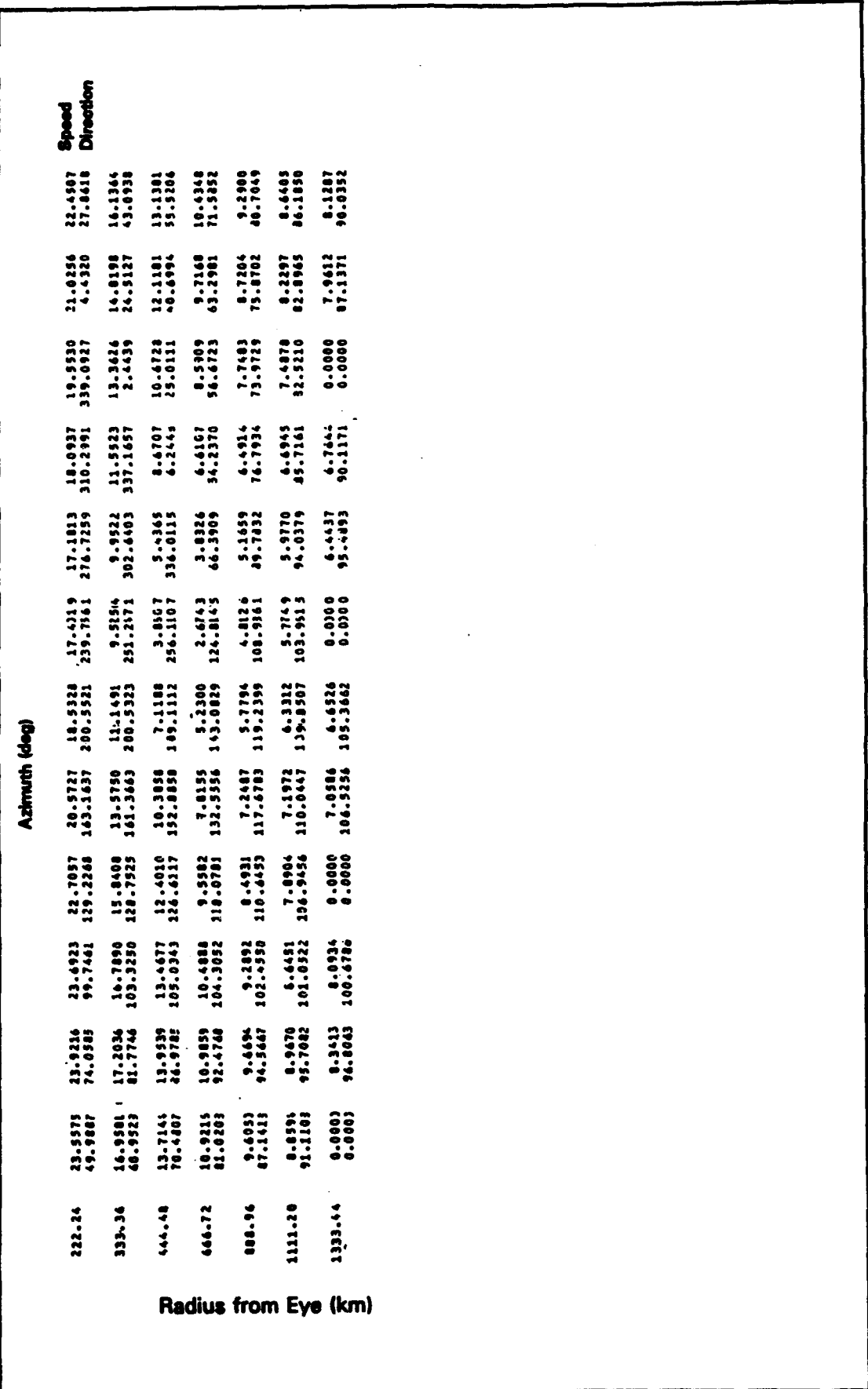


Figure C9. (Concluded)

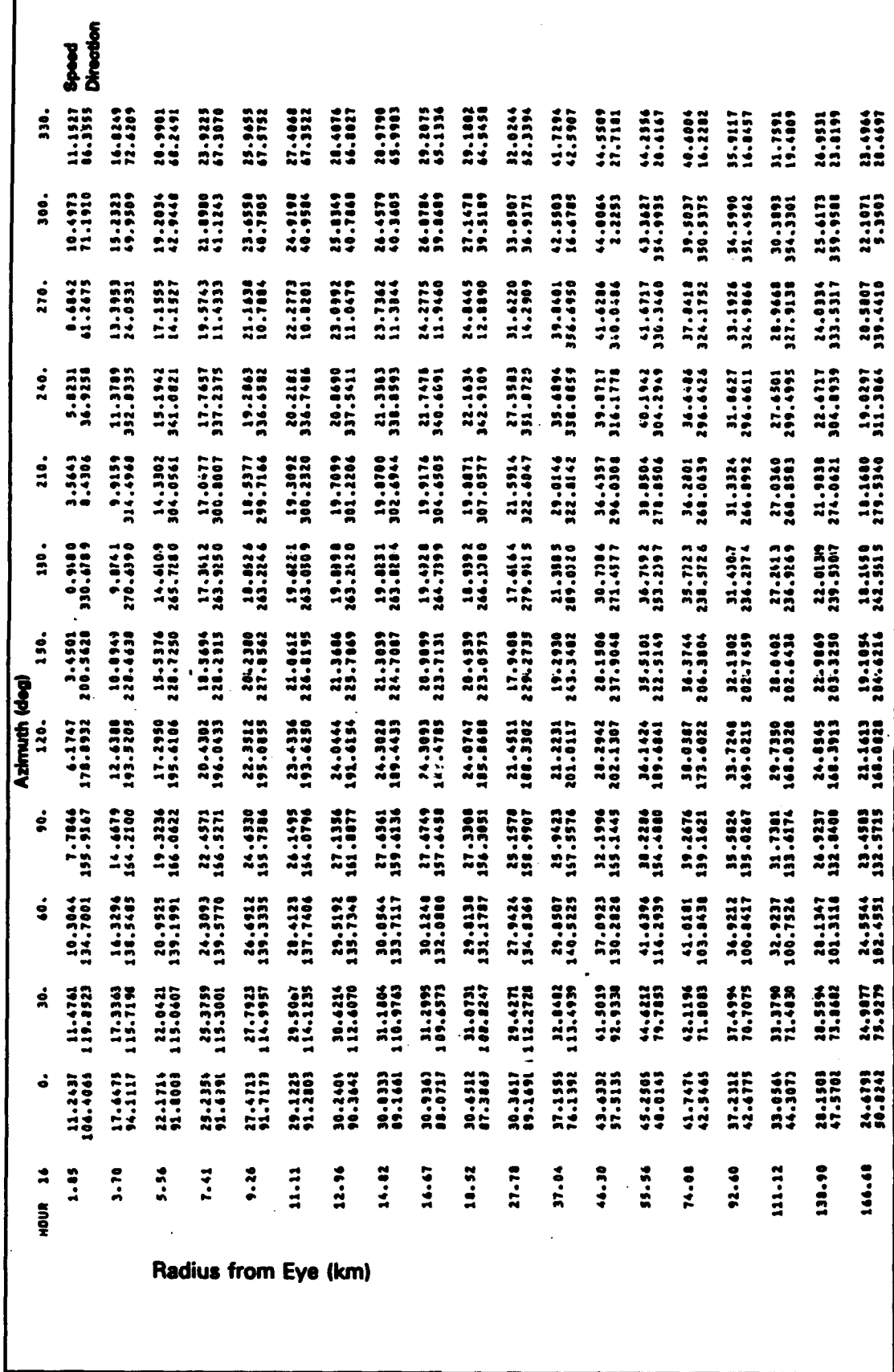


Figure C10. Wind speed and direction fields, Snapshot 9, Hurricane Gilbert (Continued)

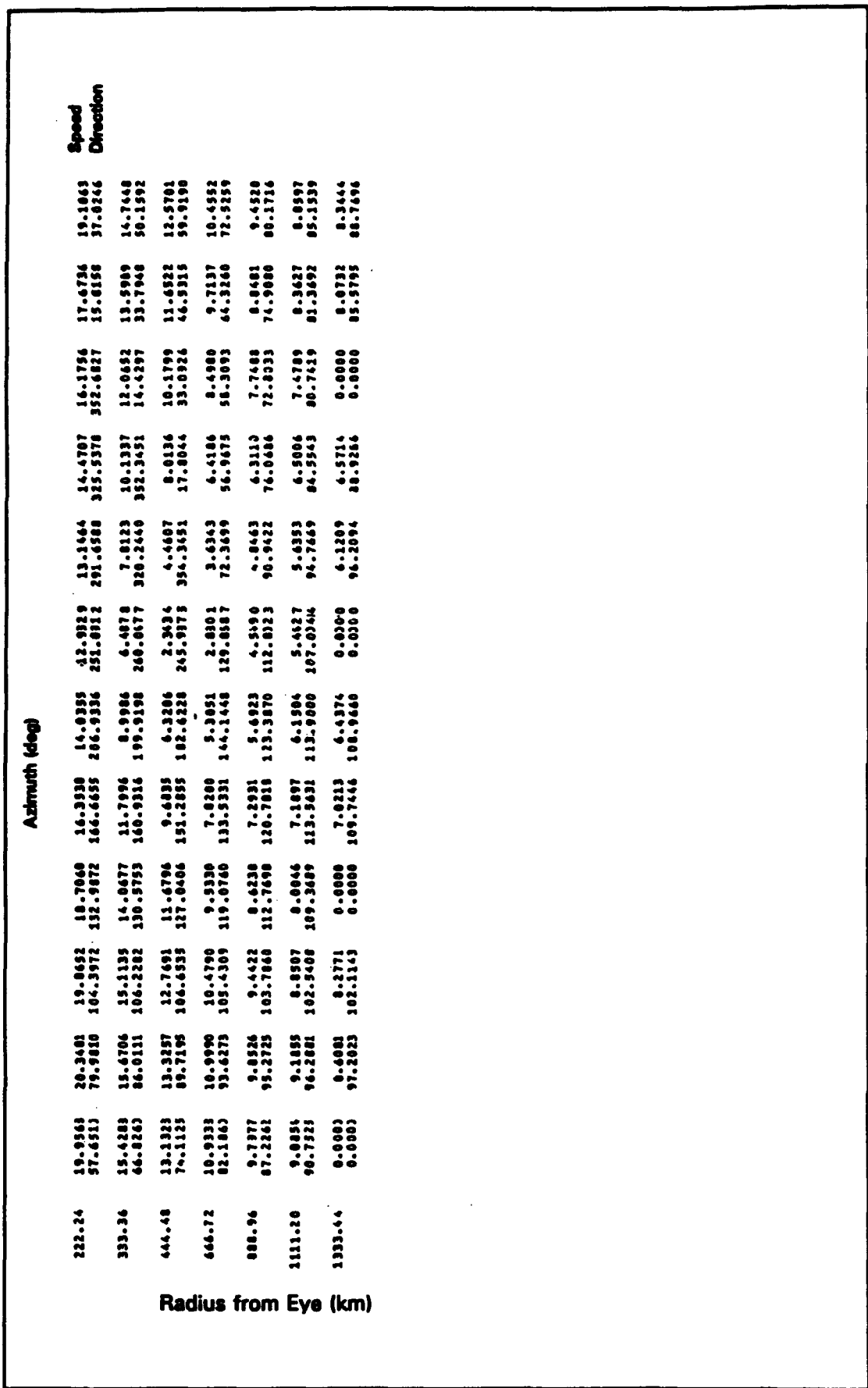


Figure C10. (Concluded)

Hour	Radius from Eye (km)	Azimuth (deg)										Speed	Direction
		0.	30.	60.	90.	120.	150.	180.	210.	240.	270.		
1.05	5.8791	5.8192	5.7591	5.724	5.7350	5.7720	5.8250	5.8780	5.9223	5.9668	5.9664	5.9486	5.9486
104.9437	105.1000	104.6491	103.6973	102.880	102.0790	101.6304	101.4965	101.1503	102.8366	103.1457	103.1457	103.5127	103.5127
3.70	4.0381	5.8556	5.4873	5.4093	5.4993	5.4977	5.8229	5.9268	6.0137	6.0592	6.1477	6.1777	6.1777
5.56	4.4052	6.2755	5.8663	5.4997	5.2914	5.2809	5.5704	5.6918	5.9702	6.2115	6.4694	6.8159	6.8159
109.5462	112.4160	113.8568	111.2192	108.4607	104.0910	100.2931	98.5566	97.4455	96.6729	101.3262	101.3262	101.3813	101.3813
7.41	8.1022	7.5052	6.7850	5.8232	4.8059	4.0650	3.9226	4.4891	5.6382	6.9329	7.9069	8.1191	8.1191
108.7143	117.0380	124.8824	128.4530	125.8730	116.1497	102.1179	91.8830	84.4838	87.8724	93.9237	100.7391	100.7391	100.7391
9.24	10.3157	9.8020	9.0202	7.4588	5.1709	2.8452	0.9344	3.0884	5.5816	7.6019	9.2662	10.1286	10.1286
105.0439	111.8488	134.0343	148.4417	160.4423	166.1832	168.8815	166.7296	168.3810	167.3143	179.2884	191.5931	191.5931	191.5931
11.11	12.8761	12.5965	11.6469	10.1689	7.8619	5.9521	2.3129	4.1879	7.2315	9.7013	11.2386	12.6221	12.6221
101.4369	120.6983	139.7655	150.4014	164.9447	217.7013	277.3317	393.4661	267.4537	47.4178	65.4497	83.5906	83.5906	83.5906
12.96	15.6671	15.4980	14.5311	13.9063	11.1054	8.8946	6.9754	7.610	9.9767	12.2262	14.1036	15.2993	15.2993
98.6277	111.9411	122.3634	136.3339	133.9177	229.0041	216.8531	326.7876	7.5710	34.4339	56.4631	77.8766	77.8766	77.8766
14.82	18.6273	18.5335	17.4727	16.1361	14.1814	11.9945	10.4265	10.7774	12.5268	14.1664	16.8134	18.1419	18.1419
96.4916	117.8137	143.2739	166.4552	197.9950	230.9480	273.6279	319.2888	397.2303	267.5179	51.5986	74.1468	74.1468	74.1468
16.47	21.4323	21.7026	20.8665	19.2667	17.1703	14.6755	13.3136	13.2873	14.9666	17.2690	19.5127	21.0934	21.0934
95.2263	110.9406	143.3261	159.1313	197.4498	230.5236	273.3225	314.0730	391.4125	21.4671	47.7105	71.8767	71.8767	71.8767
18.52	24.6191	24.8264	23.926	22.1337	19.8816	17.0102	15.2121	15.4523	16.1371	19.7091	22.1439	23.8269	23.8269
94.2877	110.9921	142.2577	160.3927	196.9398	229.3966	269.6417	310.9637	369.0617	10.6115	45.5471	69.9393	69.9393	69.9393
27.18	35.5222	36.8410	32.9125	30.1679	26.4152	23.1143	21.4590	23.1348	24.4759	30.7359	34.9766	34.9766	34.9766
85.5997	109.4270	135.0929	152.9338	192.0734	228.9399	270.0502	310.9603	344.5595	12.5334	37.2657	61.2766	61.2766	61.2766
37.04	39.3999	37.7291	34.9971	31.6346	28.3959	25.4676	23.7713	29.4886	38.5245	38.4115	40.9763	46.4726	46.4726
77.1921	103.4319	110.2506	150.2511	193.7711	232.4534	274.7313	311.4034	338.9324	2.5746	25.9047	50.4494	50.4494	50.4494
46.30	49.3423	39.2836	34.9345	31.4693	28.3984	27.0173	23.2109	33.1790	37.8322	40.4875	42.4611	46.4446	46.4446
70.6902	99.7431	120.8866	160.7063	194.4644	236.4919	273.4991	305.8359	329.1547	352.0350	15.2129	41.1493	41.1493	41.1493
55.96	41.7935	39.9269	35.9911	31.3238	28.7288	26.4614	21.8145	35.4987	38.5344	40.6359	42.3464	43.8039	43.8039
64.7161	66.4463	120.4886	162.2574	195.1939	230.4906	273.2194	299.1604	322.4314	36.9380	87.1331	36.8233	36.8233	36.8233
-0.04	51.0643	50.1187	46.2899	32.2104	20.3981	16.9071	12.9192	25.1227	36.8094	39.3970	40.2996	40.9471	40.9471
55.5161	57.4422	122.7976	160.1244	198.9955	233.5294	263.1859	286.8892	313.5711	338.4441	2.2226	27.4732	27.4732	27.4732
92.49	39.5187	39.9413	36.7864	33.3399	31.4998	31.2726	31.9172	33.3039	34.6699	36.2576	37.7727	38.7346	38.7346
138.90	34.7661	34.9126	34.9269	32.4345	30.5914	28.9449	26.3984	29.7139	30.9772	32.4236	33.6645	33.6645	33.6645
146.68	31.8693	32.9561	31.3974	30.6472	29.2689	26.3565	25.5599	26.6123	26.8729	27.976	29.5903	30.7119	30.7119
44.3329	44.3329	102.1377	134.6385	169.2289	205.6914	246.4537	272.9894	303.6312	331.7113	357.6796	371.8916	371.8916	371.8916

Figure C11. Wind speed and direction fields, Snapshot 10, Hurricane Gilbert (Continued)

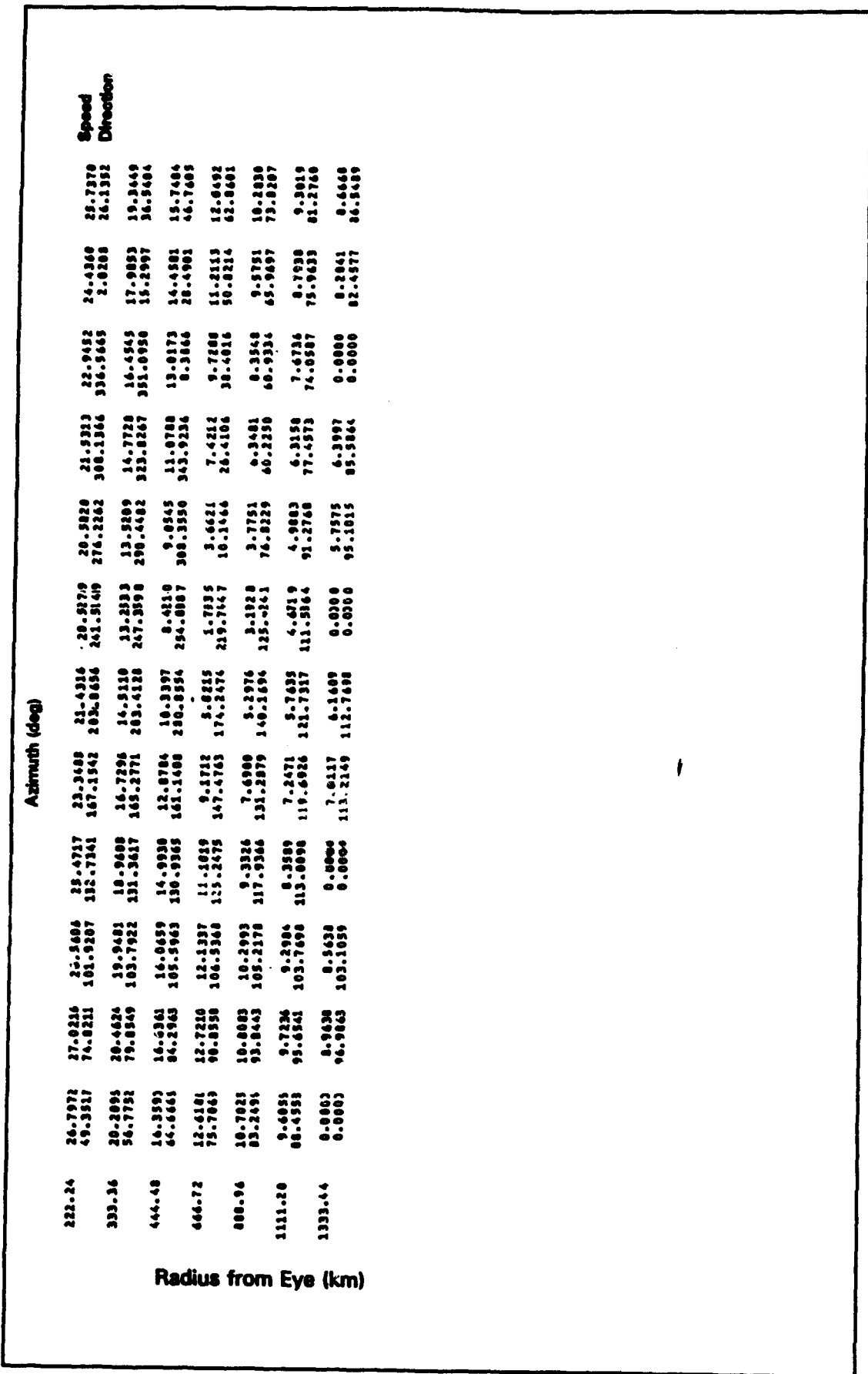
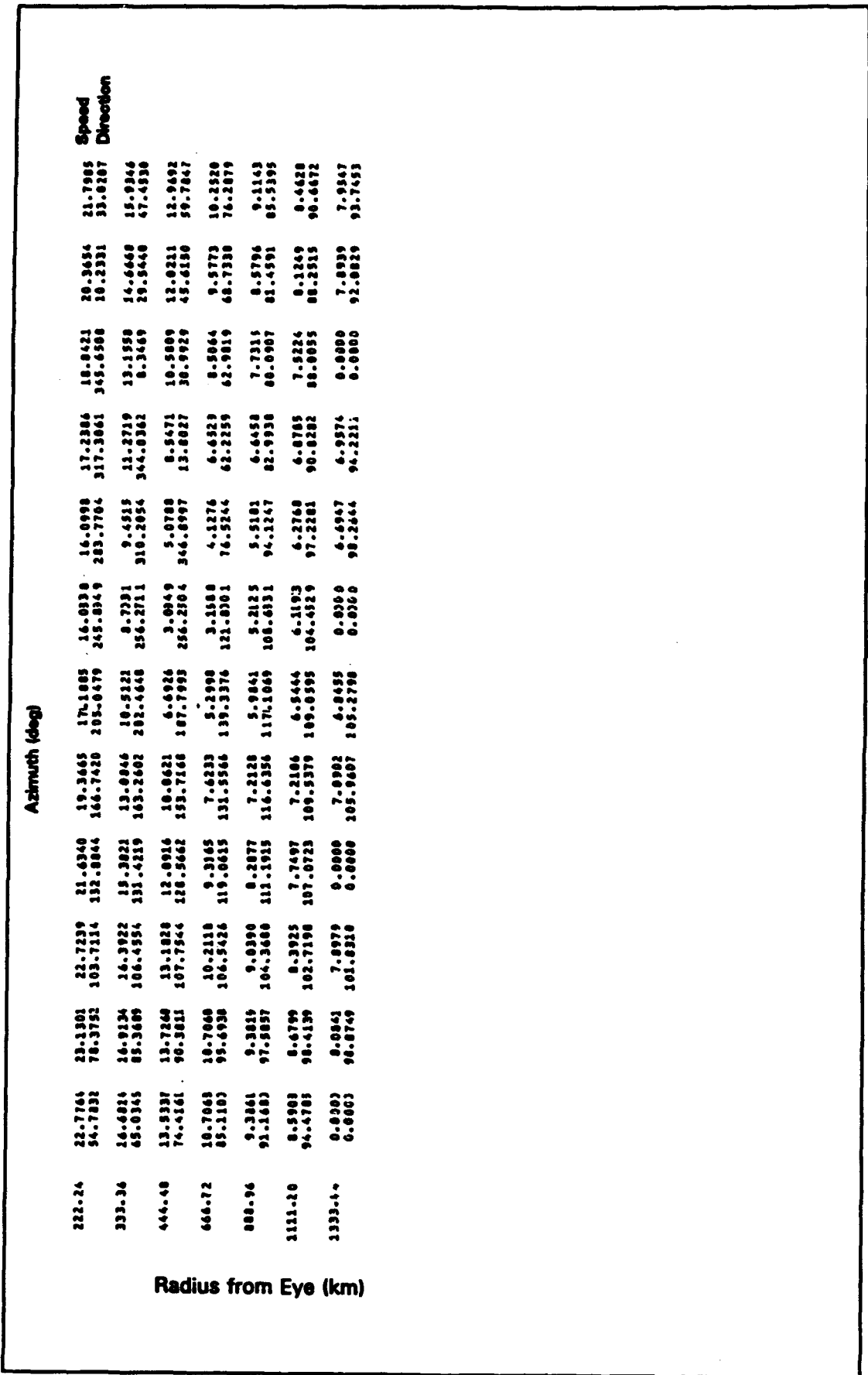


Figure C11. (Concluded)

Hour	Radius from Eye (km)	Azimuth (deg)										Speed	
		0.	10.	20.	30.	40.	50.	60.	70.	80.	90.		
1.45	5.9395	5.8823	5.8475	5.8352	5.8931	5.8916	5.9174	5.9167	6.0003	6.0003	6.0003	5.9767	
3.70	3.9811	5.8669	5.7664	5.7365	5.7774	5.8698	5.9524	5.9304	6.0798	6.1027	6.1330	6.0221	
5.56	6.1933	5.9303	5.7101	5.4101	5.4446	5.7917	5.9105	6.0720	6.1500	6.2274	6.3004	6.3446	
7.41	6.7665	6.2669	5.7929	5.781	5.3467	5.4262	5.7160	5.9119	6.1369	6.4120	6.7201	6.9235	
9.26	8.2391	7.4281	6.4723	5.7277	4.6736	4.1552	4.9163	5.2863	5.7371	6.7553	7.4339	8.1043	
11.11	10.9037	11.7212	12.47192	12.6361	12.8139	11.47497	10.0397	92.5068	87.6621	87.7064	94.8223	101.9703	
12.94	12.9992	12.5985	11.4842	10.3957	8.2692	5.3897	2.9532	4.1778	7.4666	10.8225	11.7933	12.9932	
14.82	15.9861	15.6482	14.9280	13.4136	11.7990	9.3839	7.9165	7.5269	10.2768	12.4714	14.4066	16.2130	
16.67	19.2391	19.2051	18.5467	17.1986	15.1895	12.4795	10.5149	10.4905	12.0813	15.6470	17.7775	19.9106	
18.52	22.7201	22.8847	22.2024	20.6210	18.3616	15.9631	12.9013	13.3014	15.9718	18.9824	21.0770	22.3292	
20.36	35.7231	34.5609	32.6769	29.9005	26.1567	22.3295	21.4734	25.3618	31.3325	36.2174	38.5119	37.2980	
22.20	42.5229	35.5777	32.1298	28.8985	27.0031	29.3277	36.4634	41.1668	46.4935	46.7209	46.9806	50.7563	
24.04	49.4133	38.2159	34.4094	30.4117	29.5100	26.7508	31.12416	33.4404	39.3.8004	46.1769	42.6763		
27.78	67.6465	112.6603	138.1398	165.4177	195.4956	232.7752	277.7592	318.3113	347.6441	10.5687	33.9714	52.6456	
30.64	46.0261	46.3777	39.7195	35.2557	34.9766	37.6124	39.7897	41.5712	43.2427	44.9356	49.6401		
32.40	49.4595	46.4922	39.4321	37.5463	35.8956	34.4616	33.9822	34.4173	35.1465	36.4932	37.9064	39.1431	
34.30	42.1673	37.9512	33.7562	31.3806	31.7468	35.1369	39.3362	42.5312	44.4370	46.0325	46.9325		
35.56	46.0261	46.3777	39.7195	35.2557	34.9766	37.6124	39.7897	41.5712	43.2427	44.9356	49.6401		
37.40	43.4113	43.4444	41.3370	38.4435	37.4837	36.3536	36.6192	37.4987	38.5452	39.7370	41.4629		
39.00	48.0063	77.986	112.6982	156.3196	185.6686	210.6669	249.3782	276.9476	304.2915	330.7660	355.9180	371.2849	
41.12	37.0091	37.2925	36.4285	35.3346	33.3221	31.6798	31.0519	31.3301	31.7849	32.1381	34.1381	35.8079	
44.00	44.0091	72.7627	102.6268	135.2499	171.6314	205.3594	239.2719	276.1206	299.8626	327.3006	354.2827	39.5995	
46.20	32.3885	32.1023	32.2468	31.9266	29.9466	27.2892	26.4192	26.4193	26.4194	26.3159	29.0994	31.1434	
46.2701	73.3987	101.4861	135.4826	165.0262	203.3277	238.4256	271.7739	301.9199	330.3402	357.2231	371.7717		
48.6255	28.5681	28.6026	28.4113	27.3226	25.1770	23.1919	22.3196	22.3491	22.9469	24.4161	25.9338	27.2816	
50.66	48.6255	74.5154	101.9119	135.4959	167.0395	203.3592	239.7785	274.7785	301.9199	330.3402	357.2231	371.7717	

Figure C12. Wind speed and direction fields, Snapshot 11, Hurricane Gilbert (Continued)

**Figure C12. (Concluded)**



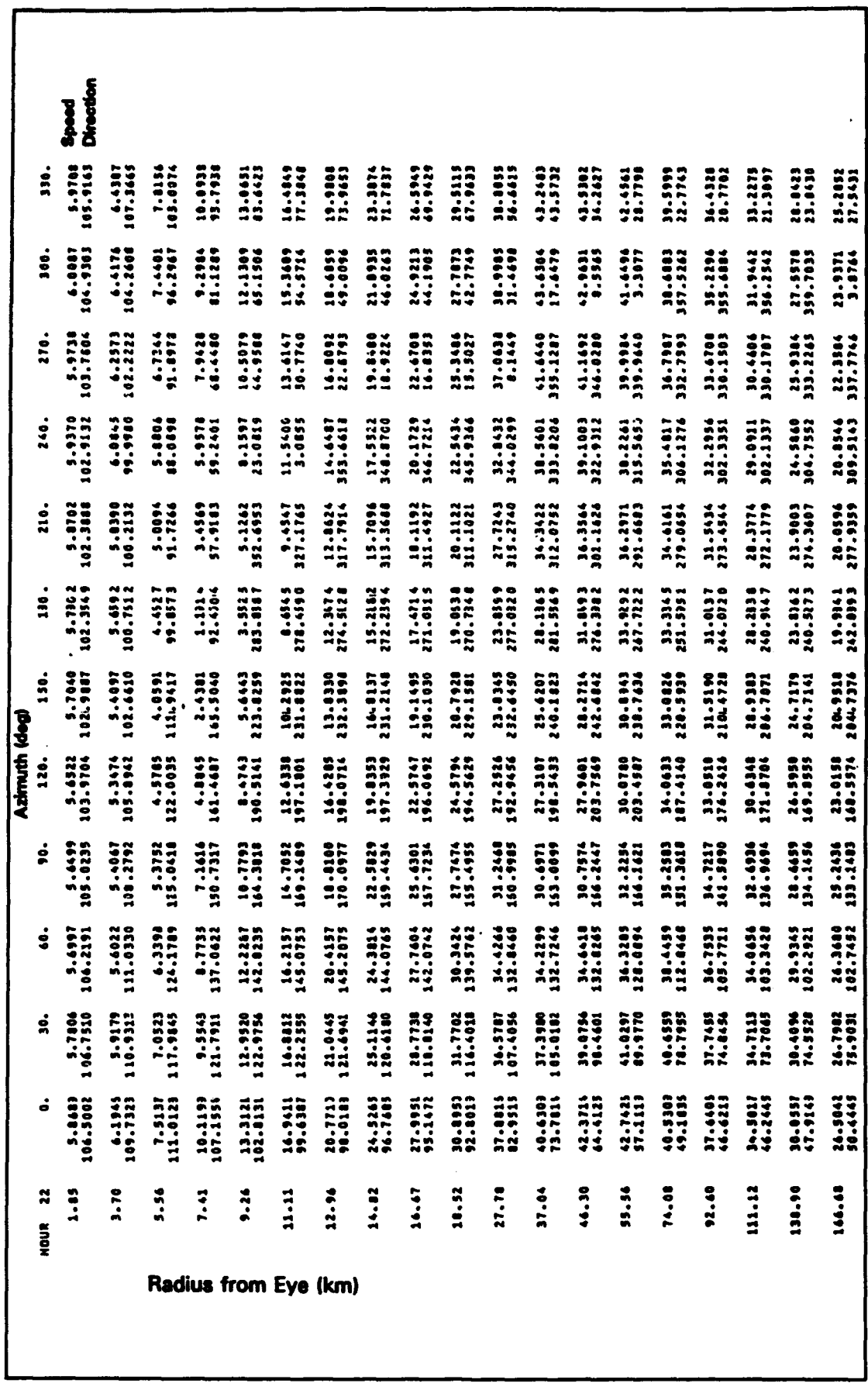


Figure C13. Wind speed and direction fields, Snapshot 12, Hurricane Gilbert (Continued)

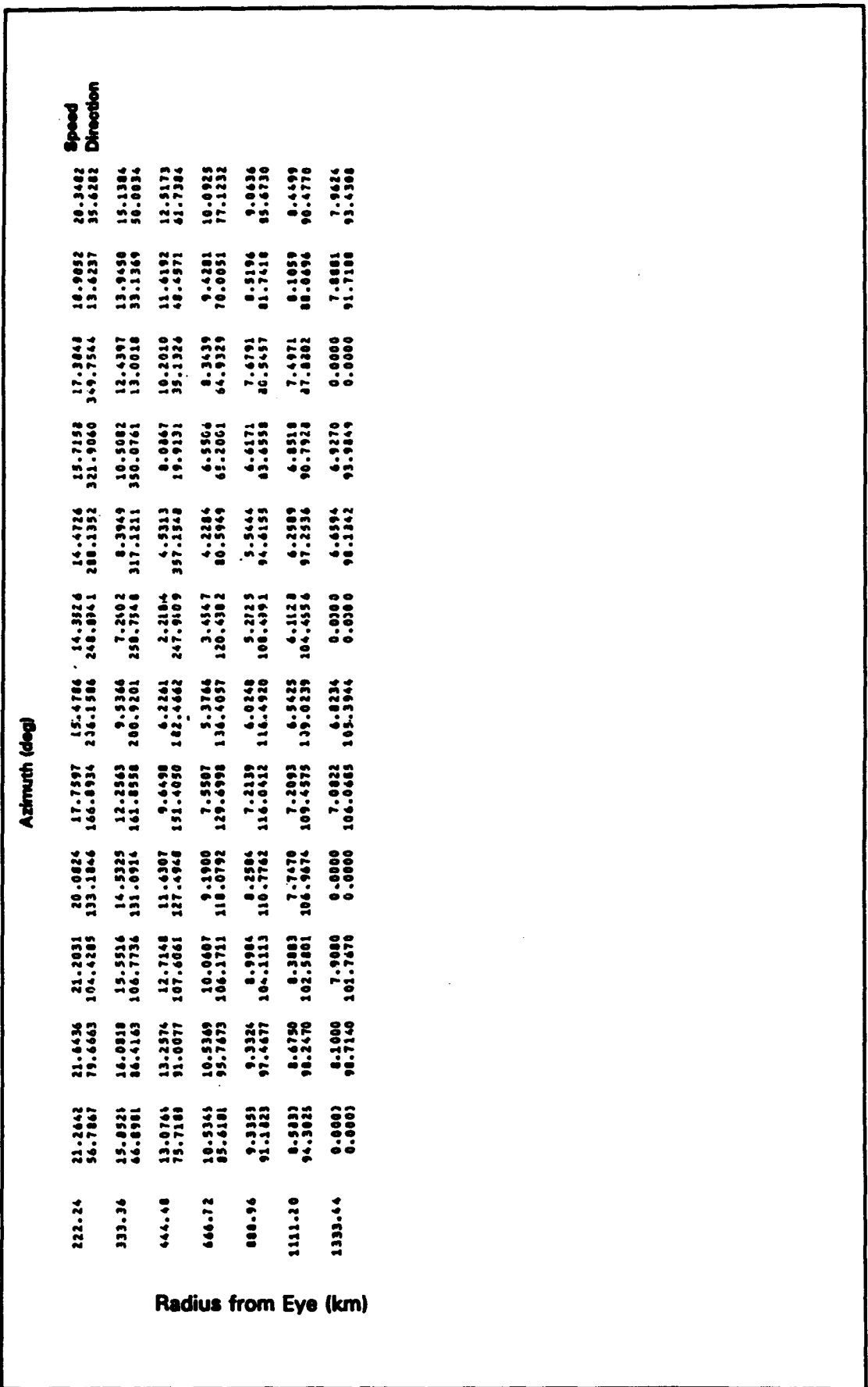


Figure C13. (Concluded)

\$ ASSIGN GILB.WIND21 FOR020  
 \$ ASSIGN GILB.WIND18 FOR018  
 \$ RUN AZIM\_AVER

Radius (n.m.)	Radius (km)	--- Wind Speed ---		Inflow Angle,
		Scalar Avg. (m/sec)	Vector Avg. (m/sec)	(+ = in, - = out) (deg)

WIND,HOUR		20	0	
1.	1.852	5.9405	0.0583	242.9772
2.	3.704	5.9437	0.1176	243.5015
3.	5.556	5.9498	0.1792	244.4864
4.	7.408	5.9595	0.2443	245.8895
5.	9.260	5.9755	0.3159	248.0143
6.	11.112	5.0049	0.4017	251.6257
7.	12.964	5.0747	0.5263	259.0292
8.	14.816	5.2682	0.7831	-85.1015
9.	16.668	5.7908	1.4971	-61.3046
10.	18.520	7.8736	3.2177	-39.8814
15.	27.780	25.7127	25.8542	0.0638
20.	37.040	39.1360	37.0043	14.4071
25.	46.300	39.8450	38.6980	21.4880
30.	55.560	39.2075	38.2327	26.3533
40.	74.080	35.9664	36.4542	35.2711
50.	92.600	36.7457	34.4134	40.8962
60.	111.120	32.1222	31.8455	43.3617
75.	138.900	27.6395	27.3607	43.5430
90.	166.680	23.5362	23.2120	41.9669
120.	222.240	17.3512	16.8293	36.0960
180.	333.360	13.8521	9.6021	23.6111
240.	444.480	7.9560	5.4558	15.0186
360.	666.720	7.4514	1.7981	10.4387
480.	888.960	7.4233	0.6930	11.4414
600.	1111.200	7.4100	0.3141	6.7318
720.	1333.440	6.9126	0.1089	-12.1050

WIND,HOUR		20	1	
1.	1.852	5.9644	0.0565	240.5800
2.	3.704	5.9677	0.1138	241.0424
3.	5.556	5.9738	0.1730	241.9138
4.	7.408	5.9834	0.2350	243.1496
5.	9.260	5.9985	0.3022	245.0328
6.	11.112	5.0250	0.3803	248.1936
7.	12.964	5.0830	0.4864	254.5270
8.	14.816	5.2368	0.6847	268.6367
9.	16.668	5.6499	1.2092	-68.0856
10.	18.520	7.5427	2.5093	-45.4020
15.	27.780	23.5379	22.5697	-2.4338
20.	37.040	33.3208	37.1779	14.3794
25.	46.300	42.0500	41.0345	23.7352
30.	55.560	41.5028	40.6994	29.0430
40.	74.080	37.9929	37.5078	35.4472
50.	92.600	36.9229	34.5727	39.4681
60.	111.120	32.1931	31.8974	41.7004
75.	138.900	23.1118	27.8268	42.5412
90.	166.680	24.3038	23.9868	41.6276
120.	222.240	13.2532	17.7728	36.8113
180.	333.360	11.5444	10.4276	25.1562
240.	444.480	3.2821	6.0906	15.3304
360.	666.720	7.4668	2.0921	10.6132
480.	888.960	7.4237	0.8189	11.3564
600.	1111.200	7.4093	0.3746	7.6189
720.	1333.440	6.9128	0.1289	-8.0063

Snapshot 1

Interpolation between  
Snapshots 1 & 2

Figure C14. Azimuthally averaged speed and inflow angle, Hurricane Gilbert (Sheet 1 of 12)

Radius (n.m.)	Radius (km)	Scalar Avg. (m/sec)	Vector Avg. (m/sec)	Inflow Angle, (+ = in, - = out) (deg)
---- Wind Speed ----				
WIND,HOUR		20	2	
1.	1.852	5.9885	0.0548	238.0248
2.	3.704	5.9919	0.1102	238.4156
3.	5.556	5.9982	0.1672	239.1560
4.	7.408	5.0076	0.2264	240.1999
5.	9.260	5.0220	0.2895	241.7754
6.	11.112	5.0457	0.3604	244.3654
7.	12.964	5.0921	0.4500	249.2603
8.	14.816	5.2074	0.5968	263.4110
9.	16.668	5.5173	0.9457	-78.7729
10.	18.520	7.2460	1.8151	-55.4724
15.	27.780	20.4553	19.1466	-5.2852
20.	37.040	33.5064	37.3467	14.3384
25.	46.300	46.2971	43.3895	25.7404
30.	55.560	43.8676	43.1995	31.4260
40.	74.080	39.0180	38.5573	35.6167
50.	92.600	35.1224	34.7513	38.0579
60.	111.120	32.2916	31.9735	40.0499
75.	138.900	23.5935	28.3006	41.5780
90.	166.680	25.0731	24.7614	41.3158
120.	222.240	19.1630	18.7172	37.4373
180.	333.360	12.2446	11.2392	26.5320
240.	444.480	3.6870	6.7227	17.4240
360.	666.720	7.4862	2.3823	10.7159
480.	888.960	7.4253	0.9447	11.2861
600.	1111.200	7.4090	0.4350	8.2587
720.	1333.440	4.9130	0.1493	-5.0173
WIND,HOUR		20	3	
1.	1.852	5.8402	0.7731	-75.1767
2.	3.704	5.4599	3.0543	-50.1969
3.	5.556	5.9973	8.7711	-22.2437
4.	7.408	17.1276	16.4325	-8.7850
5.	9.260	23.7617	23.2580	-1.7680
6.	11.112	27.9470	27.5536	2.6972
7.	12.964	29.9794	29.6319	6.0785
8.	14.816	30.5931	30.2645	8.6527
9.	16.668	30.4137	30.1121	10.4360
10.	18.520	29.9044	29.6449	11.3989
15.	27.780	33.3389	32.9973	10.4108
20.	37.040	33.8700	38.9509	15.7391
25.	46.300	43.8779	39.9576	22.2504
30.	55.560	39.5400	36.7501	26.6865
40.	74.080	35.3129	35.8119	33.3749
50.	92.600	33.4908	33.1396	37.8682
60.	111.120	33.9005	30.6016	40.2691
75.	138.900	27.0636	26.7709	41.2536
90.	166.680	23.5050	23.1748	40.4313
120.	222.240	17.8497	17.3439	35.7290
180.	333.360	11.4874	10.3226	24.5473
240.	444.480	3.3587	6.1182	16.4950
360.	666.720	7.5436	2.1977	11.5892
480.	888.960	7.4797	0.9074	12.1303
600.	1111.200	7.4515	0.4313	9.1300
720.	1333.440	4.9283	0.1473	-3.2681

Figure C14. (Sheet 2 of 12)

Radius (n.m.)	Radius (km)	---	Wind Speed	---	Inflow Angle, (+ = in, - = out)
		Scalar Avg.	Vector Avg.	(m/sec)	(deg)
<b>WIND, HOUR</b>					
		20		4	
1.	1.852	5.8323	1.5088	-73.7257	
2.	3.704	7.6811	5.8655	-48.3018	Snapshot 3
3.	5.556	17.0601	16.3827	-18.8441	
4.	7.408	31.1340	30.6660	-5.6326	
5.	9.260	44.1059	43.7016	1.0484	
6.	11.112	52.0694	51.6435	5.5470	
7.	12.964	55.7219	55.1891	8.9149	
8.	14.816	55.9171	56.2661	11.6026	
9.	16.668	55.6530	55.9352	13.6930	
10.	18.520	55.4595	54.7346	15.2657	
15.	27.780	47.2739	46.6246	17.3370	
20.	37.040	41.2928	40.5148	17.0706	
25.	46.300	37.5578	36.6132	18.1098	
30.	55.560	35.4703	34.4779	20.7272	
40.	74.080	33.6395	33.0831	30.7598	
50.	92.600	31.8519	31.5189	37.6681	
60.	111.120	29.5078	29.2248	40.5194	
75.	138.900	25.5316	25.2342	40.8956	
90.	166.680	21.9416	21.5849	39.4102	
120.	222.240	15.5657	15.9818	33.7018	
180.	333.360	10.7602	9.3951	22.2754	
240.	444.480	3.1825	5.5112	15.3905	
360.	666.720	7.6131	2.0124	12.5970	
480.	888.960	7.5401	0.8702	13.0439	
600.	1111.200	7.4989	0.4276	10.0139	
720.	1333.440	6.9463	0.1454	-1.4962	
<b>WIND, HOUR</b>					
		20		5	
1.	1.852	5.2252	2.7628	-65.8165	Interpolation between Snapshots 3 & 4
2.	3.704	10.8849	9.7729	-34.6276	
3.	5.556	23.9177	23.3696	-10.5852	
4.	7.408	38.7603	38.3208	-0.9444	
5.	9.260	43.6471	49.2128	4.1015	
6.	11.112	55.1260	54.6246	7.4212	
7.	12.964	57.2447	56.6338	9.9296	
8.	14.816	57.5303	56.8154	11.9629	
9.	16.668	55.7618	55.9895	13.5702	
10.	18.520	55.3013	54.5162	14.8087	
15.	27.780	47.1459	46.3588	16.6690	
20.	37.040	41.7828	40.8349	17.7450	
25.	46.300	38.5645	37.6181	21.1510	
30.	55.560	35.6946	35.9205	25.7857	
40.	74.080	34.4778	34.0738	35.2891	
50.	92.600	31.8423	31.5568	40.0867	
60.	111.120	28.8347	28.5661	41.5009	
75.	138.900	24.3943	24.0850	40.6594	
90.	166.680	23.6857	20.2947	38.4191	
120.	222.240	15.4411	14.7694	31.7297	
180.	333.360	10.0126	8.4136	20.0608	
240.	444.480	3.0213	4.8038	13.9795	
360.	666.720	7.6176	1.7291	12.1352	
480.	888.960	7.5582	0.7501	12.4990	
600.	1111.200	7.5163	0.3689	9.0158	
720.	1333.440	6.9548	0.1238	-3.6095	

Figure C14. (Sheet 3 of 12)

Radius (n.m.)	Radius (km)	--- Wind Speed ---		Inflow Angle, (+ = in, - = out)
		Scalar Avg. (m/sec)	Vector Avg. (m/sec)	
<b>WIND, HOUR</b>				
1.	1.852	5.7256	3.9907	-62.4913
2.	3.704	14.5032	13.6544	-28.3991
3.	5.556	30.8972	30.3899	-6.2408
4.	7.408	45.3251	45.8593	2.2482
5.	9.260	54.9773	54.4563	6.4809
6.	11.112	58.0636	57.4492	9.0340
7.	12.964	53.7361	58.0230	10.8773
8.	14.816	53.1499	57.3589	12.3154
9.	16.668	55.8714	56.0365	13.4475
10.	18.520	55.1522	54.2988	14.3488
15.	27.780	47.0437	46.0940	15.9946
20.	37.040	42.3020	41.1548	16.4114
25.	46.300	39.6646	38.7001	24.0330
30.	55.560	33.1960	37.5633	30.4291
40.	74.080	35.5348	35.2260	39.5457
50.	92.600	31.8955	31.6439	42.5023
60.	111.120	28.1750	27.9150	42.5365
75.	138.900	23.2591	22.9323	40.3630
90.	166.680	19.4405	19.0049	37.2775
120.	222.240	14.3366	13.5521	29.3917
180.	333.360	9.3352	7.4333	17.3851
240.	444.480	7.9289	4.0952	12.1178
360.	666.720	7.6295	1.4431	11.4411
480.	888.960	7.5739	0.6301	11.7333
600.	1111.200	7.5351	0.3103	7.6245
720.	1333.440	6.9639	0.1025	-6.6188
<b>WIND, HOUR</b>				
		20	7	
1.	1.852	5.8491	4.5236	-58.1521
2.	3.704	15.3031	15.0616	-22.8319
3.	5.556	31.6745	31.1321	-4.0379
4.	7.408	45.2941	44.7367	3.0175
5.	9.260	52.8056	52.1772	6.3979
6.	11.112	55.6764	54.9776	8.3532
7.	12.964	55.5360	55.7612	9.8517
8.	14.816	55.2909	55.4289	11.1628
9.	16.668	55.4900	54.5386	12.3841
10.	18.520	54.2968	53.2621	13.5252
15.	27.780	48.6838	47.4276	18.2287
20.	37.040	45.1281	44.1740	25.3132
25.	46.300	42.5121	41.9100	32.3032
30.	55.560	40.5284	40.1261	37.4110
40.	74.080	35.1586	35.9069	42.6494
50.	92.600	31.4613	31.2270	43.5405
60.	111.120	27.2626	27.0013	42.3935
75.	138.900	22.2634	21.9178	39.4404
90.	166.680	13.5853	18.1153	35.9769
120.	222.240	13.8112	12.9681	27.9865
180.	333.360	9.1801	7.2034	16.8972
240.	444.480	7.9265	4.0666	12.5087
360.	666.720	7.6258	1.5307	12.1834
480.	888.960	7.5713	0.7078	12.4845
600.	1111.200	7.5257	0.3684	8.9790
720.	1333.440	6.9587	0.1301	-2.1435

Figure C14. (Sheet 4 of 12)

Radius (n.m.)	Radius (km)	--- Wind Speed ---		Inflow Angle, (+ = in, - = out) (deg)
		Scalar Avg. (m/sec)	Vector Avg. (m/sec)	
<b>WIND, HOUR</b>				
1.	1.852	7.0426	5.0716	-54.7408
2.	3.704	17.1757	16.5115	-18.2037
3.	5.556	32.4857	31.9070	-1.9445
4.	7.408	44.2867	43.6128	3.8353
5.	9.260	53.5559	49.7581	6.2712
6.	11.112	53.2640	52.4012	7.5746
7.	12.964	54.2964	53.3844	8.7047
8.	14.816	54.4636	53.4694	9.9306
9.	16.668	54.1409	53.0254	11.2704
10.	18.520	53.4684	52.2117	12.6752
15.	27.780	51.3944	48.7947	20.3304
20.	37.040	43.4448	47.5966	31.2649
25.	46.300	45.0761	45.6723	39.2970
30.	55.560	43.3528	43.0839	43.4863
40.	74.080	35.8795	36.6723	45.6317
50.	92.600	31.0389	30.8200	44.6116
60.	111.120	25.3489	26.0853	42.2429
75.	138.900	21.2724	20.9049	38.3987
90.	166.680	17.7416	17.2313	34.5203
120.	222.240	13.2931	12.3823	26.4577
180.	333.360	9.0301	6.9736	16.3809
240.	444.480	7.9248	4.0382	12.9052
360.	666.720	7.6209	1.6167	12.8425
480.	888.960	7.5641	0.7856	13.0809
600.	1111.200	7.5185	0.4267	9.9572
720.	1333.440	6.9536	0.1582	0.7499
<b>WIND, HOUR</b>				
	20		9	
1.	1.852	5.9981	5.0795	-54.8159
2.	3.704	17.1768	16.5351	-18.2056
3.	5.556	32.5058	31.9429	-1.9150
4.	7.408	44.2801	43.6174	3.8725
5.	9.260	53.4746	49.6803	6.2548
6.	11.112	53.1378	52.2742	7.4287
7.	12.964	54.1663	53.2625	8.4029
8.	14.816	54.3547	53.3862	9.4955
9.	16.668	56.0787	53.0050	10.7557
10.	18.520	53.4631	52.2558	12.1347
15.	27.780	53.7277	49.1375	19.9558
20.	37.040	49.0489	46.2190	31.2943
25.	46.300	45.7582	46.3703	39.4880
30.	55.560	44.0145	43.7565	43.6872
40.	74.080	37.4074	37.2072	45.7600
50.	92.600	31.4470	31.2338	44.6753
60.	111.120	25.6654	26.4072	42.2520
75.	138.900	21.4959	21.1338	38.3407
90.	166.680	17.9024	17.3978	34.4100
120.	222.240	13.3829	12.4762	26.2241
180.	333.360	9.0683	7.0029	15.9467
240.	444.480	7.9528	4.0419	12.4316
360.	666.720	7.6355	1.6109	12.3296
480.	888.960	7.5744	0.7805	12.4548
600.	1111.200	7.5258	0.4218	9.4619
720.	1333.440	6.9565	0.1548	0.8799

Snapshot 5

Interpolation between  
Snapshots 5 & 6

Figure C14. (Sheet 5 of 12)

Radius (n.m.)	Radius (km)	--- Wind Speed ---	Inflow Angle, (+ = in, - = out)
		Scalar Avg. (m/sec)	Vector Avg. (m/sec)
WIND, HOUR		20	10
1.	1.852	5.9537	5.0869
2.	3.704	17.1782	16.5585
3.	5.556	32.5267	31.9786
4.	7.408	44.2750	43.6215
5.	9.260	53.3961	49.6013
6.	11.112	53.0167	52.1647
7.	12.964	54.0441	53.1380
8.	14.816	54.2563	53.3016
9.	16.668	54.0279	52.9847
10.	18.520	53.4681	52.3011
15.	27.780	51.0640	49.4815
20.	37.040	49.6522	48.8398
25.	46.300	47.4393	47.0666
30.	55.560	44.6752	44.4276
40.	74.080	37.9347	37.7411
50.	92.600	31.8548	31.6470
60.	111.120	25.9819	26.7288
75.	138.900	21.7196	21.3627
90.	166.680	13.0638	17.5646
120.	222.240	13.4730	12.5704
180.	333.360	9.1069	7.0325
240.	444.480	7.9816	4.0458
360.	666.720	7.6511	1.6052
480.	888.960	7.3856	0.7755
600.	1111.200	7.5338	0.4170
720.	1333.440	4.9598	0.1515
WIND, HOUR		20	11
1.	1.852	3.7297	7.8357
2.	3.704	15.9519	16.5147
3.	5.556	25.1567	25.7571
4.	7.408	32.9936	32.5674
5.	9.260	35.6307	36.1683
6.	11.112	33.3153	37.6633
7.	12.964	39.0787	38.6623
8.	14.816	39.2626	38.8826
9.	16.668	39.0661	38.7132
10.	18.520	33.3591	38.2241
15.	27.780	35.5052	36.1724
20.	37.040	35.8351	36.5306
25.	46.300	38.2610	37.9182
30.	55.560	39.2255	38.8999
40.	74.080	35.8223	36.6041
50.	92.600	32.2816	32.0769
60.	111.120	29.2033	27.9708
75.	138.900	23.4524	23.1454
90.	166.680	23.0079	19.6021
120.	222.240	15.5677	14.8986
180.	333.360	11.1093	9.7741
240.	444.480	8.9368	6.8459
360.	666.720	7.8636	3.9343
480.	888.960	7.6628	2.5745
600.	1111.200	7.5550	1.8281
720.	1333.440	4.9576	0.9003

Snapshot 6

Interpolation between  
Snapshots 6 & 7

Figure C14. (Sheet 6 of 12)

Radius (n.m.)	Radius (km)	--- Wind Speed ---	Inflow Angle,	
		Scalar Avg. (m/sec)	Vector Avg. (m/sec)	(+ = in, - = out) (deg)
WIND,HOUR		20	12	
1.	1.852	12.3410	11.8551	3.7051
2.	3.704	17.3732	17.0704	5.5010
3.	5.556	19.8249	19.5672	4.8894
4.	7.408	21.3645	21.1058	4.0851
5.	9.260	22.3264	22.0409	3.5390
6.	11.112	22.9808	22.6516	3.4733
7.	12.964	23.4277	23.0439	3.8438
8.	14.816	23.6688	23.2223	4.4859
9.	16.668	23.7225	23.2100	5.1796
10.	18.520	23.5859	23.0055	5.6476
15.	27.780	23.2624	22.4453	1.8611
20.	37.040	25.1342	25.5009	0.3552
25.	46.300	31.0352	30.4071	10.2215
30.	55.560	35.0799	34.4948	21.2548
40.	74.080	35.0679	35.7961	34.1508
50.	92.600	32.8376	32.6266	37.4436
60.	111.120	29.4805	29.2604	37.3449
75.	138.900	25.2107	24.9394	35.4033
90.	166.680	21.9817	21.6405	33.0628
120.	222.240	17.7000	17.1812	28.0628
180.	333.360	13.3470	12.4114	21.4082
240.	444.480	10.9123	9.5324	17.4889
360.	666.720	8.6205	6.1845	15.2893
480.	888.960	7.9491	4.2965	15.4385
600.	1111.200	7.6724	3.1780	14.7235
720.	1333.440	5.0044	1.6352	13.5201
WIND,HOUR		20	13	
1.	1.852	7.7009	6.5613	-2.0170
2.	3.704	11.4624	10.8461	-1.3424
3.	5.556	14.6585	14.2437	-0.4667
4.	7.408	17.3708	17.0409	0.1374
5.	9.260	19.5312	19.2268	0.5209
6.	11.112	21.1956	20.8754	0.9853
7.	12.964	22.4706	22.1060	1.7251
8.	14.816	23.3862	22.9570	2.6858
9.	16.668	23.9666	23.4606	3.6873
10.	18.520	24.2226	23.6335	4.4648
15.	27.780	24.8182	23.9490	1.5678
20.	37.040	23.1526	27.4695	0.8347
25.	46.300	33.2867	32.4993	10.3299
30.	55.560	37.8870	37.1112	21.6899
40.	74.080	40.1685	39.6787	37.0295
50.	92.600	37.2299	37.0326	41.6416
60.	111.120	33.6495	33.4597	42.3094
75.	138.900	23.6322	28.4091	40.7412
90.	166.680	24.6445	24.3656	38.3392
120.	222.240	19.1697	18.7279	32.5782
180.	333.360	13.6240	12.7291	23.5062
240.	444.480	10.6611	9.2116	17.6683
360.	666.720	8.2944	5.3560	14.5539
480.	888.960	7.7899	3.4564	14.7954
600.	1111.200	7.5948	2.4277	14.0900
720.	1333.440	6.9736	1.1949	12.8509

Snapshot 7

Interpolation between  
Snapshots 7 & 8

Figure C14. (Sheet 7 of 12)

Radius (n.m.)	Radius (km)	--- Wind Speed ---	Scalar Avg. (m/sec)	Vector Avg. (m/sec)	Inflow Angle, (deg)
<b>WIND, HOUR</b>					
1.	1.852	20	5.7881	1.0245	-54.9114
2.	3.704		5.4541	3.9720	-24.5178
3.	5.556		9.4686	8.6090	-11.9362
4.	7.408		13.4829	13.0106	-6.3961
5.	9.260		15.7968	16.4585	-3.6516
6.	11.112		19.4415	19.1273	-2.0103
7.	12.964		21.5386	21.1914	-0.5934
8.	14.816		23.1255	22.7110	0.8438
9.	16.668		24.2274	23.7256	2.2362
10.	18.520		24.8698	24.2708	3.3539
15.	27.780		25.3710	25.4490	1.3220
20.	37.040		30.1687	29.4218	1.2605
25.	46.300		35.5447	34.5681	10.4418
30.	55.560		40.6915	39.6964	22.0873
40.	74.080		44.2657	43.9524	39.3821
50.	92.600		41.6690	41.4767	44.9398
60.	111.120		37.9086	37.7362	46.1393
75.	138.900		32.1717	31.9795	44.8648
90.	166.680		27.4255	27.1891	42.4840
120.	222.240		23.7241	20.3404	35.3204
180.	333.360		13.3054	13.0482	25.5059
240.	444.480		10.4115	8.8880	17.8943
360.	666.720		3.0717	4.5179	13.6535
480.	888.960		7.6928	2.6034	13.7065
600.	1111.200		7.5579	1.6662	12.8807
720.	1333.440		4.9537	0.7413	11.2863
<b>WIND, HOUR</b>					
		20		15	
1.	1.852		5.2786	3.6952	-21.4673
2.	3.704		9.6598	8.8585	-8.8558
3.	5.556		13.9015	13.4537	-3.6465
4.	7.408		17.2845	16.9501	-1.3335
5.	9.260		19.9031	19.5926	-0.1562
6.	11.112		21.8548	21.5198	0.7374
7.	12.964		23.2916	22.9027	1.7017
8.	14.816		24.2837	23.8207	2.7128
9.	16.668		24.8923	24.3430	3.6006
10.	18.520		25.1624	24.5209	4.1324
15.	27.780		25.3268	25.4590	0.4130
20.	37.040		30.7382	30.0349	2.6953
25.	46.300		35.3498	35.5371	14.4592
30.	55.560		40.5023	39.6200	25.8454
40.	74.080		41.5230	41.2674	39.3602
50.	92.600		37.9830	37.7975	43.0899
60.	111.120		34.0207	33.8370	43.3371
75.	138.900		23.6710	26.4499	41.4519
90.	166.680		24.4793	24.1978	39.8258
120.	222.240		13.7628	18.3017	32.6069
180.	333.360		13.0273	12.0419	22.6556
240.	444.480		10.0310	8.3815	16.5407
360.	666.720		9.0627	4.5075	13.6395
480.	888.960		7.6978	2.7350	13.7344
600.	1111.200		7.5589	1.8231	12.9673
720.	1333.440		4.9534	0.8437	11.6417

Figure C14. (Sheet 8 of 12)

Radius (n.m.)	Radius (km)	--- Wind Speed ---		Inflow Angle, (+ = in, - = out)
		Scalar Avg. (m/sec)	Vector Avg. (m/sec)	
<b>WIND, HOUR</b>				
		20	16	
1.	1.852	7.5921	6.3574	-15.8577
2.	3.704	13.8447	13.4131	-2.9746
3.	5.556	13.2339	17.9469	0.7354
4.	7.408	21.1606	20.8925	1.7934
5.	9.260	23.0540	22.7538	2.2868
6.	11.112	24.2866	23.9272	2.8904
7.	12.964	25.0617	24.6285	3.6555
8.	14.816	25.4596	24.9436	4.4044
9.	16.668	25.5713	24.9689	4.8958
10.	18.520	25.4633	24.7739	4.8956
15.	27.780	25.2953	25.4727	-0.4949
20.	37.040	31.3771	30.6556	4.0804
25.	46.300	37.3395	36.6335	18.2633
30.	55.560	41.5397	40.0771	29.5947
40.	74.080	33.7619	38.5545	39.3625
50.	92.600	34.2823	34.0974	40.8550
60.	111.120	33.1596	29.9541	39.8027
75.	138.900	25.2403	24.9730	37.0471
90.	166.680	21.6228	21.2727	34.0914
120.	222.240	15.8975	16.3266	27.8725
180.	333.360	12.1601	11.0181	19.3734
240.	444.480	9.6775	7.8774	15.0447
360.	666.720	3.0558	4.4971	13.6266
480.	888.960	7.7047	2.8664	13.7609
600.	1111.200	7.5622	1.9796	13.0339
720.	1333.440	4.9545	0.9461	11.9152
<b>WIND, HOUR</b>				
		20	17	
1.	1.852	5.1944	3.3138	-17.8760
2.	3.704	3.2681	7.2138	-6.8815
3.	5.556	13.7056	10.0051	-6.1496
4.	7.408	12.7647	12.1956	-3.0712
5.	9.260	14.7353	14.2314	-2.2659
6.	11.112	15.6943	16.2217	-1.2967
7.	12.964	13.5415	18.0779	-0.2965
8.	14.816	23.2149	19.7445	0.5915
9.	16.668	21.6830	21.1906	1.2304
10.	18.520	22.9397	22.4105	1.6022
15.	27.780	27.8821	27.2105	1.1748
20.	37.040	32.6080	32.0467	5.5850
25.	46.300	35.3954	35.8652	14.8451
30.	55.560	38.1757	37.7211	22.5590
40.	74.080	37.0872	36.7704	30.7857
50.	92.600	34.6084	34.3532	34.4098
60.	111.120	32.1141	31.8807	36.0672
75.	138.900	28.4567	28.2119	36.6382
90.	166.680	25.2441	24.9620	35.9514
120.	222.240	23.3278	19.9233	32.5304
180.	333.360	16.6386	13.8605	25.1756
240.	444.480	11.3865	10.1154	19.1383
360.	666.720	8.4428	5.7836	14.1522
480.	888.960	7.8172	3.5385	13.6463
600.	1111.200	7.5980	2.3437	12.9271
720.	1333.440	4.9691	1.0852	11.8318

Interpolation between  
Snapshots 9 & 10

Figure C14. (Sheet 9 of 12)

Radius (n.m.)	Radius (km)	--- Wind Speed ---		Inflow Angle,
		Scalar Avg. (m/sec)	Vector Avg. (m/sec)	(+ = in, - = out) (deg)
<b>WIND, HOUR</b>				
		20	18	
1.	1.852	5.8467	0.1474	-88.3850
2.	3.704	5.8913	0.3323	-80.3511
3.	5.556	5.9854	0.7624	-51.3616
4.	7.408	5.1382	2.1004	-27.6604
5.	9.260	5.7706	4.7446	-17.3690
6.	11.112	9.0271	8.0799	-12.3260
7.	12.964	12.0708	11.4742	-8.8906
8.	14.816	15.0533	14.6107	-6.1866
9.	16.668	17.8664	17.4786	-4.1897
10.	18.520	23.4882	20.1007	-2.5294
15.	27.780	29.5051	28.9509	2.6555
20.	37.040	33.9718	33.4147	6.9510
25.	46.300	35.6832	35.1937	11.2949
30.	55.560	35.3991	35.8866	14.7093
40.	74.080	35.2753	35.7456	21.5719
50.	92.600	35.3740	34.9881	28.1950
60.	111.120	34.2038	33.9125	32.8383
75.	138.900	31.6678	31.4230	36.3589
90.	166.680	28.8703	28.6221	37.3360
120.	222.240	23.8659	23.5513	35.6325
180.	333.360	17.1794	16.6087	29.1446
240.	444.480	13.2542	12.2959	22.2227
360.	666.720	9.1195	7.0444	14.5881
480.	888.960	7.9716	4.2027	13.5547
600.	1111.200	7.6452	2.7066	12.8437
720.	1333.440	4.9840	1.2224	11.7472
<b>WIND, HOUR</b>				
		20	19	
1.	1.852	5.8873	0.1315	267.8173
2.	3.704	5.9185	0.2864	-85.9611
3.	5.556	5.9876	0.5704	-62.3600
4.	7.408	5.0828	1.4068	-35.5898
5.	9.260	5.4022	3.4218	-21.5389
6.	11.112	7.7488	6.4805	-15.1524
7.	12.964	10.6217	9.8852	-11.4492
8.	14.816	13.7639	13.2437	-8.3193
9.	16.668	15.7812	16.3407	-5.9519
10.	18.520	13.6647	19.2310	-4.1128
15.	27.780	30.2064	29.6647	1.3036
20.	37.040	35.6643	35.1813	7.1232
25.	46.300	37.6751	37.1826	12.9720
30.	55.560	33.4773	37.9349	17.8365
40.	74.080	37.8872	37.4660	26.6277
50.	92.600	35.1374	35.8437	32.4841
60.	111.120	34.0912	33.8478	35.6165
75.	138.900	33.5693	30.3335	37.1984
90.	166.680	27.2103	26.9485	36.9100
120.	222.240	21.8017	21.4339	33.6695
180.	333.360	15.3121	14.5863	25.7770
240.	444.480	11.6306	10.3863	18.7814
360.	666.720	3.3756	5.5758	13.0014
480.	888.960	7.7792	3.2149	12.4173
600.	1111.200	7.5839	2.0212	11.7434
720.	1333.440	4.9611	0.8834	10.6389

Snapshot 10

Interpolation between  
Snapshots 10 & 11

Figure C14. (Sheet 10 of 12)

Radius (n.m.)	Radius (km)	--- Wind Speed ---		Inflow Angle, (+ = in, - = out) (deg)
		Scalar Avg. (m/sec)	Vector Avg. (m/sec)	
<b>WIND, HOUR</b>		<b>20</b>	<b>20</b>	
1.	1.852	5.9287	0.1162	262.9969
2.	3.704	5.9470	0.2442	266.3879
3.	5.556	5.9963	0.4185	-82.6926
4.	7.408	5.0763	0.7876	-57.0778
5.	9.260	5.1921	2.0833	-30.7253
6.	11.112	5.8094	4.8376	-19.6630
7.	12.964	3.1999	8.2625	-14.5830
8.	14.816	12.4422	11.8214	-10.8999
9.	16.668	15.7084	15.2023	-7.9758
10.	18.520	18.8605	18.3726	-5.8433
15.	27.780	33.9314	30.3868	0.0276
20.	37.040	37.4365	36.9167	7.2898
25.	46.300	39.7792	39.1634	14.4881
30.	55.560	40.6823	40.0401	20.6426
40.	74.080	33.7404	39.3892	31.2106
50.	92.600	37.0910	36.8561	36.5571
60.	111.120	34.0673	33.8533	38.4093
75.	138.900	23.4841	29.2478	38.1131
90.	166.680	25.5521	25.2662	36.4341
120.	222.240	13.7706	19.3250	31.2195
180.	333.360	13.5125	12.5523	21.3094
240.	444.480	13.1318	8.4430	14.2101
360.	666.720	3.0124	4.0795	10.4747
480.	888.960	7.6745	2.2099	10.1812
600.	1111.200	7.5460	1.3164	9.3948
720.	1333.440	6.9515	0.5429	8.0716
<b>WIND, HOUR</b>		<b>20</b>	<b>21</b>	
1.	1.852	5.8757	0.1576	268.9495
2.	3.704	5.9111	0.3922	-77.2274
3.	5.556	5.9792	1.0670	-45.1869
4.	7.408	5.2267	2.7191	-27.0611
5.	9.260	7.1538	5.5461	-17.8151
6.	11.112	9.9381	9.1108	-12.9344
7.	12.964	13.2739	12.7167	-9.3226
8.	14.816	15.5174	16.0578	-5.5766
9.	16.668	13.5786	19.1314	-4.5214
10.	18.520	22.3568	21.8765	-2.8559
15.	27.780	31.7253	31.1325	1.6857
20.	37.040	35.4453	35.8979	7.4276
25.	46.300	33.1408	37.5264	13.7821
30.	55.560	33.9178	38.2712	19.6641
40.	74.080	33.2284	37.8720	30.4967
50.	92.600	35.6980	35.4598	35.9404
60.	111.120	32.7401	32.5198	37.7223
75.	138.900	23.2836	28.0357	37.3035
90.	166.680	24.4976	24.1939	35.5394
120.	222.240	13.9903	18.5127	30.2212
180.	333.360	13.0686	12.0446	20.4458
240.	444.480	9.6837	8.1095	13.8851
360.	666.720	7.9783	3.9614	10.7447
480.	888.960	7.5647	2.1807	10.4799
600.	1111.200	7.5406	1.3178	9.6954
720.	1333.440	6.9487	0.5516	8.3981

Snapshot 11

Interpolation between  
Snapshots 11 & 12

Figure C14. (Sheet 11 of 12)

Radius (n.m.)	Radius (km)	--- Wind Speed ---		Inflow Angle, (+ = in, - = out)
		Scalar Avg. (m/sec)	Vector Avg. (m/sec)	(deg)
WIND, HOUR		20	22	
1.	1.852	5.8255	0.2000	-87.6107
2.	3.704	5.8812	0.5546	-70.1721
3.	5.556	5.0218	1.8204	-37.1198
4.	7.408	5.7394	4.6981	-21.8820
5.	9.260	9.6611	8.8197	-14.1624
6.	11.112	13.5649	13.0636	-9.2704
7.	12.964	17.2198	16.8280	-6.1336
8.	14.816	20.5720	20.1906	-3.9692
9.	16.668	23.4862	23.0649	-2.2587
10.	18.520	25.8745	25.3865	-0.7408
15.	27.780	32.5430	31.8957	3.2647
20.	37.040	35.4582	34.8746	7.5786
25.	46.300	35.5038	35.8823	13.0151
30.	55.560	37.1546	36.4978	18.5939
40.	74.080	35.7130	36.3500	29.7262
50.	92.600	38.3014	34.0590	35.2759
60.	111.120	31.4108	31.1831	36.9782
75.	138.900	27.0841	26.8226	36.4202
90.	166.680	23.4467	23.1226	34.5579
120.	222.240	13.2176	17.7032	29.1176
180.	333.360	12.6231	11.5294	19.5335
240.	444.480	9.6441	7.7750	13.5450
360.	666.720	7.9456	3.8433	11.0326
480.	888.960	7.6550	2.1516	10.7810
600.	1111.200	7.5351	1.3193	9.9973
720.	1333.440	6.9459	0.5603	8.7143
FORTRAN STOP				

Snapshot 12

Figure C14. (Sheet 12 of 12)

# **Appendix D**

## **Sample Application of Upgraded CE Model to Simulation of 36-Hr Period of Hurricane Gilbert in the Gulf of Mexico**

---

This appendix provides information related to a 36-hr simulation of Hurricane Gilbert in the Gulf of Mexico. The simulation was performed by OWI as an additional test with the upgraded CE model. The simulation time period begins 1200 UTC (Universal Time Coordinate, formerly known as Greenwich Mean Time) 15 September 1988. The four snapshots used in the simulation all took advantage of the double exponential form for pressure profile specification. Input file information on the snapshots and storm track specification is provided in this appendix.

The appendix also includes plots of Hurricane Gilbert wind fields. Model wind fields at 19-m elevation are given at 6-hr intervals throughout the simulation period. Wind speed and direction is represented with the conventional weather map "wind barb" notation. The shaft of each wind arrow indicates the direction and the barbs or "feathers" indicate wind speed. A half-barb denotes 5 knots, full barb denotes 10 knots, and solid flag denotes 50 knots.

```

$ type 05gilbert88.dat
$name1 Kzm = 8809, Kdh = 151100, Kmin = 60, inside=1,
    nstres=17227, Kstres = 0, kwind = 19, nwind = 4661, hh=500. $end
    lns2 eyelat=22, eypres=951, pfar=1012, radius=11.88,46.85, holl=.56,2.52,
    dpi=45.07, direc=290, speed=11, sqw=7, oni=120 $end
$name2 eyelat=23, eypres=949, pfar=1010, radius=11.88,43.53, holl=.75,2.52,
    dpi=40.67, sqw=8 $end
$name2 eyelat=24, eypres=953, pfar=1010, radius=27,64.21, holl=1.33,2.52,
    dpi=46.62, sqw=9 $end
$name2 eyelat=24, eypres=954, pfar=1009, radius=21.6,60.61, holl=1.19,2.52,
    dpi=44.98 $end
$name2 eyelat = 999 $end
    0 21 54 -91 42 1
    1 21 54 -91 42 1
    7 22 5 -92 48
    13 22 30 -93 48 2
    19 22 54 -94 48
    25 23 42 -95 54
    31 23 54 -97 0 3
    37 24 24 -98 12 4
999
$what Kstep2 = 37 $enc

```

**Figure D1.** Snapshot and storm track specification, Hurricane Gilbert

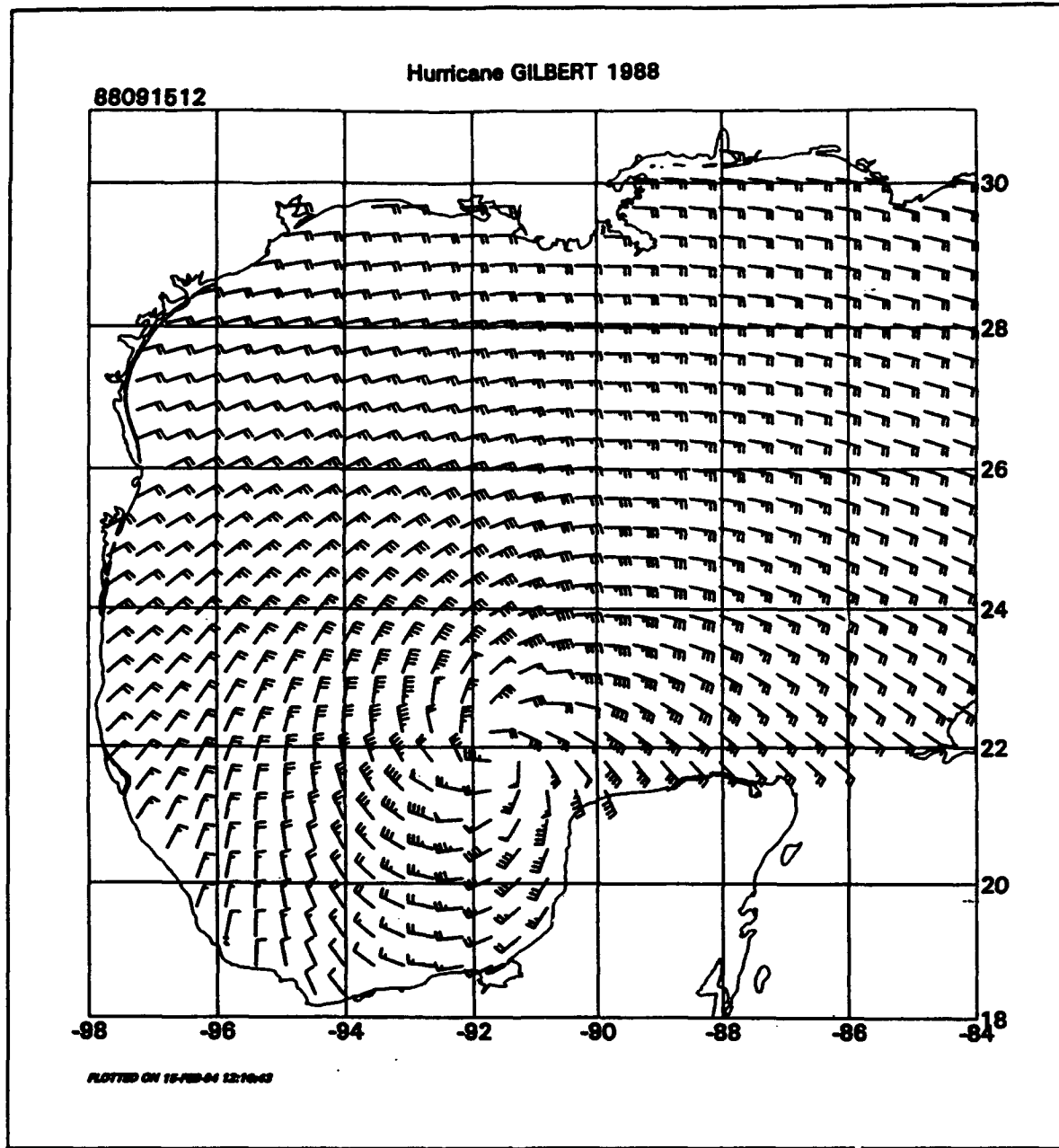


Figure D2. Modelled surface wind field in Hurricane Gilbert (Sheet 1 of 7)

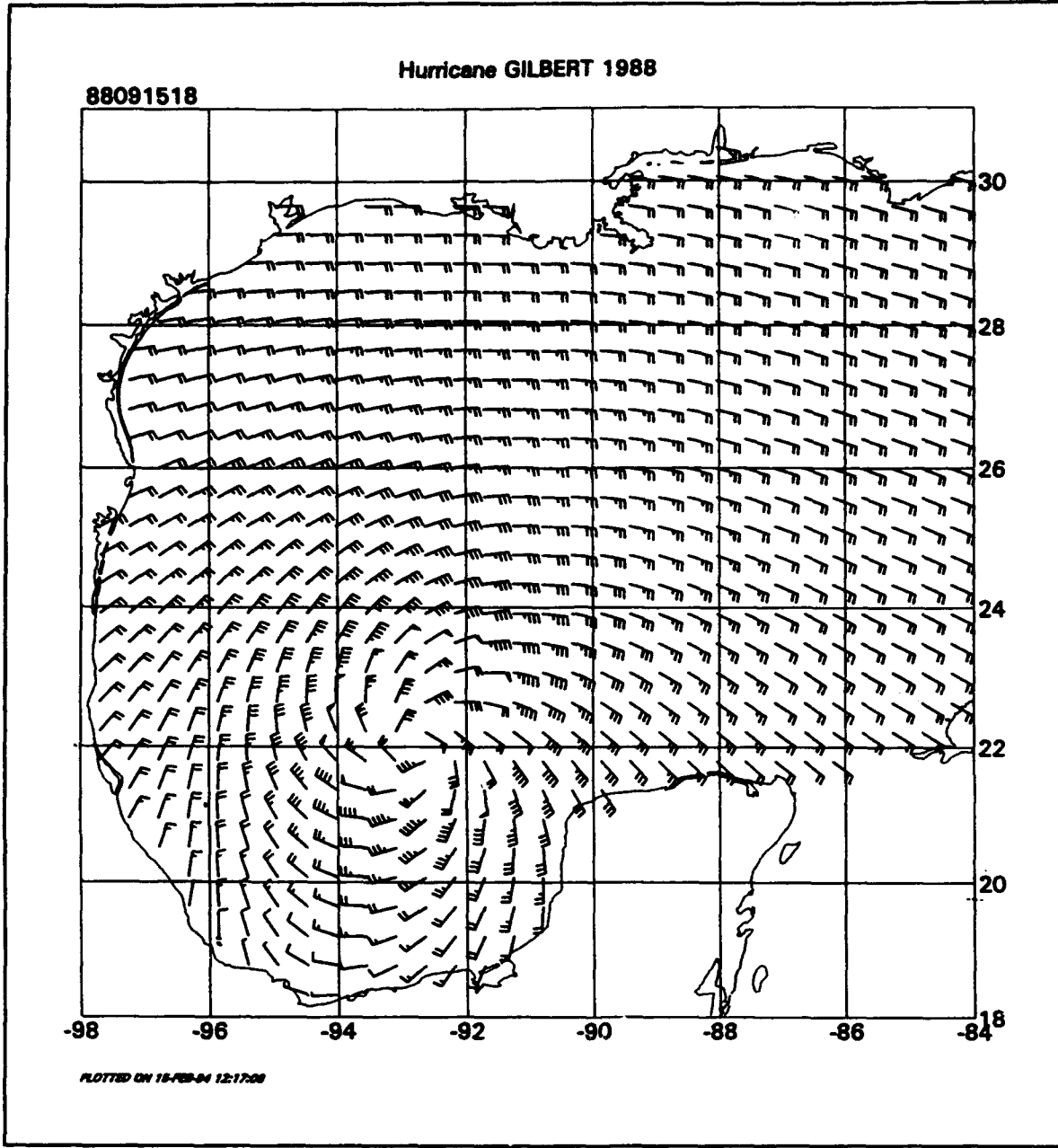


Figure D2. (Sheet 2 of 7)

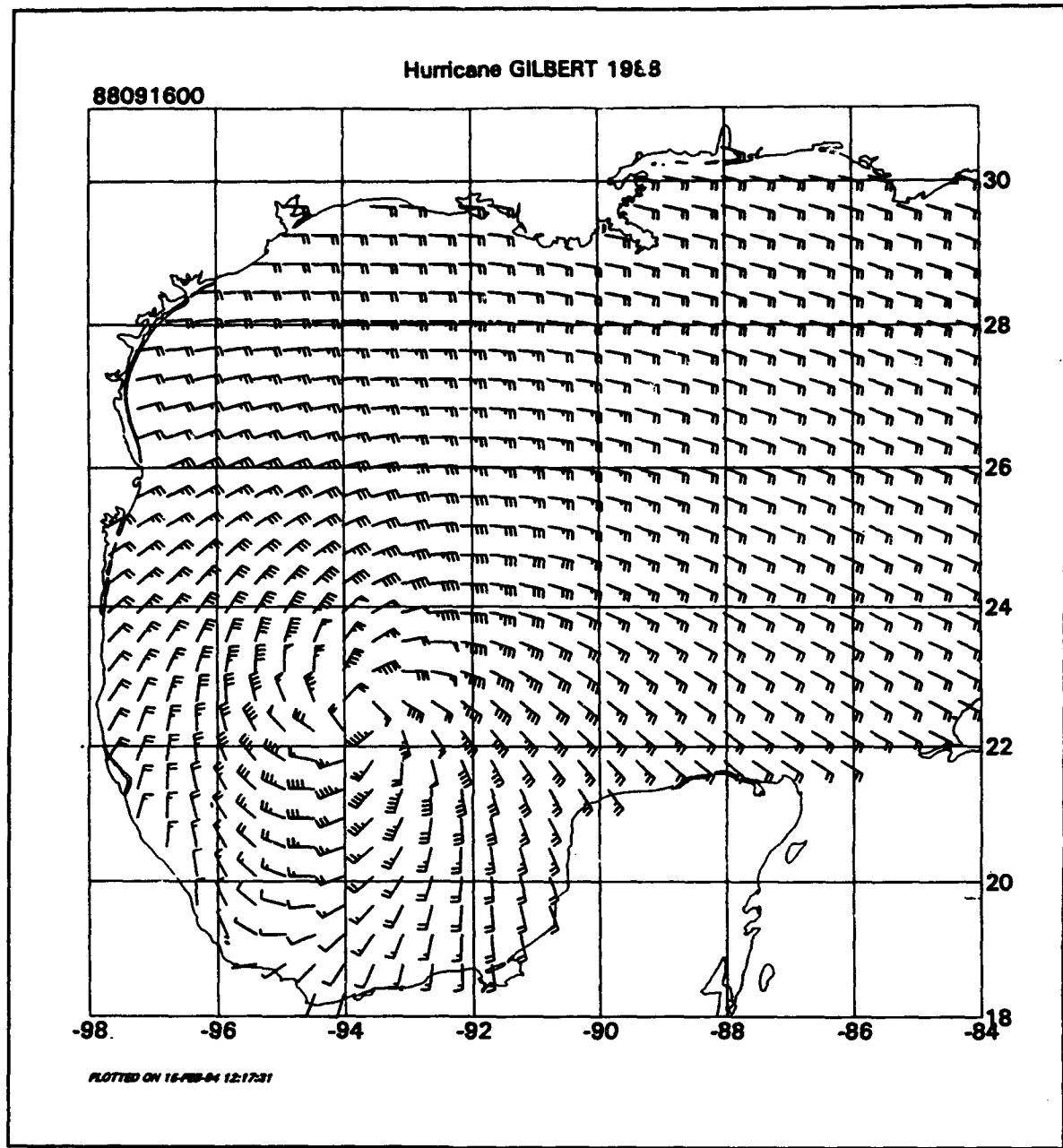


Figure D2. (Sheet 3 of 7)

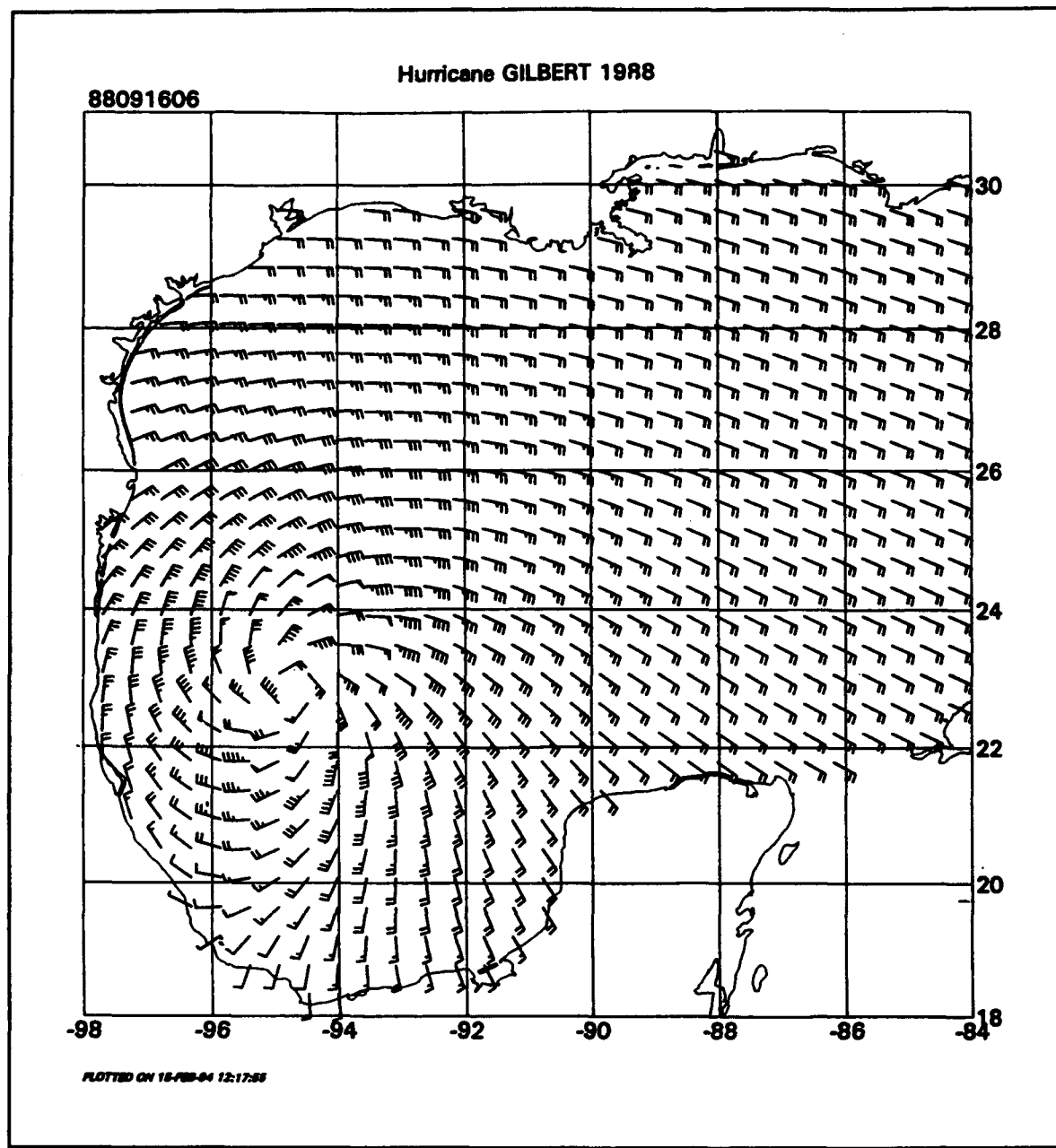


Figure D2. (Sheet 4 of 7)

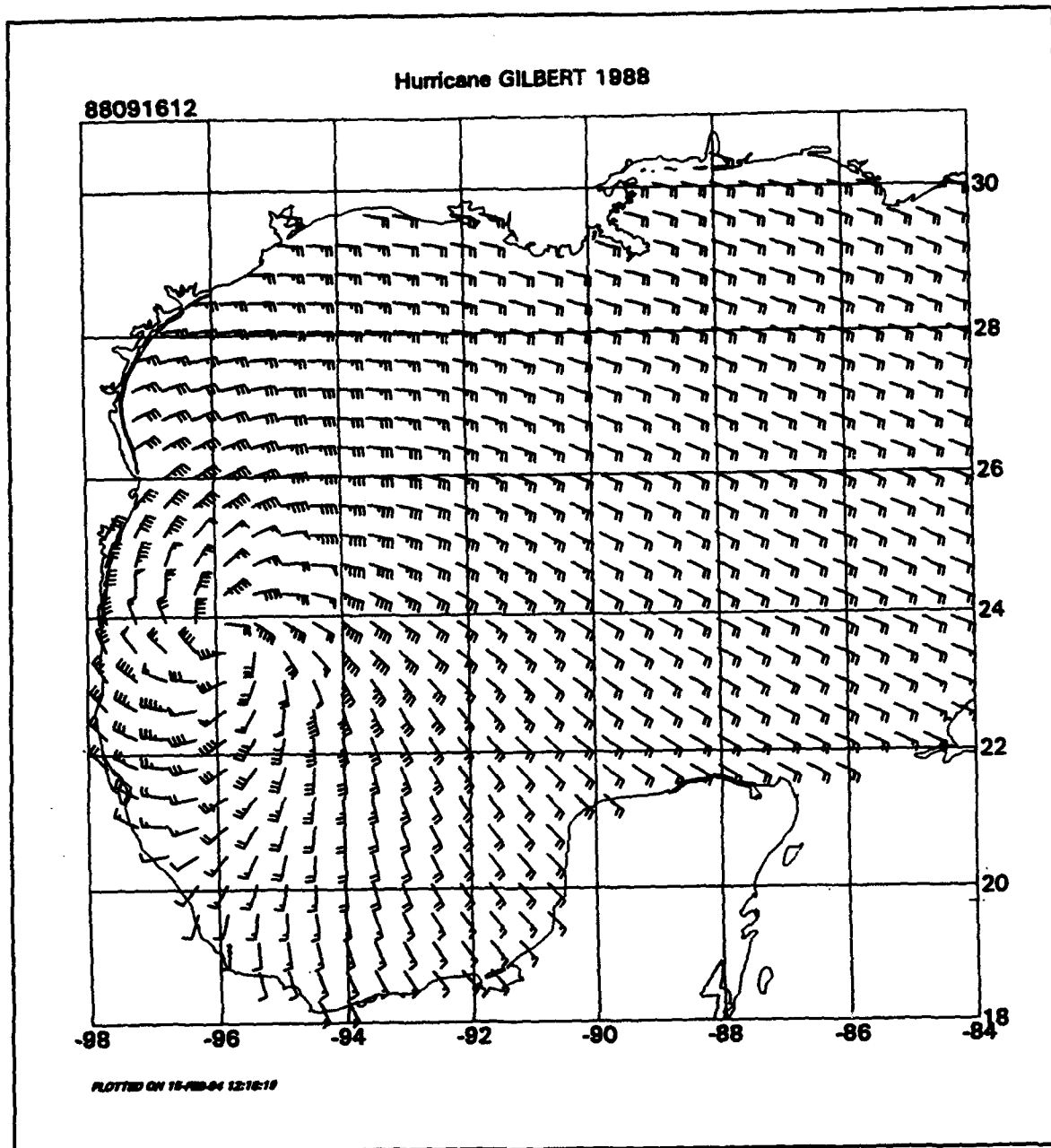


Figure D2. (Sheet 5 of 7)

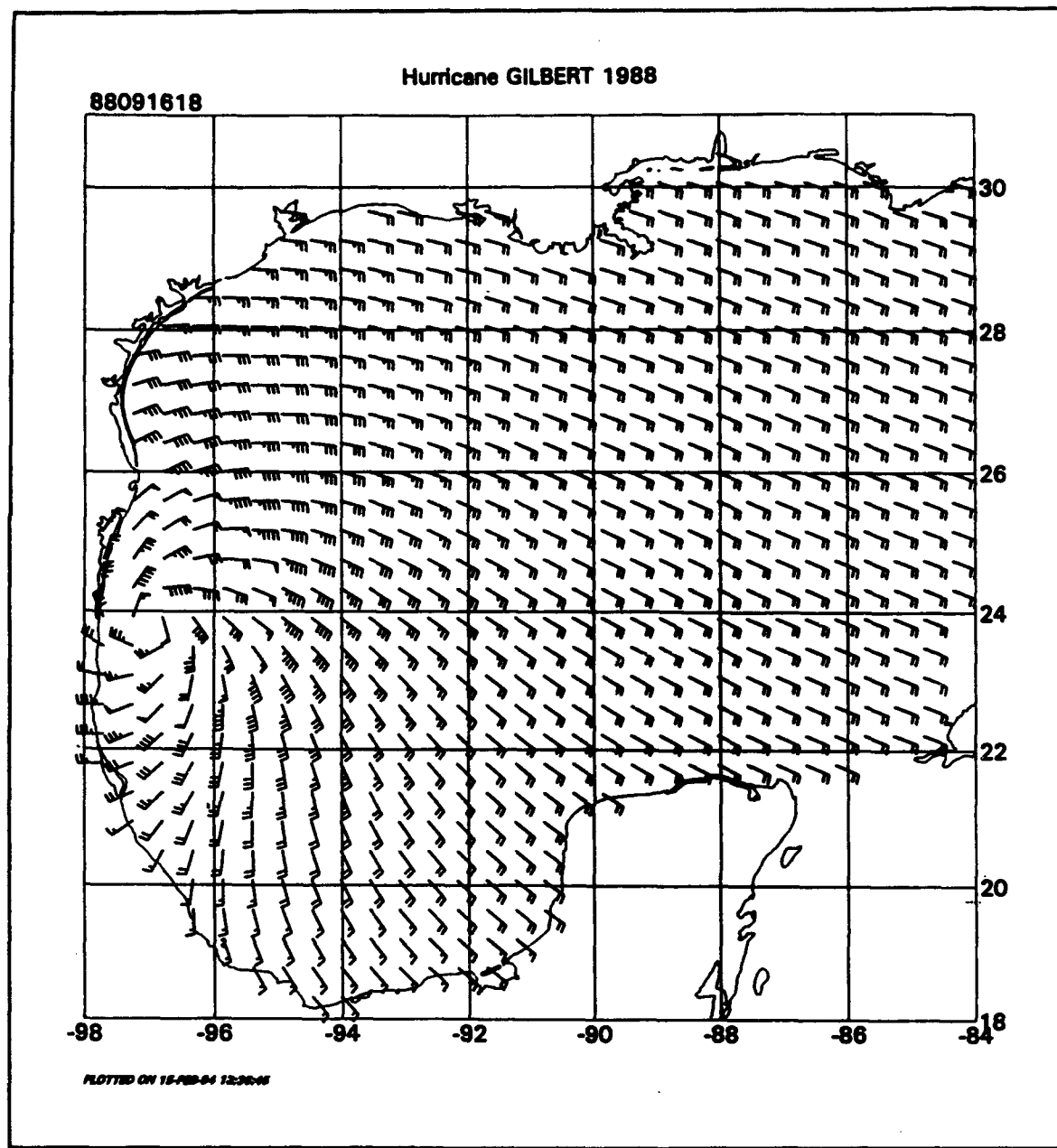


Figure D2. (Sheet 6 of 7)

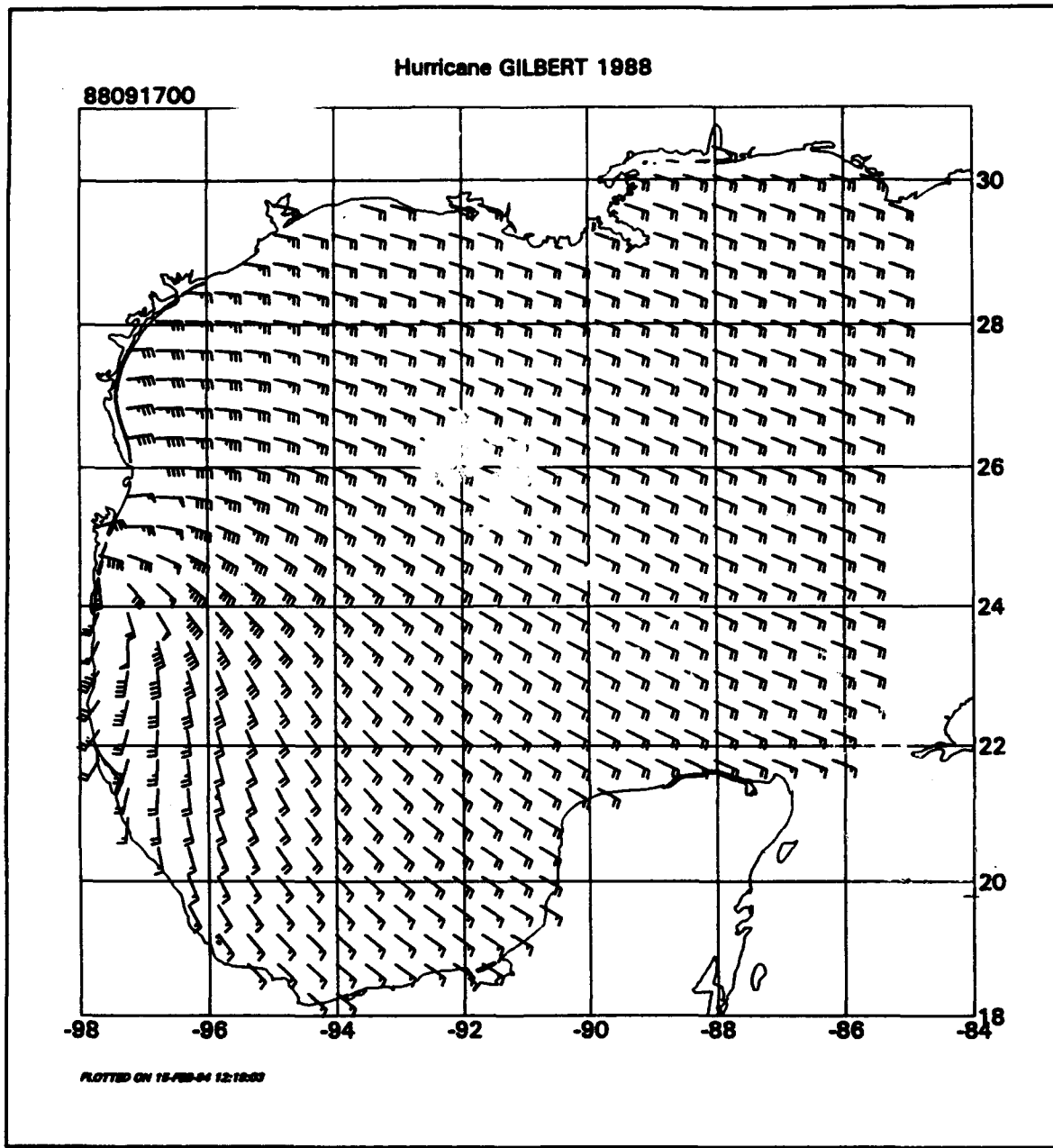


Figure D2. (Sheet 7 of 7)

# REPORT DOCUMENTATION PAGE

Form Approved  
OMB No. 0704-0188

Public reporting burden for this collection of information is estimated to average 1 hour per response, including the time for reviewing instructions, searching existing data sources, gathering and maintaining the data needed, and completing and reviewing the collection of information. Send comments regarding this burden estimate or any other aspect of this collection of information, including suggestions for reducing this burden, to Washington Headquarters Services, Directorate for Information Operations and Reports, 1215 Jefferson Davis Highway, Suite 1204, Arlington, VA 22202-4302, and to the Office of Management and Budget, Paperwork Reduction Project (0704-0188), Washington, DC 20503.

1. AGENCY USE ONLY (Leave blank)	2. REPORT DATE	3. REPORT TYPE AND DATES COVERED
	July 1994	Final report
4. TITLE AND SUBTITLE Upgrade of Tropical Cyclone Surface Wind Field Model		5. FUNDING NUMBERS WU 32683
6. AUTHOR(S) Vincent J. Cardone, Andrew T. Cox, J. Arthur Greenwood, Edward F. Thompson		8. PERFORMING ORGANIZATION REPORT NUMBER Miscellaneous Paper CERC-94-14
7. PERFORMING ORGANIZATION NAME(S) AND ADDRESS(ES) Oceanweather, Inc., 5 River Road, Suite 1, Cos Cob, CT 06807 U.S. Army Engineer Waterways Experiment Station 3909 Halls Ferry Road, Vicksburg, MS 39180-6199		
9. SPONSORING/MONITORING AGENCY NAME(S) AND ADDRESS(ES) U.S. Army Corps of Engineers Washington, DC 20314-1000		10. SPONSORING/MONITORING AGENCY REPORT NUMBER
11. SUPPLEMENTARY NOTES Available from National Technical Information Service, 5285 Port Royal Road, Springfield, VA 22161.		
12a. DISTRIBUTION/AVAILABILITY STATEMENT Approved for public release; distribution is unlimited.		12b. DISTRIBUTION CODE

**13. ABSTRACT (Maximum 200 words)**

The U.S. Army Corps of Engineers (CE) tropical cyclone surface wind field model has been a very useful tool in ocean response modeling for more than a decade. Recently, its limitations were assessed in light of present knowledge and technology. Model limitations were identified and evaluated in terms of their perceived importance to ocean response modeling and the level of effort required to develop improved solutions. The limitations are summarized in this report.

Two aspects of the CE model were targeted for improvement. This report describes the improvements developed for the upgraded model. First, the model was upgraded to include more computationally intensive options which give improved resolution and areal coverage. Up to seven nested grids are now available, compared to only five nests in the standard model. In a typical application, this upgrade can be used to achieve 2-km resolution around the eye (as compared to 5-km resolution often used in the standard model) and an expanded total coverage area.

The second upgrade allows a more general specification of the axisymmetric pressure profile. This upgrade can be used to create wind fields with maxima at two different radii or with a broad maximum extending over a range of radii. It also provides more flexibility in fitting the shape of single peaked wind profiles.

(Continued)

14. SUBJECT TERMS Hurricanes Numerical modeling Tropical storms		15. NUMBER OF PAGES 101	
		16. PRICE CODE	
17. SECURITY CLASSIFICATION OF REPORT UNCLASSIFIED	18. SECURITY CLASSIFICATION OF THIS PAGE UNCLASSIFIED	19. SECURITY CLASSIFICATION OF ABSTRACT	20. LIMITATION OF ABSTRACT

13. (Concluded).

The upgraded model is demonstrated with historical hurricanes. The five-nest and seven-nest models are applied to Hurricane Camille. The fully upgraded model, with seven nests and general pressure specification, is applied to Hurricane Gilbert. This hurricane was chosen because it is well-documented by Black and Willoughby (1992) and it evolved into some nontraditional storm structures. The upgraded model was more effective than the standard CE model in simulating the storm.